Life-Cycle Reliability-Based Design and Assessment of Shield Tunnels in Coastal Regions

海洋環境にあるシールドトンネルのライフサイクル信頼性設計と評価

June, 2019

Zhengshu HE

何　政樹

Life-Cycle Reliability-Based Design and Assessment of Shield Tunnels in Coastal Regions

海洋環境にあるシールドトンネルのライフサイクル信頼性設計と評価

June, 2019

Waseda University
Graduate School of Creative Science and Engineering
Department of Civil and Environmental Engineering
Research on Concrete Structure

Zhengshu HE
何　政樹

Abstract

Corrosion of reinforcing bars is a primary source of deterioration for reinforced concrete (RC) structures, and the corrosion-induced deterioration poses a major challenge to the RC structure in an aggressive environment for providing an acceptable performance over their entire life-cycle. Especially for the RC shield tunnels located in marine environments, those tunnel structures always undergo a more complex and rapid deterioration process due to aggressive chemical attack and action of high earth-water pressure. Therefore, higher structural performance and durability for RC tunnel structures in coastal regions are required to ensure the serviceability of structures within their lifetime.

For new RC shield tunnels, the concept of Life Cycle Design has been gradually proposed and considered by engineers at structural design phase; meanwhile, for improving the accuracy of structural performance estimates for existing RC shield tunnels, updating of structural reliability has been discussed by incorporating observational information from field inspection. However, because the environmental and operational conditions of RC shield tunnels in coastal regions are complex, the primary impact factors on structural deterioration should be identified and integrated into the reliability-based performance analysis of tunnel structures, so that the reliable design for new tunnels and rational maintenance planning for deteriorated existing structures can be proposed.

To address this issue, a novel approach for estimating the life-cycle structural performance of a RC shield tunnel in a marine environment is proposed firstly, in which the hazard associated with underground chloride and the impact of hydrostatic pressure on chloride motion in RC segmental linings are taken into account. The deterioration processes of RC segmental linings are investigated based on a corrosion-accelerated experiment of bearing RC segment specimens, and the combined effects of corrosive agents and loads on

deterioration of RC segment are revealed. Monte Carlo simulation is used to estimate the time-variant failure probability of RC shield tunnels in a marine environment. In an illustrative example, the effects of structural location, hydrostatic pressure, and material properties on the life-cycle reliability of shield tunnels are discussed.

Based on the life-cycle structural performance analysis of RC shield tunnels in coastal regions, the approaches for life-cycle reliability-based design and assessment of RC shield tunnels in coastal regions are proposed, respectively. For the durability design of RC shield tunnels in coastal regions, the coupling effects of chloride and hydrostatic pressure are integrated into the reliability-based durability design of new RC shield tunnels in coastal regions. Based on the proposed durability design criterion for RC segments, the durability design factors are discussed, and the relationship between the marine environment and concrete quality (W/C) of RC segment is revealed, so that the target durability reliability level of RC tunnel structures within the prescribed lifetime will be satisfied. Meanwhile, with respect to the existing RC shield tunnels in coastal regions, a computational procedure for updating structural reliability of existing RC shield tunnels subjected to underground chloride attacks is presented. Observational information, including chloride concentration distribution in segmental linings, corrosion-induced crack width on the surface of segments and vertical convergence of shield tunnels, are used in conjunction with the calculation of time-variant reliability for existing RC shield tunnels via Sequential Monte Carlo Simulation (SMCS). And the influences of different observational information on updating the parameters of random variables, time-variant convergence and reliability of existing RC shield tunnels, are discussed, respectively.

Acknowledgements

Three-year doctoral life in Japan, at Waseda University, is close to an end. This long journey not only expands my horizons of knowledge but also makes my heart stronger. I believe the valuable experiences at Waseda has been, will always be, supporting me to fight with challenges and realize my dreams. I greatly appreciate the people who has accompanied me in the past years, it is you to give me one special and memorable time on my journal of life.

First and foremost I would like to take this opportunity to appreciate my supervisor Prof. Mitsuyoshi Akiyama who has always kept encouraging me to challenge myself for improving my competencies and knowledge, so that I can seize opportunities to get more achievements on the road of academic research and create a bright future in my life. I cannot image I can successfully complete my doctoral program within 3 years without his kind and strategic guidance. His trust and hope on me always make me feel the warmth of home. Also, working with him made me gain a lot and changed me in many aspects, he shows and teaches me how I can be an outstanding researcher and professor, his influence, I believe, will keep going serve me well beyond my doctoral time.

I am grateful to all members of my Ph. D dissertation committee, Prof. Motoi Iwanami, Prof. Yasuhiko Sato and Prof. Kiyoshi Ono, for attending my doctoral defense and providing constructive comments for me to improve my doctoral dissertation. Also, I would like to express my appreciation to Chinese Government for awarding me the CSC scholarship and sponsoring my study and life in Japan, so that I could focus on my attentions on my doctoral study.

Meanwhile, I would also like to thank Dr. Khem and all wonderful students in Akiyama laboratory from Japan, China, Thailand and Bangladesh, who create a multicultural home here and let me know this world more. Also, they always supported and encouraged me to

overcome the difficulties of study in the past three years at Waseda University, especially my junior Oat spent so much time to help me conduct the computational analysis. Furthermore, thanks to my friends in Koraku-Ryo who enriched my life in Japan.

Finally, I want to appreciate my parents for their understanding and supports, which are the source of my continuous fight for building a bright future. And a special thanks to Dear Shao who always accompanies me through the difficult time and brings me infinite happiness. If there were not all of you, I would not be where I am today. Thank all of you for your endless love!

HE Zhengshu

Waseda University

April 2019

Table of Contents

List of Figures

List of Tables

Chapter 1: Introduction

1.1 Background and motivation of research

The reliable and durable performance of tunnel structures is essential to support the stable developments of the cities located in the coastland or regions with numerous lakes and rivers. Generally, those tunnels are expected to provide acceptable service for extended periods of time, but reinforced concrete (RC) tunnel linings, owing to their inherent vulnerability, are at risk from deterioration processes due to aggressive chemical attacks and other physical damage mechanisms (Ellingwood 2005; Biondini and Frangopol 2016). In particular, for a RC shield tunnel located in a marine environment, the tunnel structure always undergoes a more complex and rapid deterioration process (Post et al. 2004, Yuan et al. 2006). For example, the Al-Shindagha undersea tunnel in Dubai (built in 1973) and the Ahmed Hamdi underwater tunnel (built in 1983) that crosses the Suez Canal had to be rehabilitated in 1983 and 1992, respectively, because of severe steel corrosion and lining damage that accrued within 10 years after construction (Liu et al. 2016). The likely reason for this phenomenon is the combined effects of multiple mechanical and environmental stressors, such as high hydrostatic pressure and highly concentrated and aggressive chemical agents. Therefore, higher structural performance and durability for tunnel linings are required to ensure the long-term safety and serviceability of tunnel structures.

For the new shield tunnels, considering the high construction costs, long target service-life and difficulties of maintenance, repair and rehabilitation, etc., the concept of Life Cycle Design have been gradually proposed and considered by engineers at structural design phase, to ensure the higher long-term structural performance and durability of tunnel structures, especially for undersea tunnels (Sun 2011; He et al. 2017). For example, because of the repaid development of nation economy in China, higher demands for

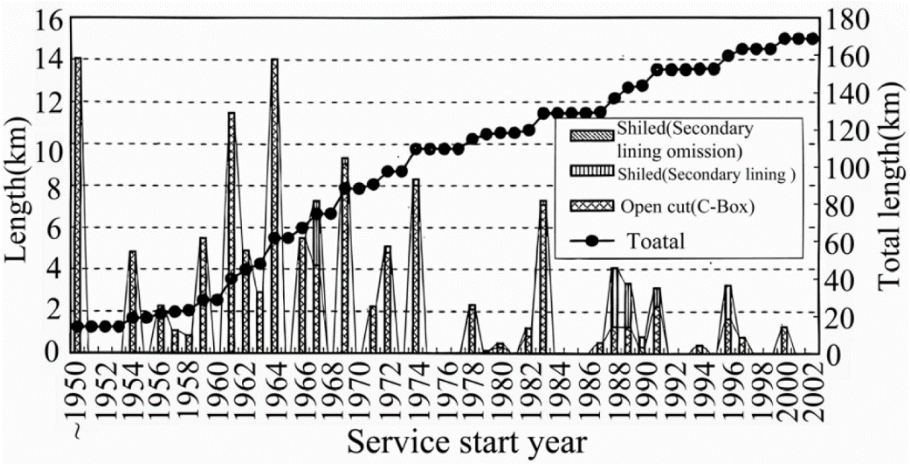

Figure 1.1 Development history of Tokyo Metro (Kimura et al. 2012)

underground infrastructure facilities, like metro in developed coastal cities, transportation tunnels cross rivers, lakes and sea, has been proposed. Therefore, a reliable durability design methodology, like Life Cycle Design, for new RC tunnel structures is very important and urgent. On the other hand, numerous existing RC tunnel structures have been constructed to support national development in many countries since last century, especially in the developed countries. Figure 1.1 presents a history of metro development in Tokyo as an example with indicators of year and tunnel length. Although the demands for new tunnel structures have been gradually decreased, amount of existing tunnel structures have been undergoing deterioration since the turning of the century (Kimura et al. 2012). Structural deterioration poses a big challenge to these existing tunnel structures for providing an acceptable service over their entire life-cycle. Meanwhile, tunnel structures cannot be simply abandoned after structural degradation, which is different from the ground structures. Therefore, a reliable predicting approach is necessary to provide precise estimates for structural performance of existing shield tunnels during their remaining lifetime, so that the repair and maintenance action plan can be carried out in time to extend structural service life.

Because of the complexity of structural deterioration process of RC shield tunnels in coastal regions, the primary impact factors on structural deterioration should be

captured and integrated into the structural performance analysis, this approach could support decision-making processes for reliable design of durable tunnels and rational planning of maintenance, repair of deteriorating existing structures. Generally, RC tunnel linings in marine environments are exposed to chemical attacks from aggressive agents. Aggressive chemicals, such as chlorides and sulfates, either diffuse under concentration gradients into segmental linings, or permeate with seawater into segmental linings due to the high water pressures on the outside wall of linings (Jin et al. 2013; Zhang et al. 2016). This process often leads to premature steel corrosion and the concrete cracking of tunnel linings. Meanwhile, the concrete cracking and spalling of tunnel linings induced by high water-soil pressures and steel corrosion allow aggressive agents to permeate more easily (Hoseini et al. 2009) and, thus, increase the rates of corrosion and structural deterioration (Otieno et al. 2016). As a result, to accurately assess the structural performance of a shield tunnel during its life-cycle, the coupling effects of aggressive chemical agents and high hydrostatic pressures on the deterioration of the shield tunnels must be considered.

Over the past few decades, significant advances have been accomplished in the fields of life-cycle structural performance assessment of RC structures (Mori and Ellingwood 1993; Frangopol and Lin 1997; Ellingwood 2005; Akiyama et al. 2010, 2012; Frangopol 2011; Biondini and Frangopol 2016). However, owing to the complex underground service conditions, the deterioration processes of shield tunnels normally is different from that of ground RC structures. In terms of the durability of tunnel structures, the attempts (Kudo and Guo 1994; Fagerlund 1995; Sun 2008, 2011; Funahashi 2013 & Lei et al. 2015) using corrosion testing of the RC component and on-sit monitoring have been addressed in the durability design, assessment and lifetime prediction of undersea tunnels. Meanwhile, probabilistic methods to evaluate the deterioration of underwater tunnels (Song et al. 2009; Bagnoli et al. 2015) have been recently reported. However, there has been a lack of research on accounting for structural deterioration performance

of the shield tunnels in a marine environment over their entire life-cycle, by considering the effects of marine environmental hazard and structural deterioration processes. Furthermore, according to the life-cycle structural performance analysis of RC shield tunnels in coastal regions, a reliable reliability-based durability design criteria for new shield tunnels and an approach for estimating structural performance of existing shield tunnels using inspection information should be established.

1.2 Objectives of research

This study focuses on the external steel corrosion of RC segmental linings due to the chloride attacks from the surrounding soil and underground water around shield tunnel. Next, life-cycle structural performance of RC shield tunnels in a marine environment is studied with emphasis on the corrosion-induced deterioration of segmental linings, according to the deterioration mechanism of RC segmental linings in a marine environment and Life-Cycle concept of RC structures.

In this study, three primary objectives are proposed as follows:

(1) Time-variant structural performance assessment of a shield tunnel in coastal regions

a. Present a framework for the time-variant structural performance assessment of a shield tunnel in a marine environment;
b. Because the deterioration of a shield tunnel depends on its location and surroundings, the hazards posed by chloride should be investigated for a tunnel in a coastal region.
c. Experimentally illustrate the deterioration processes of segmental linings under different load levels, with an emphasis on the chloride-induced corrosion of concrete segments. And propose an approach for estimating the damage level in segmental linings based on the experimental results.

d. Examine chloride transportation in the segmental linings, with an emphasis on the impact of hydrostatic pressures. Next, estimate the time to corrosion initiation of external reinforcement in segmental linings.

e. Assess the time-variant structural reliability of a shield tunnel in a marine environment considering the degradation of structural stiffness and the capacity of segmental linings induced by steel corrosion.

(2) Life-cycle reliability-based durability design for RC shield tunnels

a. Integrate the chloride hazard in coastal regions, structural location and effect of hydrostatic pressure into the reliability-based durability design of RC segmental linings with service life design format.

b. Propose a computational procedure for service life (durability) design of segmental linings using partial factors, and determine the durability partial factors of segment according to the target lifetime and target reliability.

c. Discuss the maximum design value of water to cement ratio for RC segmental linings under different hydrostatic pressure and underground chloride hazard.

(3) Performance assessment of existing RC shield tunnels based on inspection data

a. Propose a framework for estimating structural performance of existing RC shield tunnels in a marine environment during their remaining lifetime, and illustrate the updating process for structural reliability assessment using Sequential Monte Carlo Simulation (SMCS) and inspection results.

b. Discuss the influence of different types of inspection information on updating parameters of random variables and reliability of RC shield tunnels. According to the updating results, determine a maximum time interval of inspection for existing RC shield tunnels to improve the predicted precision of structural performance during their remaining lifetime.

In terms of above three primary objectives, objective (1) is treated as a fundamental aspect for the studies for other two objectives. According to the procedure for assessing the hazard associated with underground chloride around segmental linings and the effect of hydrostatic pressure on chloride transport in segmental linings, time-dependent chloride distribution around external reinforcement of segmental linings could be estimated accurately. Thus, the durability parameters of RC segmental linings could be designed based on quantitative evaluation results for shield tunnels located in different coastal regions. Meanwhile, the predicted results associated with structural performance before updating would be used to update the parameters of random variables with inspection information, then time-dependent structural reliability of existing RC segmental linings could be updated based on updated random variables.

Chapter 2: Literature Reviews

2.1 Basic concepts for deterioration of RC structures

2.1.1 Corrosion mechanism of reinforcement in concrete

Generally, microscopic pores of concrete includes high concentrations of alkaline solution, this very alkaline condition (i.e. pH 12-13) could facilitate the formulation of a thin protective oxide film (i.e. passivation film) on the surface of the reinforcement bars (Broomfield 2006; Bertolini 2008; Kapakonstantinou et al. 2013). Because of the protection of passive film on rebars, the steel corrosion can be prevented even though there are an amount of oxygen and high moisture in concrete. However, due to the chloride penetration and carbonation of concrete for real concrete structures, the passive film on rebar might be locally damaged or removed, resulting in the corrosion of reinforcement in engineering.

Chloride-induced corrosion is regarded as the most severe factors for structural deterioration of structures in coastal regions, the chlorides found in concrete are generally from two approaches. One is chloride casted into concrete, such as mixing by seawater, using admixture including chlorides. Another one is the penetration of chloride in concrete due to salt spray from seawater, drying/wetting cycles of seawater and deicing salts in winter (Broomfield 2006). In particular for the undersea tunnels, segmental linings are exposed to infinite seawater and chloride from seawater could penetrate into segmental linings, it is a big challenge for engineers to ensure the long-term safety and serviceability of tunnel structure during its life-cycle.

For structures under an aggressive environment, as the chloride concentration around rebar accumulates and reaches a critical threshold, localized corrosion on rebar would take place due to passive film broken down. According to previous reports

(Broomfield 2006; Kapakonstantinou et al. 2013), the chloride-induced corrosion is an electrochemical process, including anodic and cathodic half-cell reactions. The reactions could be illustrated using following equations:

$$Fe \rightarrow Fe^{2+} + 2e^{-} \quad (2\text{-}1)$$

$$Fe^{2+} + 2Cl^{-} \rightarrow FeCl_2 \quad (2\text{-}2)$$

$$FeCl_2 + 2H_2O \rightarrow Fe(OH)_2 + 2HCl \quad (2\text{-}3)$$

$$4Fe(OH)_2 + O_2 + 2H_2O \rightarrow 4Fe(OH)_3 \quad (2\text{-}4)$$

$$4Fe(OH)_3 \rightarrow Fe_2O_3 \cdot H_2O + 2H_2O \quad (2\text{-}5)$$

Above equations reveal that chloride ions are not consumed in the steel corrosion process, they are the catalysts for steel corrosion and could accelerate the corrosion process of reinforcement in concrete (Kapakonstantinou et al. 2013). Because of the widely distributed chloride in the world, such as in seawater, de-icing salts and air of coastal regions, significant attentions has been given to the durability of concrete structure subjected to chloride-induced corrosion (Venu et al.1965; Hausmann 1967 and Gouda 1970; Francois et al. 1999; Broomfield 2006; Angst, U. et al. 2009; Kapakonstantinou et al. 2013).

On the other hand, carbonation-induced corrosion often occurs due to the neutralization of the alkalinity condition in concrete induced by carbon dioxide from atmosphere (Bertolini 2008). With the interaction of carbon dioxide and alkaline hydroxides in concrete, the value of pH in concrete would drop to about 8.5 (Jin et al. 2014). If there are enough oxygen and moisture in concrete, passive film could be gradually removed, and reinforcement steels could corrode. Especially for the internal service environment of tunnels, there are high concentration of carbon dioxide due to bad ventilating conditions, so that the internal reinforcements of segmental linings are generally at risk from carbonation-induced corrosion (Pan et al 2005; Sun 2011).

Furthermore, the stray current induced corrosion also is a common problems for concrete structures, like metro tunnels, it could causes rapid and serious steel weight loss of reinforcements for concrete structures (Zhou et al. 1999; Angst, U. et al. 2009).

2.1.2 Impact factors for reinforcement corrosion

(1) Alkaline condition and chloride concentration around steel

As previously states, the failure of passive film is associated with the alkaline condition and chloride concentration in concrete. At the beginning time after structure construction, the initial value of pH in concrete is mainly influenced by the types of binder materials, but because of the occurrence of carbonation, leaching, hydration, etc. for concrete structures, the pH value could change and affect the property of passive film (Angst, U. et al. 2009). Meanwhile, chloride ions act the catalyst on the steel corrosion, and chloride concentration around rebar could directly affect the steel corrosion process. Generally, higher concentration of chlorides leads to higher hazard associated with corrosion of reinforcement bars in concrete, but the chloride threshold for corrosion initiation is only influenced by chloride concentration. According to the literatures (Venu et al.1965; Hausmann 1967 and Gouda 1970), the threshold value for steel corrosion initiation are associated with the results of inhibiting effect of hydroxide ions against chloride induced corrosion. Gouda (1970) experimentally found threshold value increasing with the increasing pH value. Therefore, it is suggested to determine the threshold value, C_{crit}, based on the Cl^-/OH^- ratios.

(2) External environment (e.g. Temperature, Moisture and Oxygen)

As a matter of fact, both water and oxygen are the basic elements for steel corrosion, anyone of them lacked could be facilitate to inhibit steel corrosion. For the concrete under water saturated condition and rather dry condition, resulting in a lack of oxygen and water for the reaction of steel corrosion, respectively, higher chloride concentration is often

required for the steel corrosion initiation (Angst, U. et al. 2009). On the contrary, when concrete are subjected to wetting/drying cycles or exposed to the environment with relative humidity (RH) ranging from 90% to 95% (Zhao 2004), reinforcements might have the higher hazard associated with corrosion. In addition, temperature also plays a significant role for steel corrosion process, the corrosion rate generally increases with the increasing temperature to 40℃ according to Jin et al. (2014).

(3) Concrete properties and conditions

Steel corrosion process is significantly influenced by the concrete properties, like the ratio of water to cement, the binder type, and cracks of concrete. In term of the ratio of water to cement, it could not only determine the strength of concrete, but also affect the anti-permeability of concrete. Generally, higher ratio of water to cement could result in a worse anti-permeability of concrete, which is harmful to inhibit steel corrosion (Jin et al. 2014). Meanwhile, the electrical resistivity of concrete is associated with the binder materials of concrete, like the mineral admixture using silica fume, fly ash and blast furnace slag, and the rate of steel corrosion would change depending on the types of mineral admixture (Angst, U. et al. 2009). Furthermore, because of the action of tensile loads, effect of wetting/drying cycle, and alkali-aggregate reaction, etc., the cracking of the cover concrete might take place after structure construction. Cover concrete cracking could allow the chlorides, carbon dioxide, water and oxygen, etc., to reach the surface of steel more easily, and thus increase the rate of corrosion (Francois et al. 1999; Otieno et al. 2016).

(4) Other effects

Except for the factors illustrated previously, the steel corrosion process is also associated with the steel properties and/or conditions, like steel surface condition, steel electrochemical potential, and steel-concrete interface, and stress state of structures

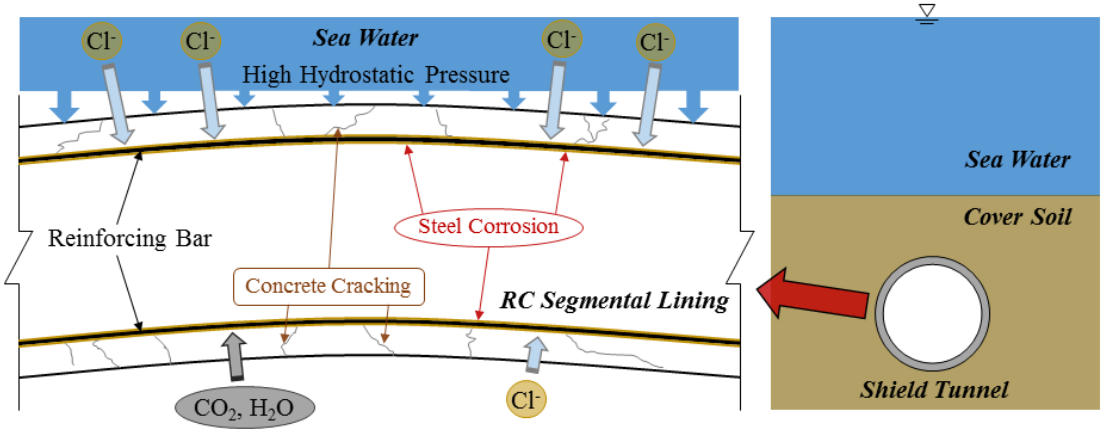

Figure 2.1 Illustration diagram of an undersea shield tunnel

(Angst, U. et al. 2009; Jin et al. 2014). Because of the variety of factors on steel corrosion involved, the uncertainties in the steel corrosion process are extremely advisable to be taken into consideration when assessing the structural deterioration performance (Biondini and Frangopol 2016).

2.2 Durability of RC tunnel structures in a marine environment

2.2.1 Deterioration mechanism of RC segmental linings

With respect to an RC shield tunnel in a marine environment, three damage mechanisms are generally observed: (1) chemical processes (e.g., carbonation and chloride-induced corrosion), (2) physical processes (e.g., expansion because of rust formation) and (3) mechanical processes (e.g., concrete cracking caused by soil-water pressure and other loads). As shown in Figure 2.1, the inside- and outside walls of segmental linings are exposed to totally different environments. Marine chloride diffuses and permeates into the outside wall of segmental linings because of high concentration gradients and significant hydrostatic pressure. Meanwhile, carbonation and chloride attacks occur at the inside wall of segmental linings due to high concentrations of CO_2 and airborne chloride, seepage and leakage of seawater. These processes can lead to steel corrosion in the segmental linings and corrosion-induced concrete cracking. In addition, concrete cracking and spalling of the segmental linings induced by high soil-water pressure might

happen at the beginning of structural service phase, so that aggressive agents can move into concrete more easily and result in severe corrosion. Therefore, the coupled effects of a corrosive environment and high water-soil pressure are considered as the most significant reasons for the decline in the long-term structural performance of undersea shield tunnels.

In term of the structural deterioration of undersea shield tunnels due to steel corrosion of external reinforcement, structural damage process is described in Figure 2.2 based on the model proposed by Tuutti (1982) using a phenomenological process (Rao et al. 2017). In this approach, segment damage is segmented into a series of states beginning with the (1) initial damage induced by loading and chloride transport through the concrete cover; (2) reinforcing steel de-passivation, steel corrosion initiation and anti-permeability decrease of segment; (3) accelerated corrosion rates, concrete cracking caused by expansion from rust formation and decreased bond strength; and (4) severe steel weight loss as well as concrete spalling and structural capacity loss. In particular, states (2), (3) and (4) represent the deteriorating damage stages induced by the coupled effects of corrosive agents and loads as shown in Figure 2.2.

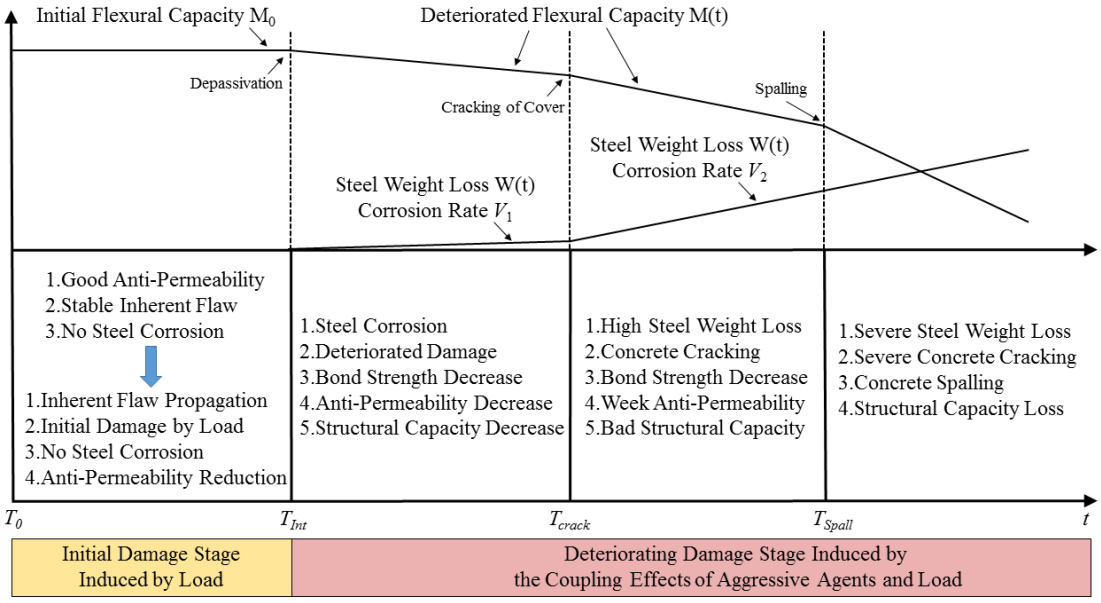

Figure 2.2 Illustration diagram of deterioration process for undersea shield tunnels

2.2.2 Study on durability performance of RC tunnels

In order to ensure undersea tunnel structures to provide an acceptable service for extended periods of time, significant advances have been accomplished in the durability of these tunnel structures. Jin et al. (2013) and Zhang et al. (2016) illustrated the chloride transport process in the concrete linings under the effect of hydrostatic pressure based on the experiments and theoretical model, the results revealed that the high hydrostatic pressure could accelerate chlorides motion in concrete linings. Meanwhile, Liu et al. (2017) presented that the chloride ions could be locally concentrated at the locations around segment joint, and the external reinforcement in segmental linings, especially for the reinforcement close to segment joint, are at high hazard from the corrosion due to the coupling effect of aggressive agent and high hydrostatic pressure.

In terms of the performance assessment of RC undersea tunnels, numerous attempts that use on-site monitoring and the corrosion testing of RC components have focused on the qualitative durability assessment and lifetime prediction of underwater tunnels. In engineering, since it is difficult to confirm steel corrosion status by visual inspection, especially for the corrosion of external reinforcement in segmental linings, Non-destructive testing (NDT) technology has been widely used on the on-site monitoring activities for confirming steel corrosion. By using different types of corrosion sensors, corrosion potential, corrosion rate and volume changes of rebar due to corrosion could be measured to reflect the status of corrosion (Wang et al. 2012). Bigaj et al. (2003) introduced an inspection system used in Green Heart Tunnel in Dutch to provide an early warning for corrosion risk of tunnel linings, and update the predicted service lifetime of tunnel. Gong et al. (2017) presented the on-site steel corrosion data for a subsea tunnel in China, including corrosion current, potential and temperature. The monitoring results revealed that corrosion current and temperature in linings had a cyclic-type variation with

seasonal changing, and the corrosion potentials were widely scattered because of the localized differences in the vicinity of rebar and concrete. Meanwhile, Fagerlund (1995) and Lei et al. (2015) carried out a lifetime prediction of underwater tunnels based on the chloride transport in concrete linings. Kimura et al. (2012) developed a methodology for evaluating and verifying the performance of existing tunnels based on the Analytic Hierarchy Process (AHP). Wang et al. (2016) proposed a maintenance framework for the existing shield tunnel based on the concept of structural life-cycle, and suggested to use the structural performance and life-cycle cost as the major indictors accounting for the structural deterioration performance. In addition, probabilistic methods to evaluate the deterioration of underwater tunnels (Song et al. 2009; Bagnoli et al. 2015) have gradually been reported in recent years.

Significant attentions have also been given to the durability-based design of new RC tunnels, especially for the tunnel structures in a marine environment. In Japan, Kudo and Guo (1994) studied the durability and anti-corrosion properties of a highway shield tunnel that crosses Tokyo Bay with a durability test, and a RC segment using blast furnace slag was recommended to improve the durability of undersea tunnels. In China, Sun (2008, 2011), based on the mechanism of durability degradation of undersea tunnels, proposed a methodology and corresponding testing methods for the durable design of a subsea tunnel in China, and, thus, eleven engineering measures were suggested to improve the durability of tunnel lining structures. Li et al. (2015a & 2015b) established a principle and procedure for the durability design of the Hong Kong-Zhuhai-Macau sea-link project based on the full probability method and a proposed partial factor method.

2.3 Life-cycle performance of deteriorating RC structures

2.3.1 Uncertainties over structural lifetime

The life-cycle performance of structures depends on the time-dependent deterioration

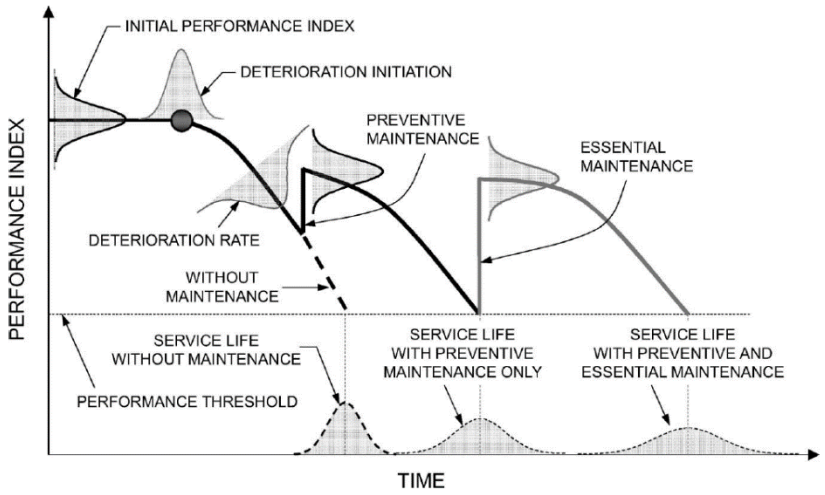

Figure 2.3 Life-cycle performance profile under uncertainties (Frangopol 2011)

effect of damage processes of structural materials and components (Estes and Frangopol 2005). Owing to the coupling effects of multiple mechanical and environmental hazards, the structural deterioration mechanisms are generally complex, and their effects and evolution over time, depending on both the damage mechanisms and type of materials and structures, are difficult to be predicated accurately due to the uncertainties in the real world (Biondini and Frangopol 2016).

As shown in Figure 2.3 proposed by Frangopol (2011), the life-cycle performance profile of structures illustrates that the uncertainties during structural life-cycle are associated with many parameters, and the uncertainties for predicting time-dependent structural performance would increase with time because of the accumulation of uncertainties using prediction models. However, the essential factors for predicting structural service life are strongly affected by the uncertainties from initial performance index, deterioration initiation time and structural deterioration rate (Frangopol 2011 & 2016).

Considering the unavoidable uncertainties when estimating structural performance over their entire life, it is extremely advisable to adopt the probabilistic methods for modelling and analysis of time-dependent structural performance (Ang and Tang 2007).

Based on the probabilistic models of structural performance, uncertainty analysis could facilitate to achieve more accurate prediction results for structural performance, and support the decision-making process to make reliable durability designs for new structures and rational engineering measures for deteriorating existing structures (Biondini and Frangopol 2016).

2.3.2 Life-cycle reliability-based structural performance

(1) Reliability assessment for structural performance

As illustrated previously, because of the uncertainties over structural entire lifetime, time-variant probability-based concepts and methods provide a rational and more scientific approach for estimating the life-cycle performance of a structural system (Ang and Tang 1984, 2007; Frangopol 2011). The failure probability of a structural system during its life-cycle is generally defined as the probability of violating any of the limit state functions that indicate its failure modes. In engineering, the functions of $R=R(t)$ and $S=S(t)$ represent the time-variant resistance and demand of a structural system, respectively, and both of them are regarded as random variables or process with time due to the uncertainties. According to different formats of structural limit state (i.e. safety and serviceability), those two functions could be described as different indictors of structural performance, and the time-variant structural failure probability can be expressed as (Frangopol 2011):

$$P_f(t) = P\big(R(t) < S(t)\big) = \int_0^\infty F_R(x,t) f_S(x,t) dx \tag{2-6}$$

where $F_R(x, t)$ is the (instantaneous) cumulative probability distribution function (CDF) of the resistance; and $f_s(x, t)$ is the (instantaneous) probability distribution function (PDF) of the demand.

Alternatively, structural safety can also be indicated using the time-variant reliability index $\beta(t)$, the relationship between structural failure probability and reliability

Table 2.1 Target reliability index based on ULT in GB 50010-2002

Safety grade	Consequence of failure	Structure category	Reliability Index β	
			Brittle failure	Ductile failure
First	Very Severe	Important	4.2	3.7
Second	Severe	Ordinary	3.7	3.2
Third	Not serious	Secondary	3.2	2.7

Note: Brittle failure is including axial tension and pure bending. Ductile failure is including axial compression, eccentric compression and shear.

Table 2.2 Target reliability for different reference periods in EN1990 (2002)

Reliability classes	Consequence of failure	Reliability Index β		Example
		1 Year	50 Year	
RC3	High	5.2	4.3	Bridges, Public building
RC2	Medium	4.7	3.8	Residences, Office
RC1	Low	4.2	3.3	Agricultural building

index can be expressed as follows (Biondini and Frangopol 2016):

$$\beta(t) = -\Phi^{-1}(P_f(t)) \tag{2-7}$$

where Φ is the cumulative distribution function of the standard normal variable.

(2) Target reliability indices for structural performance

In the structural design, two limit state formats, including ultimate limit state (ULT) and serviceability limit state (SLT), are generally considered. According to different limit state format and consequence of structural failure, target reliability indices, β_{target}, may be different. Table 2.1 indicates the target reliability level for a new structure based on ULT in China (GB 50010-2002), three reliability levels were classified based on the consequence of structural failure, and the reliability indices were given according to structural failure mode. Meanwhile, EN1990 (2002) and *fib* Model Code (2012) proposed a similar reliability classes as shown in Table 2.2, but the detail reliability indices were suggested based on different reference periods. With respect to the SLT, JSCE Standard Specifications (2002) and RILEM (1998) proposed the reliability indices ranging from 1.5 to 2.5 for RC structures.

In recent decades, as the durability of RC structures becomes more and more important, a new category of limit state (i.e. durability limit state) has been introduced. It may be formally regarded as belonging in the SLS (*fib* 2018), *fib* Model Code (2012) recommended the target durability reliability equal to 1.5. Meanwhile, the Code for Durability Design of Concrete Structure of China (2008) indicated that structural damage, like corrosion and cracking, should be controlled under repairable conditions and cannot affect structural bearing capacity, which is different from that in JSCE Code that does not allow structures to have any corrosion during structural lifetime. According to the consequence of structural failure, failure probability of RC structures ranging from 5% to 10% (i.e. β_{target} ranges from 1.282 to 1.645) was suggested to be used in the durability design and assessment of a RC structure in China.

However, target reliability levels in codes are generally used for new structures. For the existing structures, requirements to reach the same target reliability levels with new structures seems to be uneconomical (Sykora et al. 2017), thus an effort to determine the target reliability for existing structures were introduced based on the economic and societal aspects during structural life cycle (Sykora et al. 2017).

2.3.3 On-site inspection for updating structural reliability

As a matter of fact, life-cycle models are very sensitive with the changing of input parameters of random variables (Frangopol 2011; Biondini and Frangopol 2016). Due to the limit information from structural systems or limit knowledge for engineers, time-variant structural performance is generally overestimated or underestimated during structural design phase or service phase as shown in Figure 2.4. In order to reduce the level of uncertainty and support the decision-making process to carry out necessary measures of maintenance and repair for existing structures in time, information obtained from the on-site monitoring are recognized as a useful approach (Frangopol 2011).

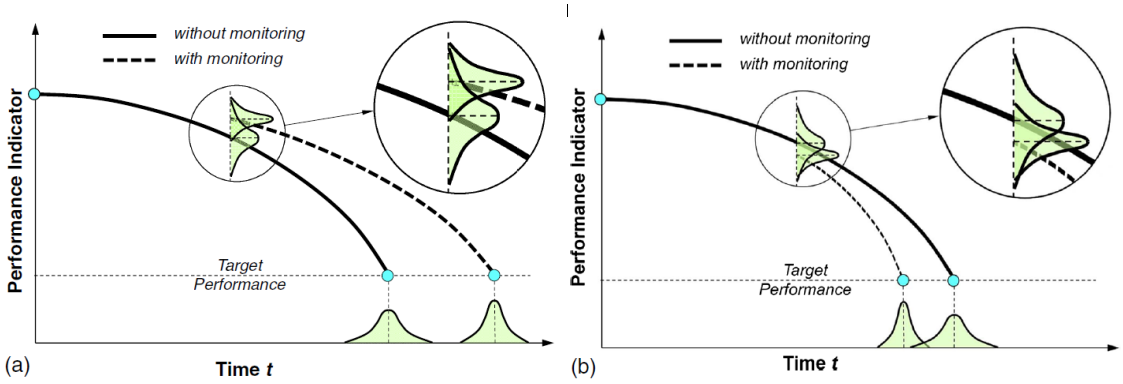

Figure 2.4 Updating structural reliability compared with that without updating (Biondini and Frangopol 2016)

In recent years, multiple attempts have been given to update the prediction functions of existing structures based on inspection data. Frangopol and Strauss (2008a & 2008b) proposed a methodology to develop structural performance function using monitored extreme data and estimate the possible monitoring intervals, then applied them for a bridge using Bayesian updating approach. Akiyama et al. (2010), based on Sequential Monte Carlo Simulation (SMCS), presented a procedure to predicate the reliability of existing structures by updating random variables using observed crack widths and chloride concentration distribution. Oksha et al. (2012) proposed and illustrated an approach for updating structural reliability of an existing bridge based on automated finite element model integrated with monitored strain data. However, there is lack of research on the updating structural performance of existing shield tunnels based on the inspection results.

2.4 Chapter Summary

(1) Steel corrosion in concrete takes place when the passive film on the steel surface is broken down by chloride attack or carbonation, and the critical threshold of corrosion initiation and corrosion rate are associated with multiply impact factors, such as alkaline condition, chloride concentration, temperature, moisture and oxygen, but corrosion of steel bar is just a form of the reaction of iron, water and oxygen.

(2) With respect to the durability of RC tunnel structures in coastal regions, three damage mechanisms were illustrated, including chemical processes, physical processes and mechanical processes. Considering the coupling effects of these three mechanisms on deterioration of RC segmental linings, an illustration diagram for the deteriorating process of RC shield tunnels subjected to the attacks from aggressive agents and high water-soil pressure was presented, including initial damage stage induced by load and deteriorating damage stage induced by the coupling effects of aggressive agents and load.

(3) In term of the research on durability of shield tunnels, the time-dependent performance indicators have not been taken into consideration for the life cycle performance analysis of tunnel structures. Based on the concept of Life Cycle Analysis, it is crucial to apply probabilistic methodology on modeling and analysis of time-dependent structural performance due to the uncertainty over structural lifetime, and inspection information could provide a powerful aid to reduce the level of uncertainty and to improve the accuracy of predictive probabilistic models.

Chapter 3: Life-Cycle Reliability Analysis of Shield Tunnels in Coastal Regions

3.1 Procedure for the life-cycle reliability assessment of shield tunnels in a marine environment

For RC shield tunnels exposed to an aggressive environment, the deteriorative processes that result from aggressive chemical attacks and other physical damage mechanisms put their structural systems at risk. Therefore, the life-cycle performance of structural systems must be considered time-dependent (Ellingwood 2005; Frangopol 2011).

Generally, to accurately assess the deterioration processes of structural systems in different regions, their environmental hazards should first be quantitatively assessed. Then, the damage level of structural systems can be described as a function of the steel weight loss of RC segments. Finally, the time-variant performance of these structural systems can be estimated. All factors that affect structural deterioration are considered, and the basic equations to compute the life-cycle structural performance of shield tunnels in a marine environment are expressed as follows:

(a) Hazard assessment

$$Hazard = g_1\left(C_{soil}\right) = g_{1'}\left(C_{sea}, d\right) \tag{3-1}$$

(b) Damage assessment

$$\rho(t) = g_2\left(Hazard, P_w, m_{RC}, f, t_1, t_2, t\right) \tag{3-2}$$

$$D(t) = g_3\left(f, \rho(t)\right) \tag{3-3}$$

(c) Mechanical performance assessment

$$(M(t), F(t)) = f_1\left(L, EI(t_0), D(t), m_{soil}\right) \tag{3-4}$$

$$M_u(t) = f_2\left(M_u(t_0), \rho(t), F(t)\right) \tag{3-5}$$

where *Hazard* is associated with the chloride concentration, C_{soil}, around the tunnels, which is a function of the chloride concentration of seawater, C_{sea}, and the distance, d, from the coastline to the structures. P_w is the hydrostatic pressure on the tunnels. m_{RC} represents the material properties of the RC segments, including the diameter of rebar (ϕ), the number of rebar (n), the water to cement ratio (W/C) and the concrete cover (c). t_1 and t_2 are the time of corrosion initiation and the corrosion crack occurrence, respectively. $\rho(t)$ is the steel weight loss in time after structural construction, and $D(t)$ is the damage level of the segments in time after structural construction. f is the load level of the segments that is induced by water-soil pressure and/or other loads. L is the Loads that include soil pressure, P_s, and hydrostatic pressure, P_w. m_{soil} represents the material properties of the soil around the tunnel. $EI(t_0)$ is the flexural stiffness of an undamaged segment, $M(t)$ and $F(t)$ are the time-variant bending moment and axial force of segmental linings, respectively. $M_u(t_0)$ is the flexural capacity of no corroded segmental linings, depending on the size of segment section, amount of rebar and axial force. $M_u(t)$ is the flexural capacity of corroded segmental linings.

In addition, because of the uncertainties in the material, and geometric properties, both in the physical models of the deterioration process and in the mechanical and environmental stressors, a measure of the time-variant structural performance is realistically possible only in probabilistic terms. Figure 3.1 illustrates a flowchart that describes the framework to compute the life-cycle reliability of a shield tunnel in a marine environment. When estimating life-cycle reliability based on the flowchart shown in Figure 3.1, a given performance limit state should be considered that relates to the predefined damage level of the RC segmental linings.

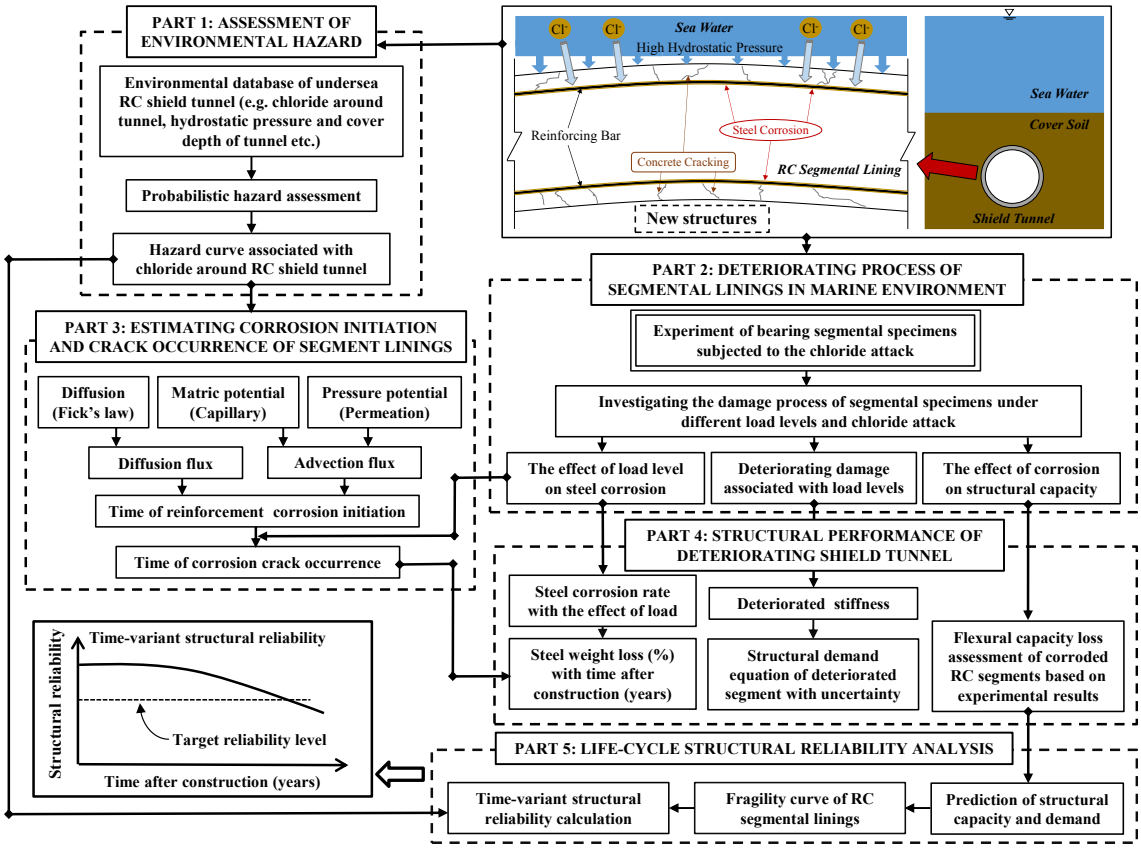

Figure 3.1 Flowchart to estimate the life-cycle reliability of shield tunnels in coastal regions affected by chloride corrosion

This flowchart consists of the following five main parts: (1) defining the process of hazard assessment for underground chloride in a coastal region; (2) investigating the chloride-induced deterioration process of segmental linings in a marine environment to propose an estimation method for a deteriorated damage level of segmental linings and the steel corrosion associated with the load level; (3) estimating the time to corrosion initiation and crack occurrence of the segmental linings with the impact of hydrostatic pressure; (4) proposing an approach to assess the time-variant structural performance of the segmental linings with corrosion-induced deterioration based on parts (2) and (3); and (5) computing the time-variant structural reliability of shield tunnels with an emphasis on corrosion-induced structural performance deterioration.

3.2 Hazard assessment of marine chloride

3.2.1 Attenuation of underground chloride in coastal regions

The deterioration of RC structures is influenced by the local environments where these structures are located. Because different environmental conditions cause RC structures to undergo different deterioration processes, it is necessary to quantitatively assess these environmental conditions. This evaluation of environmental hazards should be reflected in the life-cycle assessments of the RC structures in coastal regions.

For shield tunnels located in coastal regions, it is assumed that the attenuation of underground chloride ions around tunnels, C_{soil} (ppm, i.e., 1 mg/L), only depends on the chloride concentration of coastal waters, C_{sea} (ppm), and the distance d (km) from the coastline to the structures. The observed values from Xiamen (Guo et al. 2004) are used herein to ascertain the attenuation relationship between the underground chloride content, C_{soil}, and the distance from the coastline. There are 18 sites on Xiamen Island to collect data on C_{soil}, and a regression analysis using least squares method to reflect non-linear attenuation trend of coastal hazards associated with chloride was conducted based on Akiyama et al. (2010), as shown in Figure 3.2. Considering the influence of the chloride content in coastal waters, C_{sea}, the attenuation of C_{soil} in the horizontal direction is:

$$C_{soil} = 0.62 \cdot C_{sea} \cdot 0.63^{d} \tag{3-6}$$

Underground environments around a shield tunnel are complex, non-continuous and uncertain. Because the data on underground chlorides in different coastal regions are very limited, it is difficult to consider the influence of geological formations, geotechnical properties around structures, dilution of fresh water on the surface, precipitation, tunnel depth and differences in coastal topography on the content of underground chlorides collected at each location. To consider the uncertainties involved in the prediction of underground chlorides around tunnels, a parameter associated with model error must be

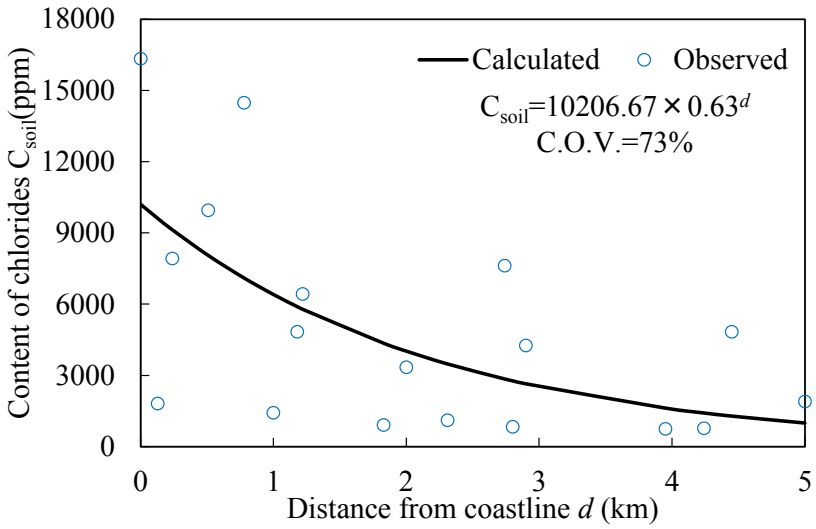

Figure 3.2 Underground chloride content compared with the distance from the coastline in Xiamen

included in the attenuation equations. Meanwhile, if there are more on-site information for underground chloride, uncertainty of prediction model could be reduced, and the accuracy of performance estimation could be improved.

3.2.2 Hazards associated with chlorides around tunnels

Considering model uncertainty, attenuation (Equation 3-6) can be expressed as:

$$C_{soil} = X_R \cdot \left[0.62 \cdot \left(X_S \cdot C_{sea} \right) \cdot 0.63^d \right] \tag{3-7}$$

where X_R is a lognormal random variable that relates to the estimation of the chloride content in the soil, and X_S is a normal random variable associated with the marine chloride content in different coastal regions.

The probability that C_{soil} at a specific site exceeds an assigned value, c_{soil}, is described as follows:

$$q(c_{soil}) = P(C_{soil} > c_{soil}) = \int_0^\infty P(X_R > \frac{c_{soil}}{0.62 \cdot X_S C_{sea} \cdot 0.63^d}) f(x_S) dx_S \tag{3-8}$$

where $f(x_S)$ is the probability density function of X_S.

The hazard curves for the tunnel structures in different cities that were obtained with Equation 3-8 are shown in Figure 3.3. The assigned value of c_{soil} ranges from 0 to

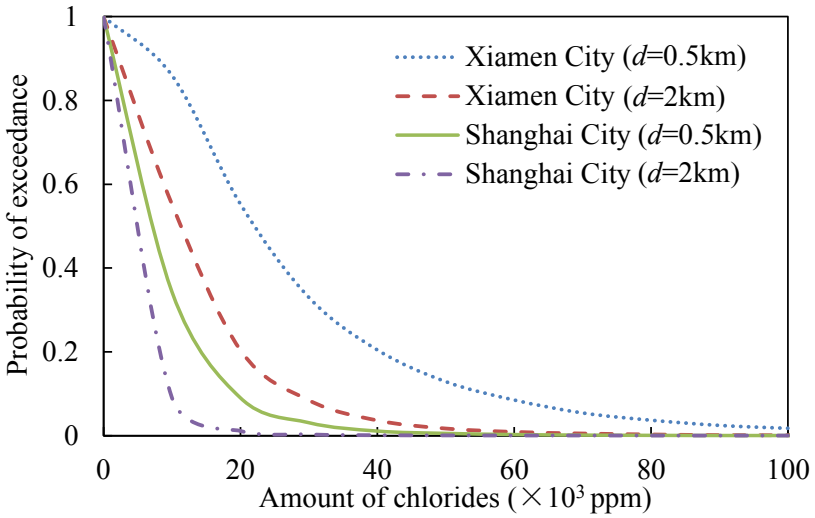

Figure 3.3 Hazard curves for the underground chloride content at two coastal cities with a distance of 0.5 km and 2 km from the coastline

100,000 ppm; X_S for Xiamen city is a normal random variable with a mean value of 1.0 and coefficient of variation (C.O.V.) of 0.043, and X_S for Shanghai is a normal random variable with a mean value of 1.0 and C.O.V. of 0.155.

3.3 Structural damage process of shield tunnels due to reinforcement corrosion

3.3.1 Deteriorating experimental programme of segmental specimens

3.3.1.1 Overview of experimental plan

An experimental plan was established to characterize the deterioration of a load-bearing segmental lining in an aggressive environment. Because of the difficulty of using a prototype segment under a loading to conduct an electrolytic experimental test, a simplified segmental specimen (see Figure 3.4) was designed based on the segmental linings in the shield tunnel of the Xiamen Metro Line No. 2 Project (see Figure 3.5) (Sun 2011; Liu et al. 2015). As shown in Figure 3.4, the specimen is 1360 mm long, whereas the experimental zone is 660 mm long. For each specimen, the cross section is 290 mm × 350 mm in the middle region and 290 mm × 600 mm in both end regions.

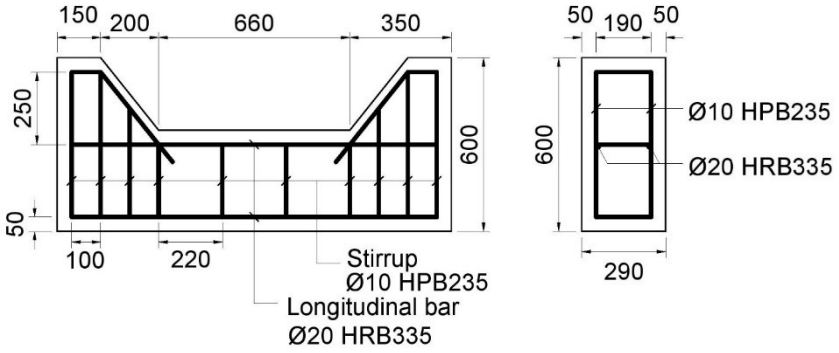

Figure 3.4 Simplified segmental specimen (dimensions are in mm)

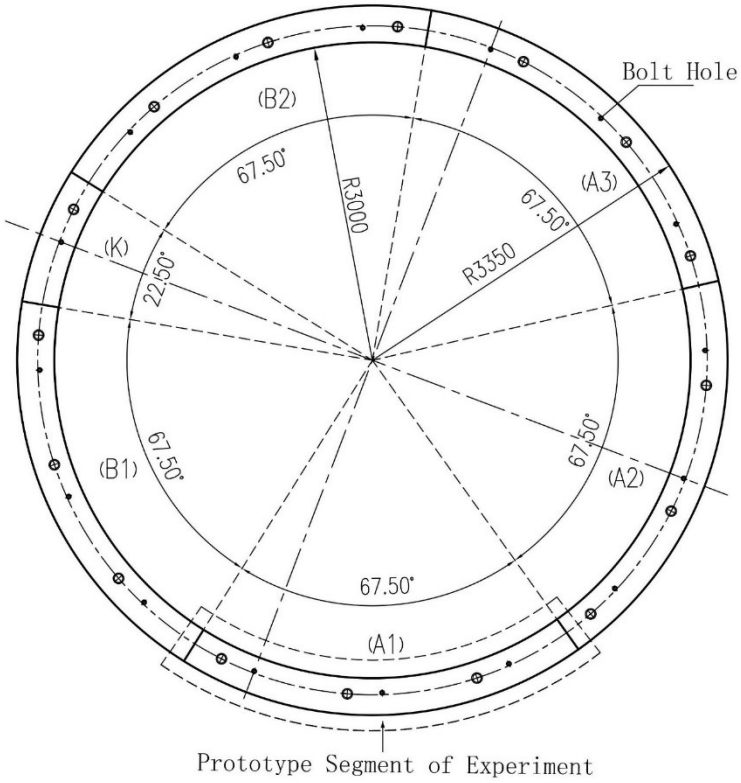

Figure 3.5 Segmental lining of the shield tunnel

To study the deterioration processes of segmental linings under different load levels and determine how the mechanical performance of the segmental lining deteriorates, five groups of two segmental specimens (F1, F2, F3, F4 and F0) were designated in the experiments. Groups F1, F2 and F3 were corrosion-accelerated specimens without cracking, with a small number of cracks, and with severe cracking, respectively. F4 was a control group of corrosion-accelerated specimens without loading. F0 was also a control group used to determine the ultimate bearing capacity without corrosion. Moreover, three

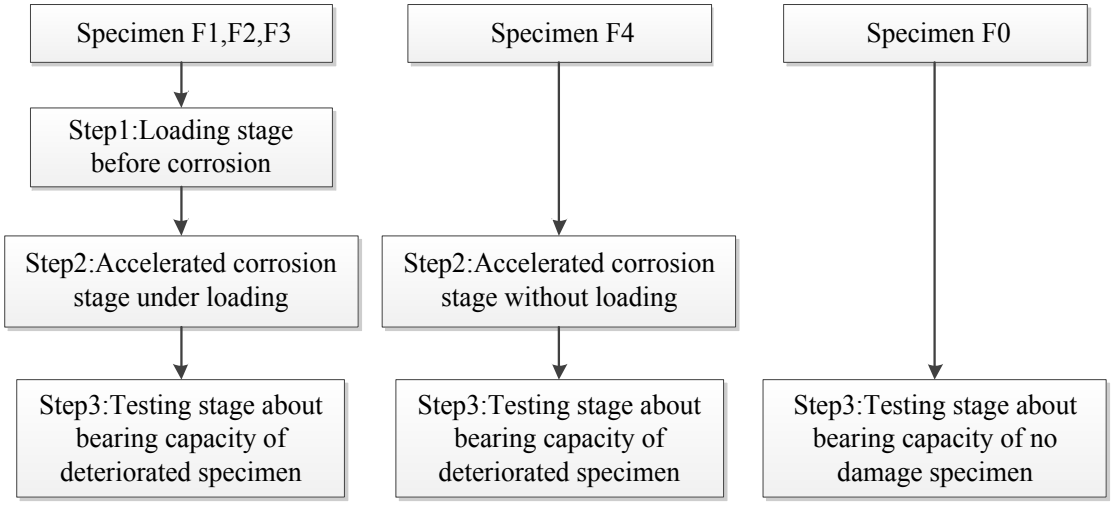

Figure 3.6 Experimental process of the specimens in each group

different stages were considered in the experiment, as indicated in Figure 3.6. During the testing process, a specified load was provided during the first stage (Step 1), which enabled the specimens to be tested under different load levels. In the second stage, the load level of the specimens remained constant, and an accelerated corrosion test was conducted (Step 2). Finally, in the third stage, an ultimate limit load was provided to cause the deteriorated specimens to fail (Step 3).

3.3.1.2 Material and fabrication of specimens

All specimens were fabricated using identical material constituents. The concrete used in the specimens had a compressive strength of 32.5 MPa and a tensile strength of 2.65 MPa. Portland cement, sand and gravel with a maximum aggregate size of 25 mm were used. The proportions of cement: sand: gravel by weight were determined as 1:1.34:3.28 with a water-to-cement (W/C) ratio of 0.37 in the concrete mix design. Four deformed bars (two tensile bars and two compressive bars), each with a diameter of 22 mm, were used as longitudinal bars. The reinforcement grade was HRB335 (i.e., hot-rolled ribbed-steel bar), which has a yield strength of 335 MPa. The diameter of the stirrups was 10 mm, and the steel grade was HPB235 (i.e., hot-rolled plain-steel bar), which has a yield strength

Table 3.1 Material parameters of the rebar

Material	Diameter (mm)	Yield Strength (MPa)	Ultimate Strength (MPa)	Modulus of Elasticity (GPa)	Elongation (%)
HPB235	10	235	370	210	25
HRB335	22	335	455	200	16

of 235 MPa. The material parameters of the rebar are provided in Table 3.1. To improve the experimental efficiency, a sodium chloride (NaCl) solution with a chloride concentration of 2% was added into the concrete during mixing.

3.3.1.3 Deteriorating experimental procedure

To achieve the combined effects of loads and corrosive agents on the segmental specimens, a loading jack and electrical corrosion technique were applied in the experiments. As shown in Figure 3.7, loads were placed on both ends of the segmental specimens using the loading jack, which caused the specimen to be subjected to the combined effects of an axial force and a bearing moment. Then, a NaCl solution pool with a chloride content of 20% was placed on the top surface to corrode the tensile rebar, as indicated in Figure 3.7 (a). Subsequently, the steel corrosion process was initiated using an electrolytic technique and the corrosion process continued for 22 days.

3.3.1.4 Failure mode of the segmental specimens under different deterioration states

The corrosion products expand and cause corrosion-induced cracking when the resulting tensile stress in the surrounding concrete reaches its tensile strength limit. Moreover, the corrosion-induced cracking patterns of the segmental specimens in each group are different because of the effects of the load level. For unloaded specimen F4, corrosion-induced cracks along the direction of the rebar occurred in the cover concrete, and as the corrosion developed, the longitudinal cracks became interconnected and grew wider. Finally, the maximum crack width of specimen F4, which was measured by the crack

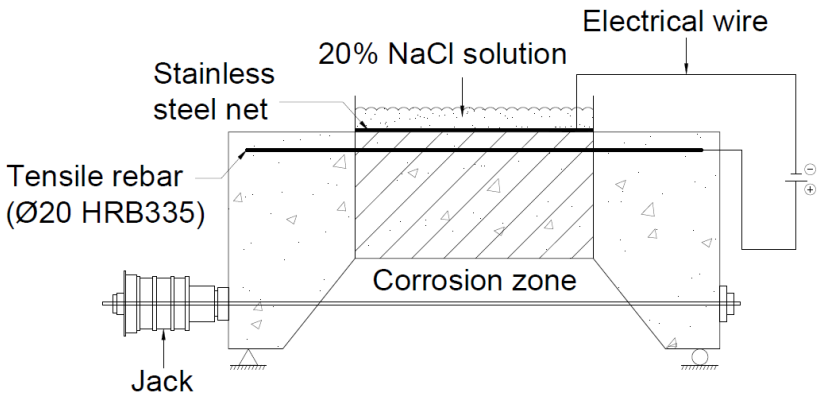

(a)

(b)

Figure 3.7 (a) Schematic diagram of an experimental corrosion specimen and (b) photograph of the experimental setup for the bearing specimens

scale, was approximately 2.2 mm.

For bearing specimens F1, F2 and F3, with initial load-induced crack widths of 0 mm, 0.2 mm and 0.45 mm, respectively, segmented corrosion-induced cracks along the direction of the rebar occurred primarily between the tensile cracks in the cover concrete. As the steel weight loss increased, the corrosion-induced cracks became interconnected with tensile cracks and propagated together. For example, the tensile crack widths on the top surface of specimen F3 near the location of the maximum bending moment ranged from 2.1 mm to 2.6 mm.

Because cracking propagation induces further degradation of the steel-concrete interface and exposes more of the steel surface to corrosive agents, a higher loading level

(a)

(b)

(c)

Figure 3.8 Failure modes of specimens (a) without corrosion (F0); (b) corrosion without cracks (F1); and (c) corrosion with cracks (F3)

led to greater steel weight loss and more severe cracking. Considering that different deteriorated states of specimens might lead to different failure modes, after corrosion testing of the segmental specimens, the load acting on the specimens was increased, and

the failure modes of the segmental specimens under differently deteriorated states were identified as shown in Figure 3.8.

For the non-corrosion specimens, F0, Figure 3.8(a) shows that the tensile cracks propagated a substantial distance in the tensile zone of each specimen, and the largest crack occurred at the mid-span; moreover, the concrete was crushed in the compressive zone of each specimen. As shown in Figure 3.8(b), specimens F1 and F4, which did not exhibit significant degrees of corrosion, exhibited larger tensile cracks than specimen F0, and the two largest failure cracks appeared at the mid-span. Finally, Figure 3.8(c) shows that specimens F2 and F3, which had more steel weight loss, exhibited interconnected failure cracks and spalling of the cover concrete.

3.3.2 Damage definition of segmental linings

The life-cycle structural performance of a RC shield tunnel is influenced by three factors: environmental stressors, service time (t), and the provided load level (f). Because the RC segmental linings are subjected to chemical-physical damage, the structural and material performance will deteriorate and the structural stiffness will decrease with time after construction. As the structural stiffness decreases, deformation of the segmental linings will increase significantly. This can be regarded as a macroscopic phenomenon of structural deterioration. Moreover, structural deformation is an important part of the on-site monitoring of a tunnel structure. Therefore, a damage index denoted by the level of deformation facilitates assessments of the level of deterioration in a tunnel structure.

Based on the stiffness damage theory reported in Liu (2011), a damage index of segmental specimens is defined as:

$$D = 1 - \frac{E'I'}{E_0 I_0} \tag{3-9}$$

where $E'I'$ and E_0I_0 are the residual stiffness and initial stiffness of the specimen, respectively.

Thus, according to the relationship between the displacement at the mid-span and the stiffness of the beam is:

$$u=\frac{Ml^2}{8EI} \tag{3-10}$$

Therefore, Equation 3-9 can also be expressed as:

$$D=1-\frac{M'u_e}{M_e u'} \tag{3-11}$$

where M' is the bending moment of the specimen; u' is the displacement of the damaged specimen, which can be measured experimentally; M_e and u_e are the bending moment at the elastic limit of the specimen and its corresponding displacement, respectively; and D is the damage value of the segmental specimen.

Furthermore, the specimen damage is expressed by D_0, D_1 and D_2 according to the testing stage. D_0 is the initial damage induced by loading during the first stage (i.e., loading stage before corrosion), and D_1 and D_2 are the total damages of the specimens during the second stage (i.e., accelerated corrosion stage) and third stage (i.e., loading stage after corrosion), respectively. In particular, the second stage D_1 contains the initial damage D_0 and deteriorating damage Δd. Therefore, D_1 is expressed as follows:

$$D_1 = D_0 + \Delta d \tag{3-12}$$

where Δd is the damage increment of the specimen induced by the combined effects of loading and corrosion during the accelerated corrosion stage.

3.3.3 Damage evolution of the segmental specimens

Based on the damage equation for the segmental specimens (Equation 3-11), the damage value D_0, D_1 and D_2 of the specimens in each group can be derived from the measured displacement value u' of the specimens. The damage curves for the five groups of specimens at all loading stages are shown in Figures 3.9, 3.10 and 3.11.

These figures show that for the specimens with higher load levels (e.g., specimens

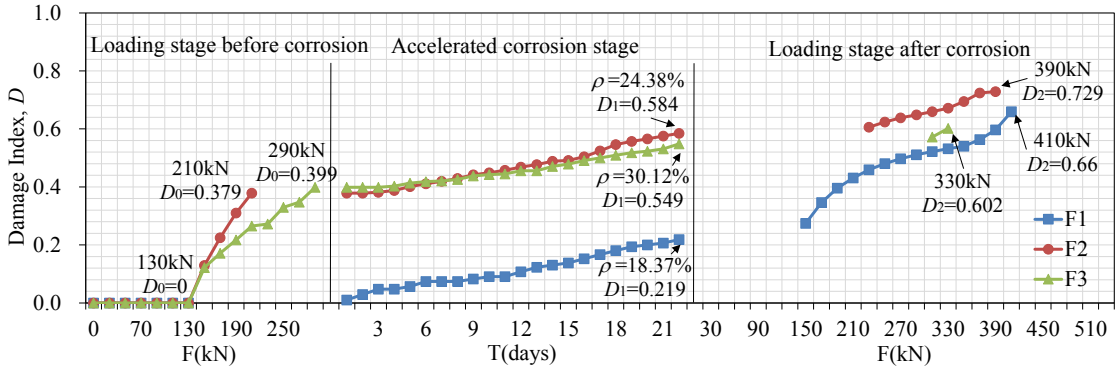

Figure 3.9 Damage index curves of specimens under different load levels (F1-F3)

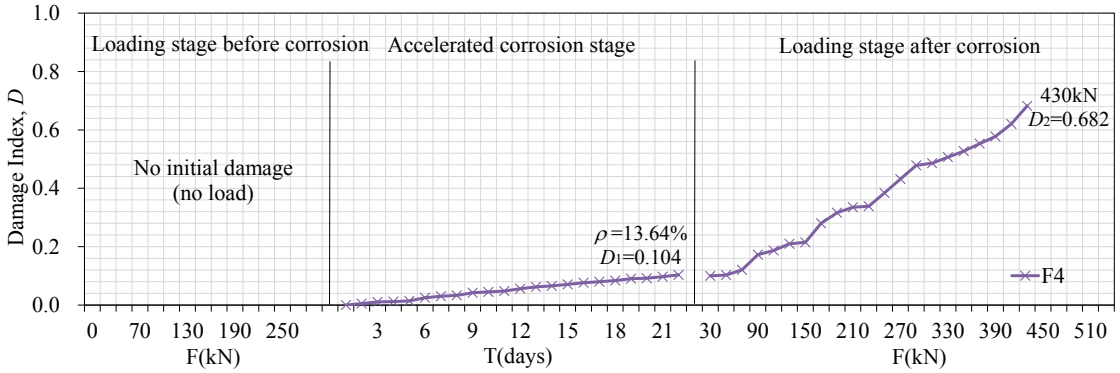

Figure 3.10 Damage index curve of the specimen without initial damage (F4)

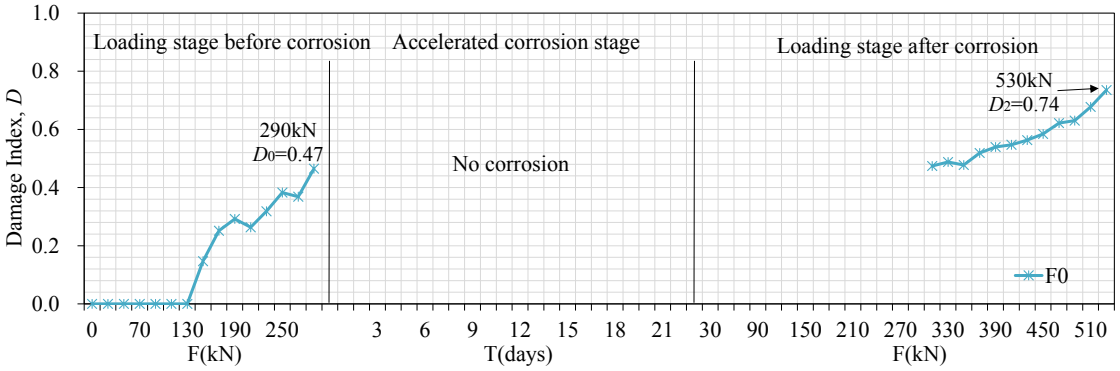

Figure 3.11 Damage index curve of the specimen without corrosion (F0)

F2 and F3), the initial damage occurred before the corrosion began. However, specimens F1 and F4 remained in an undamaged state and cracking did not occur before the corrosion began. Thus, with the development of steel corrosion, the damage of specimens increased linearly with time. In addition, the ingress of chloride was accelerated because of the effect of the load, which led to a higher corrosion rate with increases in the load levels during corrosion testing. Finally, at the end of the corrosion test, the measured ultimate steel weight losses were 18%, 24% 30% and 14% for specimens F1, F2, F3, and

F4, respectively.

With respect to the ultimate bearing capacity of the deteriorating specimens, the ultimate bearing capacity of the specimens showed greater decreases when the steel weight losses were higher. As shown in Figures 3.9, 3.10 and 3.11, the ultimate bearing capacities of specimens F1, F2, F3 and F4 decreased by 23%, 26%, 38% and 18%, respectively.

Finally, in terms of the ultimate damage value of the specimens, flexural failure occurred when the loading reached the ultimate load of the deteriorating specimen. However, because the failure specimen still had a slight residual stiffness, *E'I'* was greater than zero and the ultimate damage value from Equation 3.9 was less than one.

3.3.4 Damage modeling for the segmental specimens

3.3.4.1 Initial damage under load

Because of the construction load, ground load and high soil-water pressure, concrete cracking of segmental linings may have occurred at the beginning of service time, which indicates that the structural damage occurs. In particular, when the concrete cracks occur at the tension zone of the segmental linings, it is harmful to the long-term structural performance of shield tunnels. With respect to a shield tunnel in an aggressive environment, the damage induced by loads before structural deterioration initiation is regarded as the initial damage D_0. To perform a long-term structural performance assessment of shield tunnels in an aggressive environment, the initial damage must first be estimated.

According to a regression analysis for the experimental results on specimens F0 for loading without corrosion, the relationship between the damage D_0 caused by the load and load level f is:

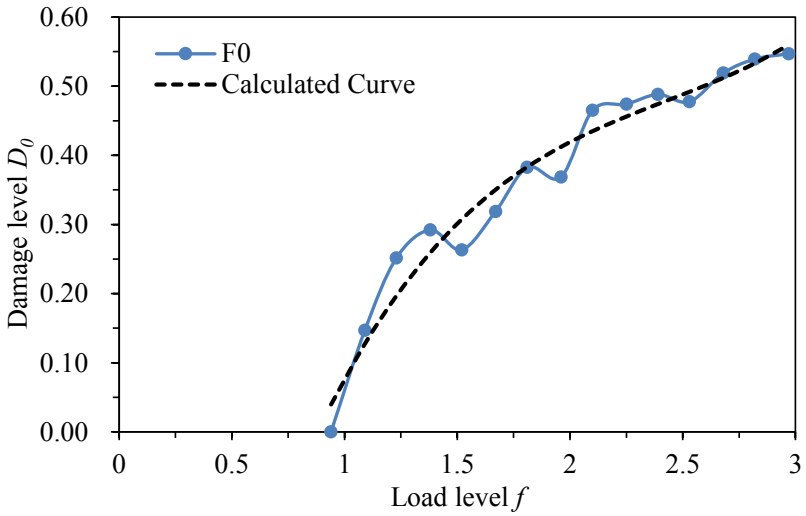

Figure 3.12 Damage associated with the load level

$$D_0 = \begin{cases} 0, & 0 \le f < 0.94 \\ 0.077f^3 - 0.559f^2 + 1.482f - 0.923, & 0.94 \le f \le 3 \end{cases} \tag{3-13}$$

$$f = \frac{\sigma}{\sigma_t} = \frac{E_0 \varepsilon}{\sigma_t} = \left(\frac{M \cdot y_s}{I} - \frac{F}{A_c} \right) \Big/ \sigma_t \tag{3-14}$$

where σ and ε are the average stress and average strain on the positions of the rebar in the RC, respectively; E_0 is the elastic modulus of the RC; σ_t is the equivalent cracking stress of the RC; y_s is the distance from the rebar position to the neutral axis of the specimen; I is the moment of inertia of the specimen; and A_c is the cross-sectional area of the specimen.

As shown in Figure 3.12, the calculated curve can appropriately reflect the damage growth trend with an increase in load level. When the load exceeds the elastic limit of RC member (f = 0.94), crack initiation and propagation lead to damage accumulation in segmental specimens. With an increase in load level, the increase in damage tends to be slow and gradual. However, in term of the shield tunnels, the bending moment, M and axial force, F in Equation 3-14 vary from case to case, depending on the structural shape and loading condition, segmental linings will yield at different value of load level, f.

3.3.4.2 Deteriorating damage due to coupling effects

Table 3.2 Deteriorating damage Δd and steel weight loss ρ (%) of the segmental specimens

Experimental Time/days		0	3	6	9	12	15	18	22
F1	Deteriorating Damage, Δd	0	0.048	0.074	0.083	0.107	0.138	0.180	0.219
	Steel Weight Loss, ρ	0	6.42	9.42	13.74	15.67	16.54	17.54	18.37
F2	Deteriorating Damage, Δd	0	0.004	0.033	0.064	0.090	0.113	0.168	0.206
	Steel Weight Loss, ρ	0	8.87	12.73	16.11	19.36	20.9	22.74	24.38
F3	Deteriorating Damage, Δd	0	0.001	0.020	0.040	0.058	0.081	0.111	0.151
	Steel Weight Loss, ρ	0	11.21	16.85	20.11	23.18	25.94	27.53	30.12
F4	Deteriorating Damage, Δd	0	0.012	0.030	0.045	0.062	0.077	0.090	0.111
	Steel Weight Loss, ρ	0	3.61	7.49	9.97	10.99	11.78	12.5	13.64

The deteriorating deformation u_t is regarded as a macroscopic phenomenon for the damage of the segmental lining's stiffness, and it is typically determined by the load level f of the segmental linings and the steel weight loss. Therefore, the function of displacement can be expressed as $u_t=u_t(f, \rho)$. Immediately after tunnel construction, the rebar is not corroded and $\rho = 0$; thus, the structure presents only the loading damage D_0. Since corrosive agents and high water-soil pressure affect the segmental linings, the deteriorating damage Δd accumulates gradually. As a result, the deteriorating damage Δd is a function of the load level f and the steel weight loss ρ as follows:

$$\Delta d = D_1 - D_0 = g(f, \rho) \tag{3-15}$$

According to the Liu et al. (2015) that experimentally investigated the relationship between steel weight loss and accelerated corrosion time, the details of deteriorating damage and steel weight loss are shown in Table 3.2.

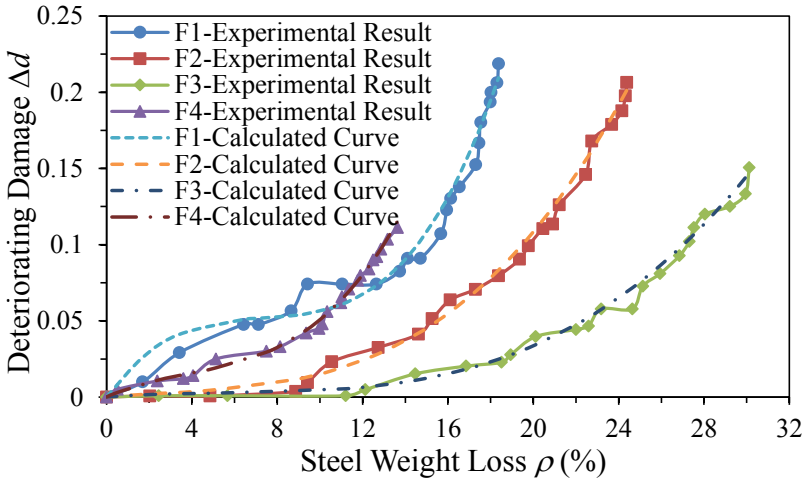

Figure 3.13 Deteriorating damage associated with steel weight loss under different load levels

Based on this Table, a deteriorating damage formula for a segmental specimen as denoted by steel weight loss and load level can be expressed as:

$$\Delta d = (A\rho^2 + B\rho + C)\rho \tag{3-16}$$

where A, B and C are influence coefficients given by regression analysis.

For the specimens without initial cracks subjected to corrosion, the value of f ranges from 0 to 0.94, and A, B and C can be expressed as:

$$\begin{aligned} A &= 36.2f + 76.6 \\ B &= -(16.7f + 8.9) \\ C &= 1.6f + 0.94 \end{aligned} \tag{3-17}$$

For the specimens with initial cracks subjected to corrosion, the value of f ranges from 0.94 to 2.07, and A, B and C can be expressed as:

$$\begin{aligned} A &= 125.7f^2 - 469.4f + 440.8 \\ B &= -(34.5f^2 - 124.7f + 111.3) \\ C &= 2.6f^2 - 9.6f + 8.6 \end{aligned} \tag{3-18}$$

The experimental results for the relationships between the deteriorating damage and steel weight loss of the segmental specimen under different load levels are shown in Figure 3.13.

This figure reveals that a higher loading level led to greater steel weight loss and

severe cracks accelerated the rebar corrosion process. However, the effect of rebar corrosion on the deteriorating damage of specimens with a higher loading level (i.e. more cracks induced by loading before corrosion) decreased. The reason for this is that more corrosive rust ran away through severe cracks with NaCl solution in the experiment, resulting in slower corrosion-induced cracking propagation and deteriorating damage. As shown in Figure 3.13, the calculated value matches the experimental results well and can accurately reflect the deteriorating damage process.

In terms of the life-cycle structural performance of an underwater shield tunnel, the use of Equations 3-16 to 3-18 represents a new approach for assessing the life-cycle structural performance of an underwater tunnel in an aggressive environment. By considering the load level and steel weight loss at different sections of the segmental linings, the deteriorating damage level of a tunnel structure can be estimated using Equations 3-16 to 3-18. Based on the deteriorating damage value of a segmental lining, the stiffness of an aging tunnel structure can be obtained and applied to the mechanical performance estimation. However, since bending moment, M, and axial force, F, of shield tunnel depend on the design conditions, segmental linings may deteriorate under higher load level, f. Meanwhile, due to the complexity of aggressive environment around tunnels, reinforcement in segment may suffer from higher steel weight loss during structural lifetime.

3.3.5 Steel corrosion associated with load level

The corrosion process of rebar for experimental specimen is normally a dynamic process in which the diffusion distances of corrosive agents increase along with the thickness of the rust layer, which causes the rate of steel corrosion to decrease (Liu and Weyers 1998a; Bhargava et al. 2006). Therefore, the rate of steel weight loss may not follow a simple linear model based on a steady state corrosion process. For uniform corrosion, the

thickness of the rust layer is proportional to the total mass of rust per unit length of the corroding bar (W_r), and the growth of rust products is given as (Liu and Weyers, 1998b)

$$\frac{dW_r}{dt} = \frac{k_p}{W_r} \tag{3-19}$$

where k_p is related to the rate of steel weight loss as $k_p = A_p \pi D_0 i_{cor}$ (Bhargava et al., 2006); i_{cor} is the annual mean corrosion rate (μA/cm^2); D_0 is the original diameter of rebar (mm); and t is presented in years.

Similarly, the relationship between the amount of steel weight loss W_s (mg/mm) per unit length and the amount of rust W_r (mg/mm) is expressed as (Bhargava et al. 2006).

$$W_s = \alpha W_r \tag{3-20}$$

By combining Equations 19 and 20, the steel weight loss rate dW_s/dt can be obtained as follows:

$$\frac{dW_s}{dt} = \frac{\alpha^2 A_p \pi D_0 i_{cor}}{W_s} \tag{3-21}$$

where the parameters α and A_p are related to the corrosion process and the amount of rust generated, respectively (Faroz et al., 2016). An estimate of these constants was given by Bhargava et al. (2006) based on the experimental evaluation by Liu (1996), and A_p=2.49 and α=0.613.

According to the experimental results, the steel corrosion rates of segmental specimens under different load levels determined using Equation 3-21 are shown in Figure 3.14. Figure 3.14 shows that the steel corrosion rates of segmental specimens tend to decrease with time, which is consistent with the results of Liu and Weyers (1998b). Besides, the average steel corrosion rate of segmental specimens increases with the loading according to Figures 3.13 and 3.14. Considering the effect of a load on the steel corrosion rate, Equation 3-21 becomes:

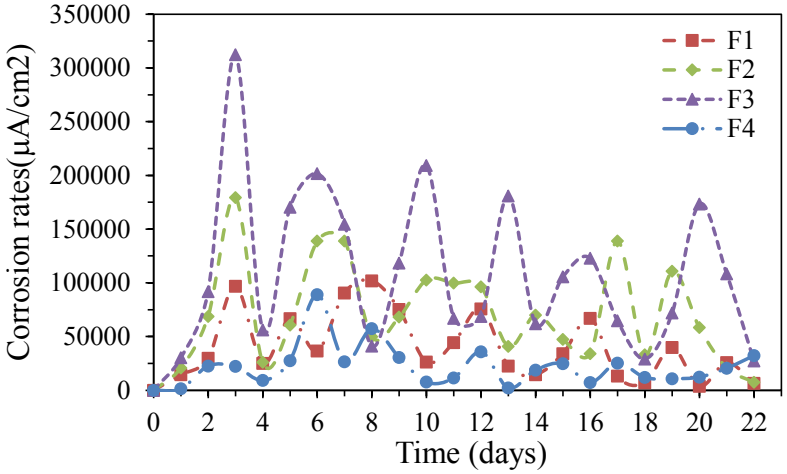

Figure 3. 14 Steel corrosion rate of RC

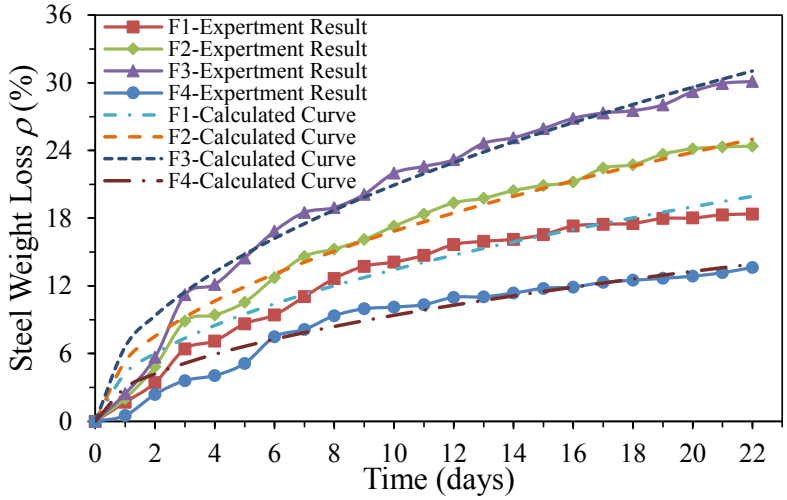

Figure 3.15 Steel weight loss associated with time

$$\frac{dW_s}{dt} = \frac{\alpha^2 A_p \beta_f \pi D_0 i_0}{W_s} \tag{3-22}$$

where the loading coefficient based on regression analysis is $\beta_f = 0.961e^{0.774f}$ and i_0 is the annual mean corrosion rate without considering the load effect.

For a constant corrosion rate, the time-variant amount of steel weight loss model W_s (mg/mm) considering the load effect can be derived based on Equation 3-22 as follows:

$$W_s = 2.375e^{0.387f}\sqrt{D_0 i_0 t} \tag{3-23}$$

$$\xi_c = e^{0.387 f} \tag{3-24}$$

where ξ_c is the influence coefficient of load level on steel corrosion.

Finally, the estimated values of the steel weight loss determined using Equation 3-23 and the average rebar corrosion rate for segmental specimens are shown in Figure 3.15. As shown in this figure, the calculated values are consistent with the experimental results.

3.4 Time-variant structural performance assessment of shield tunnel in a marine environment

3.4.1 Evaluation of corrosion initiation and crack occurrence

3.4.1.1 Chloride transportation in segmental linings under hydrostatic pressure

Until recently, researchers (Chen et al. 2008; Song et al. 2009 & Sun 2011) have estimated the life-cycle performance of undersea tunnels by only considering the diffusion of the chloride ions in RC linings. Fick's diffusion law has been adopted to predict the lifetime of undersea tunnels. However, because of the effect of high hydrostatic pressure on the tunnels, these structures withstand a large water pressure gradient between their inside and outside walls. Chloride motion in the linings is associated with external water pressure, as proven by experimental results (Van der wegen et al. 1993; Jin et al. 2013 & Zhang et al. 2015, 2016).

Therefore, considering the impact of hydrostatic pressure and the water environment, it is currently thought that the coupled effects of diffusion and advection drive chloride motion. The diffusion results in the transportation of chloride ions from a region of high ion concentration to a region of lower ion concentration. Meanwhile, advection transports ions with the bulk motion of the carrier fluid, including the matric potential (i.e., capillary) and pressure potential (i.e., permeation).

Chloride transportation in concrete is assumed to act under steady-state conditions. Therefore, a diffusion flux of free chloride ions by using Fick's 1st diffusion law is usually applied:

$$J_d = -D\nabla C_f \tag{3-25}$$

where J_d is the diffusion flux of free chloride ions, kg/(m^2·s); D is the chloride diffusion coefficient of concrete, m^2/s; ∇ is the nabla operator; and C_f is the volume concentration of free chloride dissolved in the pore solution, kg/m^3. In particular, the negative sign in Equation 3-25 indicates that diffusion occurs with the concentration reduction.

The advective flux can be expressed as:

$$J_a = C_f u \tag{3-26}$$

where J_a is the advective flux of free chloride ions, kg/(m^2·s); and u is the average velocity of chloride, m/s.

Therefore, the total flux of free chloride ions is described as follows:

$$J_{cl} = J_d + J_a \tag{3-27}$$

Based on the mass conservation law of chloride ions, the governing differential equation of chloride movement is:

$$\frac{\partial C_f}{\partial t} + \nabla J_{cl} = \frac{\partial C_f}{\partial t} + \nabla(uC_f - D\nabla C_f) = 0 \tag{3-28}$$

$$\frac{\partial C_f}{\partial t} = D\frac{\partial^2 C_f}{\partial x^2} - u\frac{\partial C_f}{\partial x} \tag{3-29}$$

With respect to Equation 3-29, Ogata and Banks (1961) presented an analytical solution for saturated concrete, described as:

$$C(x,t) = \frac{C_s}{2}\left[erf\left(\frac{x-ut}{\sqrt{4Dt}}\right) + e^{\frac{ux}{D}} erfc\left(\frac{x+ut}{\sqrt{4Dt}}\right)\right] \tag{3-30}$$

where for shield tunnel structures, x is the depth from the outside wall of the linings, mm; t is the time after structural construction in years; C_s is the chloride content at the surface,

kg/m^3; u is the average velocity of the chloride motion, mm/year; D is the chloride ion transportation coefficient in concrete, mm^2/year; *erfc* (·) is the complementary error function, *erfc*(·) = 1 − *erf* (·); and *erf* (·) is the error function.

A one-dimensional flow that seeps through concrete under pressure is regarded as a laminar flow. Thus, the velocity equation of a pressurized seeping flow is described based on Darcy's Law as follows (Murata et al. 2004 & Yoo et al. 2011):

$$u_w = -K_S \nabla H = -\frac{K_S}{\rho_w g} \nabla P_w \tag{3-31}$$

where u_w is the flow velocity of liquid, mm/year; K_s is the permeability coefficient, mm/year; H is the hydraulic head, m; ρ_w is the water density, kg/m^3; and P_w is the hydraulic pressure of the flow path, MPa.

According to Equation 3-31, Murata et al. (2004) proposed two methods to evaluate the watertight properties of concrete and the average penetration depth of water under different water pressures over time. For the Darcy seepage flow (Murata et al. 2004), since the external water pressure, P_w, is less than 0.15 MPa, the Darcy flow velocity is constant over time and space, and the hydraulic gradient becomes linear. The penetration depth of water χ (mm) by using the Darcy seepage model is

$$\chi = \sqrt{\frac{2K_s P_w}{\rho_w g} t} \tag{3-32}$$

For the seepage diffusive flow (Murata et al. 2004), the external water pressure, P_w, is larger than 0.15 MPa. As the internal deformation induced by high water pressure becomes significant, the flow velocity and hydraulic gradient vary over time and space. Thus, the penetration depth of water χ (mm) is described by using a high-pressure seepage model as:

$$\chi = \sqrt{4\frac{\gamma_0^2 \xi^2}{\alpha} t} \tag{3-33}$$

where ξ is the coefficient of water pressure, mm^2/year; and $\xi = 0.4104 \ln(P_w) + 0.995$. α is a correction factor for pressurized time (i.e., $\alpha = (365\times24\times60^2\times t)^{3/7}$), and t is pressurized time in years. γ^2_0 is the initial diffusion coefficient, mm^2/year; and $\gamma^2_0 = (K_s K_v) / (\rho_w g)$. K_v is the volumetric modulus of elasticity when considering the substances of water and concrete, expressed as $1/K_v = v / K_c + (1-v) / K_w$. K_c is the volumetric modulus of elasticity of a concrete body, K_w is the volumetric modulus of the elasticity of water, and v is the volumetric ratio of concrete body.

Because the size of a chloride ion is much smaller than the size of a water molecule, the permeation speed of a chloride ion is much slower than the permeation speed of water in concrete, and the transportation velocity of a chloride ion is approximately 53% that of water (Jin et al. 2013). The average flow velocity of a chloride ion under water pressure is

$$u = 0.53\,\chi / t \tag{3-34}$$

In particular, when the external water pressure, P_w, is very low (i.e., u is close to zero), the advection process of chloride can be ignored. Therefore, Equation 3-30 can be simplified as

$$C(x,t) = C_s\left[1 - erf\left(\frac{x}{\sqrt{4Dt}}\right)\right] \tag{3-35}$$

which is the diffusion equation of chloride based on Fick's second law.

An experimental results from Jin et al. (2013) reporting the chloride transport of concrete under hydrodynamic pressure are adopted herein to verify this proposed model. Figures 3.16 (a) and (b) depict the chloride transport under a hydrostatic pressure of 0.2 MPa in a concrete with a water-to-cement (W/C) ratio of 0.53, and the estimated results of chloride distribution obtained using Equations 3-30 to 3-34 are compared with the experimental results at time of 24 h and 480 h, respectively. As shown in figures, the

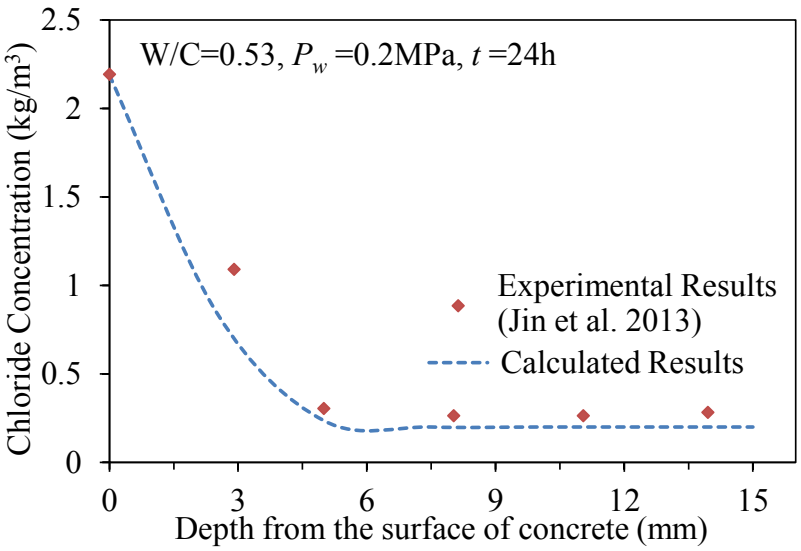

(a)

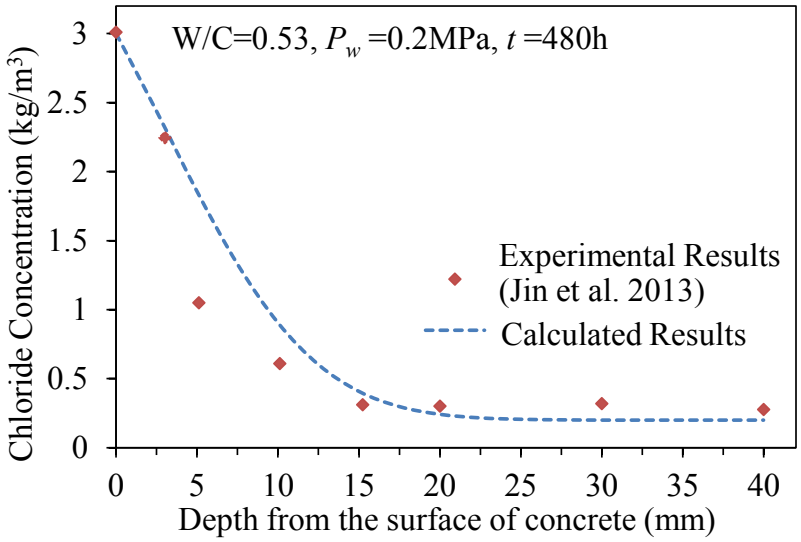

(b)

Figure 3.16 Chloride concentration distribution of concrete under the hydrostatic pressure of 0.2 MPa at (a) 24 h and (b) 480 h

proposed method provides good agreement with the experimental results.

Furthermore, according to an review about permeability of concrete (Hoseini et al. 2009), when the crack width is less than 0.2 mm, the permeability of chloride and water has not obvious change compared with that in un-cracked concrete. In engineering, the crack width of segmental linings due to load has a strict limit, it should be less than 0.2 mm; meanwhile, because of the influence of high water pressure, tensile stress in the

outside wall of segmental linings is very low, and compressive stress generally plays more significant role in the outside wall of segmental linings. Therefore, in term of effect of load-induced cracks on the diffusion of chloride, it has not been taken into consideration in this study.

3.4.1.2 Reinforcement corrosion initiation

The degree of contact with a chloride environment has a significant effect on the level of the surface chloride content, C_s. In terms of the underground environment in coastal regions, C_s of a shield tunnel is assumed to be approximately equal to the chloride content of the soil, and it may not change with time because of the chemical equilibrium for concrete that is exposed to infinite seawater (Ann et al. 2009). Therefore, C_s is described as:

$$C_s = X_1 \cdot 0.001 C_{soil} \tag{3-36}$$

where C_s is the chloride content on the outside surface of the tunnel wall, kg/m^3; C_{soil} is the chloride content of the soil, ppm; and X_1 is a lognormal random variable that represents model uncertainty.

As the total amount of chloride around rebar accumulates and reaches a critical threshold of chloride content, C_{cr} (kg/m^3), the corrosion of rebar starts. Thus, the time t_1 to corrosion initiation can be obtained by using the following event:

$$g_1 = X_2 C_{cr} - C(c,t) < 0 \tag{3-37}$$

$$C(c,t) = X_3 \frac{C_s}{2}\left[erf\left(\frac{c-ut}{\sqrt{4Dt}}\right) + e^{\frac{uc}{D}} erfc\left(\frac{c+ut}{\sqrt{4Dt}}\right)\right] \tag{3-38}$$

$$D = 10^{-6.77(W/C)^2+10.10(W/C)-1.14} \tag{3-39}$$

where C_{cr} is the critical threshold of the chloride content, kg/m^3; c is the concrete cover specified in the design, mm; t is the time after construction in years; W/C is the ratio of water to cement; D is the chloride ion transportation coefficient in concrete, mm^2/year;

and u is the average velocity of the chloride motion, mm/year. X_2 is a normal variable associated with the evaluation of C_{cr}, and X_3 is a lognormal variable that represents the model uncertainty that is associated with the estimation of $C(c, t)$.

In particular, the chloride coefficient of diffusion (Equation 3-39) (Akiyama et al. 2010) was obtained by the data reported by Maeda et al. (2004), which are used for concrete, including ordinary Portland cement (OPC). Concerning the critical threshold of chloride content C_{cr}, the value of C_{cr} exhibits a high discretization because of material properties and the environment. For an environment with frequently changing humidity or a constant humidity between 90% and 95%, the critical content is the lowest. However, for submerged structures that lack oxygen, C_{cr} is higher (Breitenbucher et al. 1999 & Zhao 2004). Based on previous reports (Breitenbucher et al. 1999; Val et al. 2003 & Jin et al. 2014), C_{cr} is assumed to be 2.8 kg/m^3, and X_2 is treated as a normal random variable with a mean and C.O.V. of 1.0 and 0.375, respectively.

3.4.1.3 Corrosion-induced crack occurrence

As the passive film is broken by chloride ions, the metallic *Fe* at the anode is oxidized to form ferrous ions that can react with hydroxyl ions to produce ferrous hydroxide, which can be further converted to hydrated ferric oxide. Because the various iron oxides have volumes that are 2 to 6 times the volume of iron (Liu et al. 1998 & Papakonstantinou et al. 2013), a large volume expansion of rust formation causes internal stress and induces cracks in the cover concrete when the total amount of the steel corrosion product, Q_b, exceeds the critical threshold of corrosion that is associated with crack initiation, Q_{cr}. According to Akiyama et al. (2010; 2012), the probability that is associated with the corrosion crack occurrence is estimated by the probability of occurrence of the event:

$$g_2 = X_4 Q_{cr}(c) - Q_b(V_1, t_1, t) < 0 \tag{3-40}$$

where

$$Q_{cr}(c) = \eta(W_{c1} + W_{c2}) \tag{3-41}$$

$$W_{c1} = \frac{\rho_s}{\pi(\gamma - 1)}\left[\alpha_0\beta_0 \frac{0.22\left\{2(c+\phi)^2 + \phi^2\right\}}{E_c(c+\phi)} f_c^{2/3}\right] \tag{3-42}$$

$$W_{c2} = \alpha_1\beta_1 \frac{\rho_s}{\pi(\gamma - 1)} \frac{c+\phi}{5c+3\phi} w_c \tag{3-43}$$

$$Q_b(V_1, t_1, t) = X_5\rho_s V_1(t - t_1) \tag{3-44}$$

ρ_s is the steel density in 7.85 mg/mm^3, γ = 3.0 is the expansion rate of the volume of the corrosion product, f_c is the concrete strength in MPa, w_c is set to 0.1 mm as the crack width of the first cracking, and E_c is the modulus of elasticity of concrete in MPa. ϕ is the diameter of the steel bar in mm, V_1 is the corrosion rate of the steel bar before the occurrence of a corrosion crack in mm/year, and α_0, β_0, α_1 and β_1 are the coefficients that consider the effects of the concrete cover, steel bar diameter and concrete strength, respectively (Qi et al. 2001). η is the correction factor, X_4 is the lognormal random variable that represents the model uncertainty that is associated with the estimation of Q_{cr}, and X_5 is the lognormal random variable associated with the corrosion rate.

Based on Equations 3-40 to 3-44, the time, t_2, to corrosion crack occurrence is

$$t_2 = t_1 + \frac{X_4 Q_{cr}(c)}{X_5\rho_s V_1} \tag{3-45}$$

The corrosion rate of the structures submerged in water or soil is generally lower than that of ground structures due to the lack of oxygen (JSCE 2010). According to the monitoring corrosion rate (see Table 3.3) of RC structures in aggressive environments, including submerged environments, and the JSCE specification (2010), a computation of the amount of rebar corrosion is made by assuming two corrosion rates, namely, (a) 7.7 μm/year before the occurrence of corrosion cracking and without loading ($V_{1,f=0}$) and (b) 30 μm/year after the occurrence of corrosion cracking and without loading ($V_{2,f=0}$). Meanwhile, X_5 is assumed as a lognormal with a mean and C.O.V. of 1.0 and 0.58, respectively (Mori et al. 1994; Frangopol et al. 1997; Nakagawa et al. 2004 & Akiyama et al. 2010).

Table 3.3 RC corrosion rate review in a submerged environment (μm/year)

	Corrosion rate	Condition	Case	
Stewart M.G. et al. (1998) & Chen D. et al. (2008)	11.6	Uncracked Moderate corrosion		
Gonzalez J.A. et al. (1995)	11.6~34.8	Active corrosion	Lab	Specimen
Costa A. et al. (2002)	<11.6 81.2	Passive condition Construction joint	On-site	Bridge (Portugal)
Walsh M. T. et al. (2016)	5~35	Pilings of undersea	On-site	Bridge
Gong C. et al. (2017)	1.16~8.12 58~116 11.6~92.8	Initiation Inside wall Outside wall	On-site	Tunnel (Xiangan Subsea Tunnel, China)

Finally, considering the effect of different loading levels on the corrosion rate that is described in Equation 3-24, the corrosion rate of the segment under different load levels is $V_{1,f} = 7.78\ e^{0.387f}$ and $V_{2,f} = 30\ e^{0.387f}$.

3.4.2 Performance assessment of the segmental linings based on steel corrosion

3.4.2.1 Steel weight loss and deteriorated flexural strength due to corrosion

Structural integrity degradation occurs after reinforcement corrosion initiation, while the flexural strength of corroded RC linings depends mainly on the total available area of the rebar in the tension zone. In this paper, the steel weight loss, $\rho(t)$, which is assumed to be uniform corrosion (Akiyama et al. 2010), is described as:

$$\rho(t) = \begin{cases} 0.0, & t \le t_1 \\ \dfrac{\pi\phi}{(\pi\phi^2)/4}(t-t_1)V_1X_5, & t_1 < t \le t_2 \\ \dfrac{\pi\phi}{(\pi\phi^2)/4}\{(t_2-t_1)V_1X_5 + (t-t_2)V_2X_5\}, & t > t_2 \end{cases} \tag{3-46}$$

where ϕ is the diameter of the steel bar, mm; V_1 is the corrosion rate of the steel bar before cracking, μm/year; V_2 is the corrosion rate of the steel bar after cracking, μm/year.

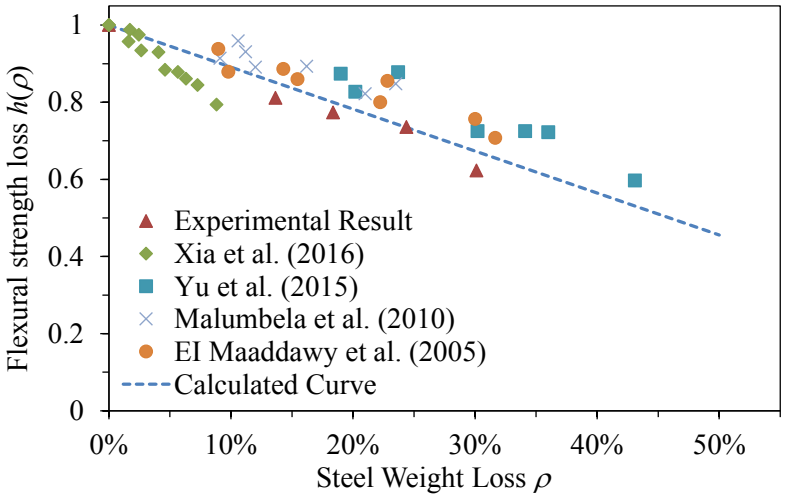

Figure 3.17 Relationship between the steel weight loss of longitudinal bars and flexural strength loss

As corrosion gradually progresses, the remaining flexural capacity is reduced. There have been many experimental studied on RC specimens with chloride-induced corrosion of rebars. Previous experimental results of corroded RC specimens (EI Maaddawy et al. 2005; Malumbela et al. 2010; Yu et al. 2015 & Xia et al. 2016) are used here. In these studies, the specimens were corroded by electric corrosion or drying/wetting conditions using salt water, and then the residual capacities of corroded RC specimens were tested under pure bending state (EI Maaddawy et al. 2005; Malumbela et al. 2010; Yu et al. 2015) or eccentric compression loading (Xia et al. 2016). Based on a regression analysis for the test results of corroded RC specimens, the flexural capacity loss of the segments with corrosion-induced deterioration in tension zones is shown in Figure 3.17. The relationship between $\rho(t)$ and the flexural strength loss, $h(\rho)$, is:

$$h(\rho) = \left(-1.089\rho + 1.000\right) \cdot X_6 \tag{3-47}$$

$$M_u(t) = M_0 \cdot h\left[\rho(t)\right] \tag{3-48}$$

where $M_u(t)$ is the deteriorated flexural capacity of the segments due to reinforcement corrosion, and M_0 is the undamaged flexural capacity of the segments, depending on the

cross-section size, amount of rebar and axial force (JSCE 2010). X_6 is a normal random variable related to the ratio of experimental to computed value by Equation 3-47 with a mean and C.O.V. of 1.0 and 0.066, respectively.

However, because the pitting corrosion of reinforcing bars is ignored here, this linear equation may lead to an overestimation of the deteriorated flexural capacity of the segmented linings with an increase of average steel weight loss.

3.4.2.2 Estimation of stiffness and demand on deteriorated segmental linings

As stated previously, the time-variant damage variable, $D_I(t)$, of the RC segments in an aggressive environment is determined by the load level, f, and steel weight loss, $\rho(t)$, which includes the initial damage, D_f, due to the load and the deteriorated damage, $D_c(t)$, due to the coupling effects of the load and corrosion. Meanwhile, because of the non-uniform distribution of the load level, f, along the different sections of segmental linings, the time-variant damage variable, $D_I(t)$, of the RC segments is also associated with the sectional position, θ, of the segmental linings. Based on Equations 3-13 to 3-18, the time-variant damage variable, $D_I(\theta, t)$, of an RC segment is assumed as (Liu 2011):

$$D_I(\theta,t)=\begin{cases} D_c(\theta,t), & 0\le f(\theta)\le 0.94 \\ D_f(\theta)+D_c(\theta,t), & 0.94\le f(\theta)\le 2.07 \end{cases} \tag{3-49}$$

$$D_f(\theta)=0.077f(\theta)^3-0.559f(\theta)^2+1.482f(\theta)-0.923 \tag{3-50}$$

$$D_c(\theta,t)=\left[A(\theta)\rho(\theta,t)^2+B(\theta)\rho(\theta,t)+C(\theta)\right]\rho(\theta,t) \tag{3-51}$$

where θ is the sectional position of the segmental linings; $f(\theta)$ is the load level at each section of the segmental linings; $D_f(\theta)$ and $D_c(\theta,t)$ are the initial damage due to the load and the deteriorated damage due to the coupling effects of the load and corrosion, respectively; and $A(\theta)$, $B(\theta)$ and $C(\theta)$ are correction coefficients depending on θ.

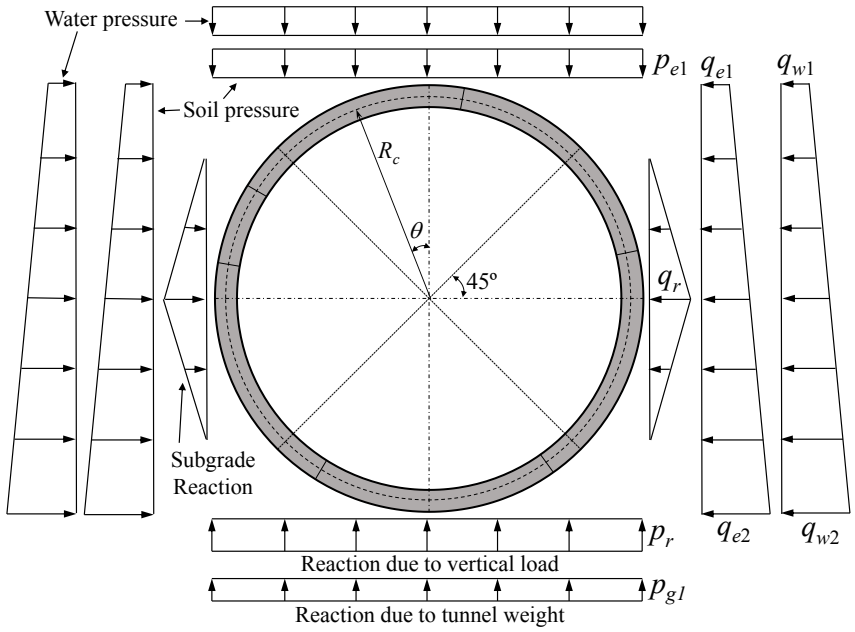

Figure 3.18 Loading structure model schematic diagram of a modified routine calculation method (adapted from JSCE 2007)

Regarding the demand calculation of deteriorated shield tunnels, a modified routine calculation method (see Figure 3.18) is adopted in this paper. This calculation method, which was proposed by Japan Society of Civil Enigneers (JSCE) (JSCE 2007), is a typical example of many loading-structure models that ignore the joint effects and that treat the shield tunnel as a uniform, rigid ring. In this paper, the average time-variant stiffness, *EI* (*t*), of the deteriorated segmental linings is defined as follows based on Equation 3-9:

$$EI(t) = \left(1 - \overline{D}_I(t)\right) \cdot EI \tag{3-52}$$

$$\overline{D}_I(t) = \frac{\int_0^{2\pi} D_I(\theta,t)d\theta}{\int_0^{2\pi} d\theta} = \frac{\int_0^{2\pi} D_I(\theta,t)d\theta}{2\pi} \tag{3-53}$$

where $\overline{D}_I(t)$ is the weighted mean value of the damage variable, $D_I(\theta, t)$, for each cross-section of the RC segmental linings, and *EI* is the undamaged stiffness of the RC segmental linings.

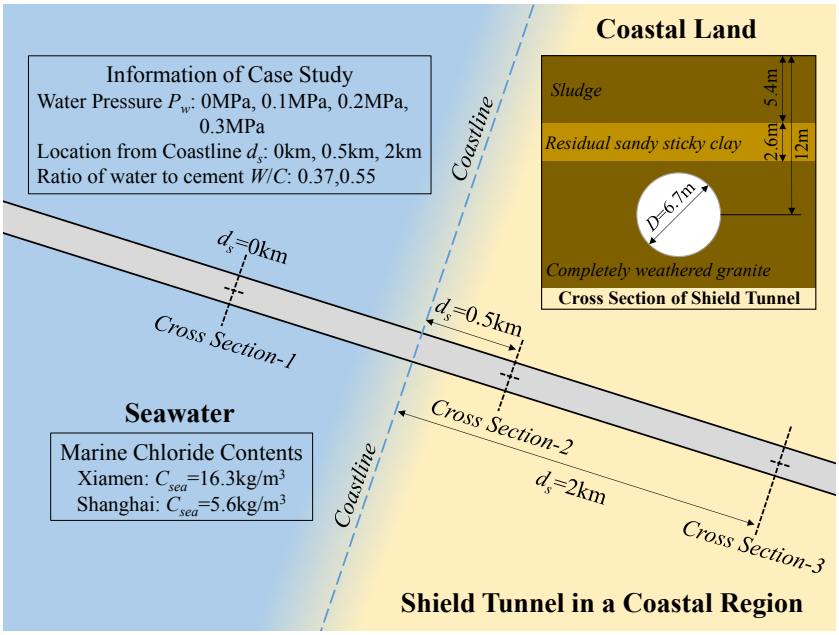

Figure 3.19 Illustration diagram of case studies of a shield tunnel in a coastal region

Furthermore, considering the uncertainty in structural properties and soil properties, these random variables are adopted in the demand calculation process of shield tunnels with corrosion-induced deterioration.

3.5 Illustrative examples

3.5.1 Time to corrosion initiation analysis

Corrosion initiation indicates the beginning of structural deterioration, and the time to corrosion initiation can be regarded as a significant index for structural durability assessments. A Monte Carlo analysis was conducted to obtain the distribution of the time to corrosion initiation of shield tunnels with a sample size of 20,000. The influence of three cases, including the hydrostatic pressure, the material properties of a segment and chloride hazard, on the time to corrosion initiation was considered for the shield tunnels in the two coastal cities of Xiamen and Shanghai (see Figure 3.19).

All the parameters of the random variable X_i (i = S, R, 1, 2, 3, 4, 5) involved in the calculation of the time to corrosion initiation by using MCS are summarized in Table 3.4.

Table 3.4 Parameters of the random variables of the deteriorating calculation

Variables	Distribution	Mean	C.O.V.
Chloride content in soil (X_R)	Lognormal	1.00	0.73
Marine chloride content (X_S)	Normal	1.00	0.043 (Xiamen)
			0.155 (Shanghai)
C_s-C_{soil} equation (X_1)	Lognormal	1.43	1.08
Critical threshold chloride content at occurrence of steel corrosion (X_2)	Normal	1.00	0.375
Estimation of chloride transport (X_3)	Lognormal	1.24	0.906
Critical threshold of corrosion amount at crack initiation (X_4)	Lognormal	1.00	0.352
Corrosion rate (X_5)	Lognormal	1.00	0.58
Corrosion-induced flexural capacity loss (X_6)	Normal	1.00	0.066

The examples illustrating the probability density functions (PDFs) for the time to corrosion initiation of the shield tunnels under different conditions are presented in Figures 3.20 to 3.22.

Figure 3.20 presents the distribution of the time to corrosion initiation for a shield tunnel located in Xiamen under the hydrostatic pressures of 0 MPa, 0.1 MPa, 0.2 MPa and 0.3 MPa. From this figure, the effect of greater hydrostatic pressure is clearly confirmed because the time to corrosion initiation occurs considerably earlier with greater hydrostatic pressure than with lower hydrostatic pressure. Notably, for a shield tunnel that is under high hydrostatic pressure conditions (i.e., P_w > 0.15 MPa), a significantly premature corrosion initiation occurs at only several years after the completion of construction. Similar results are indicated for the shield tunnels located in Shanghai.

Besides, the material properties of a segment also play a significant role in structural durability, as illustrated in Figure 3.21. Because the chloride transportation process is associated with the ratio of water to cement (i.e., K_s and D), the time to corrosion initiation of a shield tunnel in Xiamen with a higher ratio of water to cement (i.e., W/C = 0.55) is earlier than the time to corrosion of a shield tunnel in Xiamen with a lower ratio of water

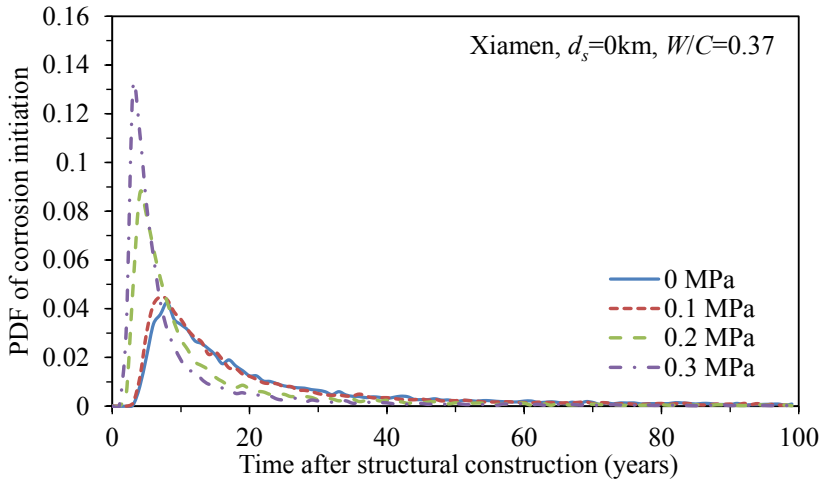

Figure 3.20 PDF of corrosion initiation over time after the structural construction of the shield tunnels in Xiamen under different hydrostatic pressures

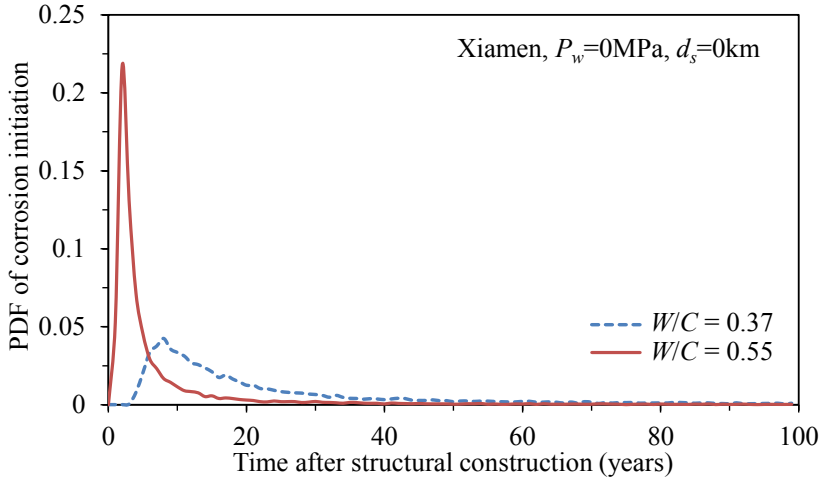

Figure 3.21 PDF of corrosion initiation over time after the structural construction of the shield tunnels in Xiamen for different ratios of water to cement

to cement (i.e., W/C = 0.37) and is approximately 8 years and with a higher probability. Similar analyses are performed for the shield tunnel in Shanghai. As expected, a RC segment that uses a lower ratio of water to cement has better anti-permeability.

Finally, Figures 3.22 (a) and (b) reveal that a higher probability of corrosion initiation occurs for a shield tunnel near a marine environment because of the higher chloride hazard and that this probability decreases with an increasing distance from the coastline. However, with the decrease of chloride hazard, the probability of corrosion

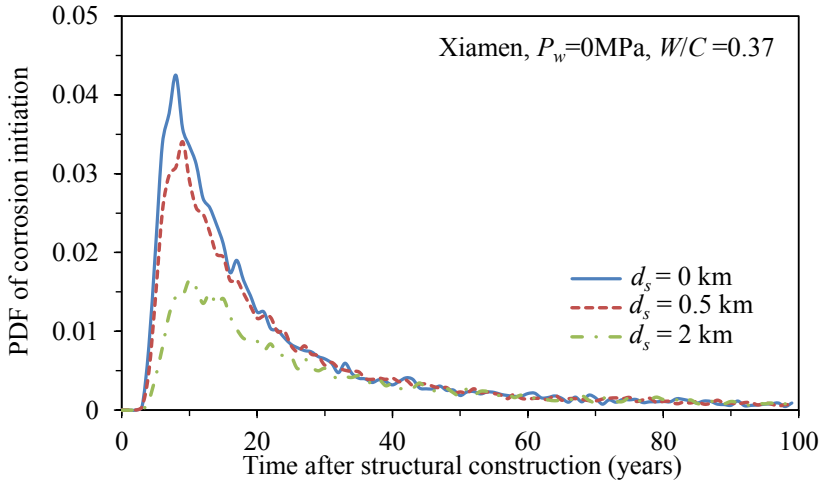

(a)

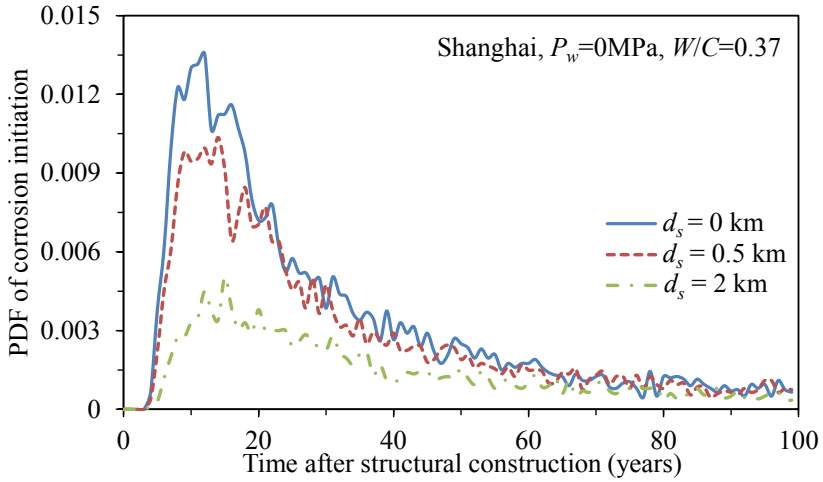

(b)

Figure 3.22 PDF of corrosion initiation over time after the structural construction of the shield tunnels in (a) Xiamen and (b) Shanghai for different distances from the coastline

initiation gradually tends to be uniform distributed with a low level during structural lifetime due to the week chloride attacks, as shown in Figure 3.22 (b).

3.5.2 Time-variant structural performance analysis

3.5.2.1 Time-variant structural reliability margin

To estimate the life-cycle performance of a structural system, time-variant probability-based concepts and methods provide a rational and more scientific basis for treating

Table 3.5 Parameters of the random variables of the demand calculation

Variables	Distribution	Mean	C.O.V.
Density of first layer of cover soil (ρ_{s1})	Lognormal	1610 kg/m^3	0.044
Density of second layer of cover soil (ρ_{s2})	Lognormal	1830 kg/m^3	0.028
Density of third layer of cover soil (ρ_{s3})	Lognormal	1880 kg/m^3	0.041
Elastic resistance coefficient of soil (kr)	Lognormal	30×10^3 kN/m^3	0.236
Side pressure coefficient of soil (λ)	Lognormal	0.330	0.175
Unit weight of RC segment (g_1)	Normal	23 kN/m^3	0.020
Elasticity modulus of concrete (E)	Normal	34.5 GPa	0.085

uncertainties (Ang and Tang 1984, 2007; Frangopol 2011). The failure probability of a structural system during its life-cycle is generally defined as the probability of violating any of the limit state functions that indicate its failure modes. In this paper, because the material properties of the segments (i.e., stiffness and strength) are the random functions of time, the time-variant margin of structural safety, $Z(t)$, is described by the flexural bending capacity, $M_u(t)$, and the bending moment, $M(t)$, of the shield tunnels. Thus, the failure probability, $P_f(t)$, is defined as:

$$P_f(t) = P\left[Z(t) = M_u(t) - M(t) < 0\right] \tag{3-54}$$

The shield tunnels studied here are located in two coastal cities of China (see Figure 3.19), namely, Xiamen and Shanghai. Notably, the depth of the shield tunnel is assumed to be 12 m, and the structure is located in a layer of completely weathered granite. The overlying stratum is sludge and residual sandy sticky clay with a depth of 5.4 m and 2.6 m, respectively. Finally, the key parameters of the random variables to calculate structural demand with uncertainty are listed in Table 3.5.

Considering the corrosion-induced deterioration of a shield tunnel under different conditions, based on Table 3.4, the time-variant failure probabilities of the shield tunnels in Xiamen and Shanghai are partly shown in Figures 3.23 to 3.28. From these figures, the failure probabilities are presented along the sections of the shield tunnels that are within

20 years of construction. In particular, the time-variant probabilities for sections regards as the hazard zones of the shield tunnels are also depicted here.

3.5.2.2 Failure probability associated with hydrostatic pressure

Figure 3.23 presents the influence of hydrostatic pressure on the failure probability of the shield tunnels located in Xiamen. Similar results are also obtained for the shield tunnels located in Shanghai. As shown in Figure 3.23, all sections of the shield tunnel can be safe for several decades after construction. As the degree of steel weight loss increases in the outside wall of the segmental lining, the failure probabilities on/around the sections with negative bending moment of the shield tunnel (i.e. the tension zone of section occurs at the outside wall of segment linings) increase. In particular, the section around 70 and 290 degrees of segmental lining gradually exhibit higher failure probabilities. However, as the degree of the hydrostatic pressure that acts on a shield tunnel and as the steel weight loss increases in the outside wall of the segmental linings, all the sections with negative bending moment are exposed to a higher hazard.

In terms of the top and bottom sections of segmental linings shown in Figure 3.23, these sections under positive bending moment exhibit to be safe over time. The steel weight loss considered in this paper only occurs on the outside wall of the segmental lining, the corrosion of external reinforcements in tensile areas due to negative bending moment greatly decrease the flexural capacity. However, the flexural capacity at the top and bottom sections of the shield tunnel depends on the reinforcing bars on the inside wall due to positive bending moment; therefore, the time-variant flexural capacity on the top and bottom sections can be considered as undamaged state. Meanwhile, the greater degree of structural stiffness deterioration that occurs because of more steel weight loss could cause a decrease in the bending moment of the segmental linings. Therefore, the top and bottom sections of the segmental linings are relatively safe compared with the

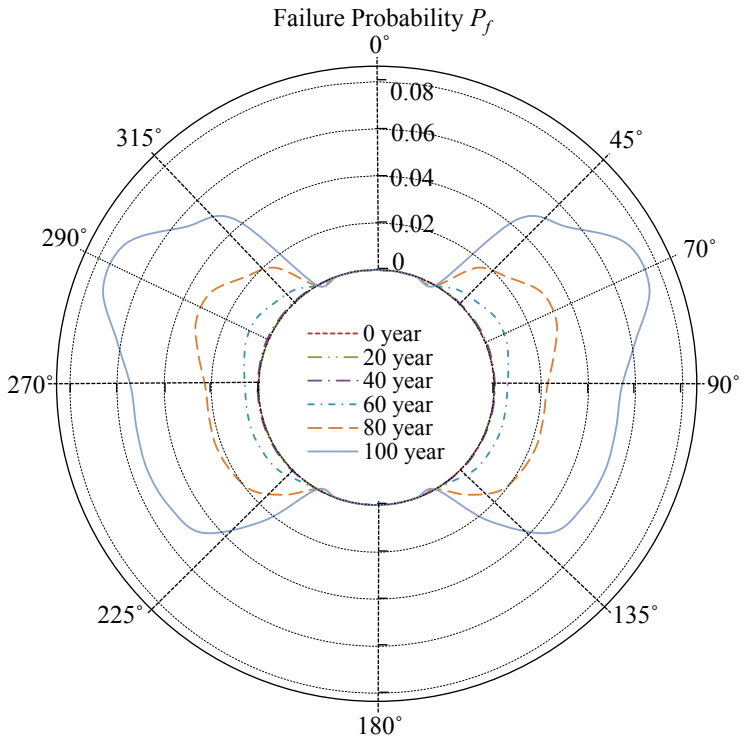

(a)

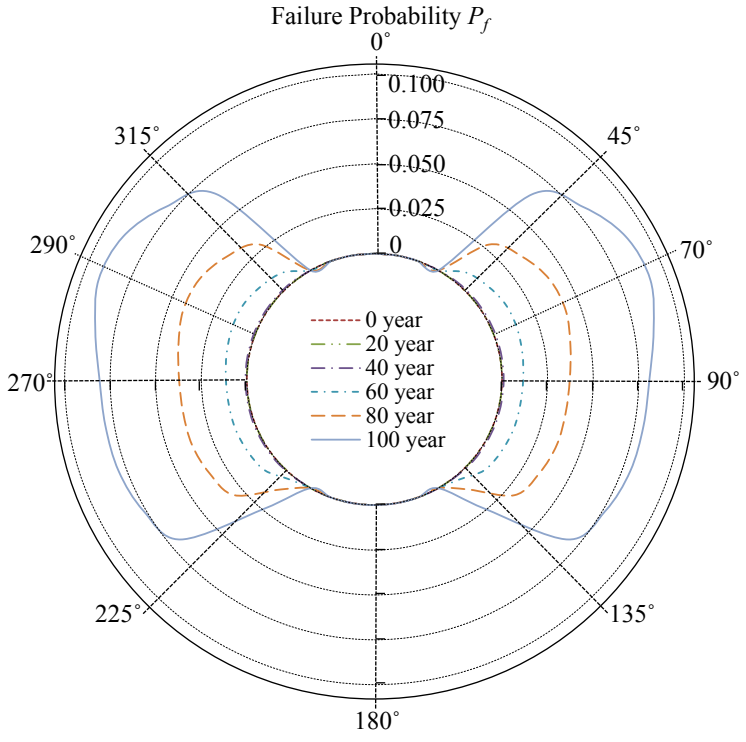

(b)

Figure 3.23 Failure probability of all sections of the shield tunnel in Xiamen (d_s = 0 km, W/C = 0.37) under the hydrostatic pressures of (a) 0 MPa and (b) 0.3 MPa at different years

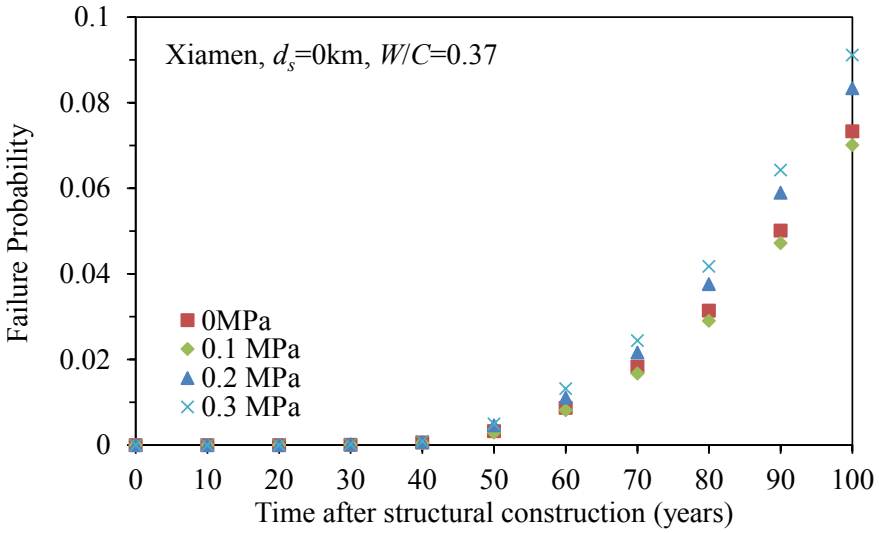

(a)

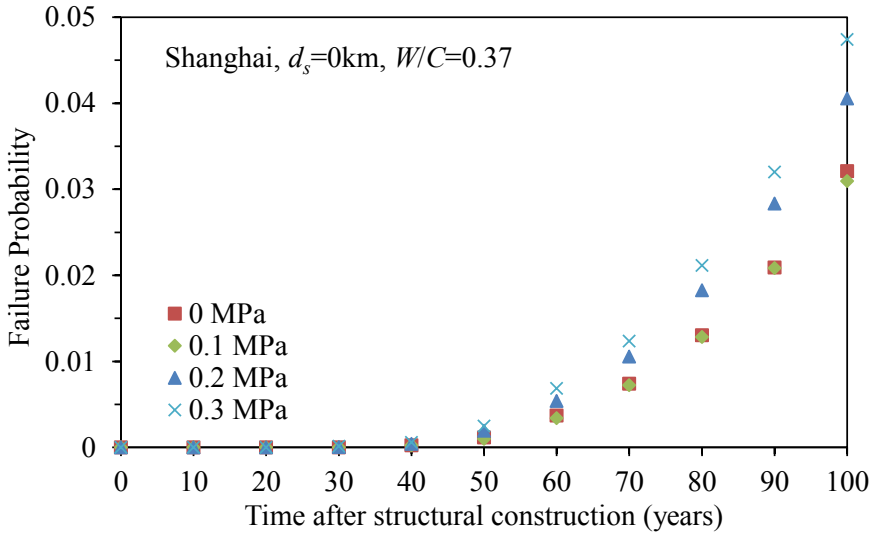

(b)

Figure 3.24 Maximum failure probability of the shield tunnels in (a) Xiamen and (b) Shanghai under different hydrostatic pressures

sections under negative bending moment based on the limit state function.

Figure 3.24 provides the maximum failure probabilities of shield tunnels in Xiamen and Shanghai under different hydrostatic pressures. Generally, a greater hydrostatic pressure leads to a higher failure probability for the shield tunnel. This is because the flexural capacity of these sections is dominated by the degree of the steel weight loss on the outside walls of the segmental linings. Although higher water pressure has a beneficial

influence on structural stress condition (i.e., the compression state), higher steel weight loss, induced by coupling effect of higher water pressure and aggressive agent, will cause the deterioration of flexural capacity more significantly. However, for a shield tunnel under low hydrostatic pressure conditions (e.g., P_w = 0.1 MPa), the influence of hydrostatic pressure on corrosion initiation is limited (see Figure 3.20). Meanwhile, because of the beneficial effect of hydrostatic pressure on the stress state of a shield tunnel, higher compressive axial force induces a decrease in the load level, which results in a lower corrosion rate. Thus, a slower deterioration process occurs in the segmental linings. This results in a slight reduction of the failure probability of a shield tunnel with low hydrostatic pressure compared with a shield tunnel without any hydrostatic pressure.

3.5.2.3 Failure probability associated with the material properties and chloride hazard

The influence of a segment's material properties on a shield tunnel's failure probability is illustrated in Figures 3.25-3.26. Figure 3.25 shows plots that correspond to the influence of the ratio of water to cement on the failure probability distribution along the sections of a shield tunnel at Shanghai. The time-variant failure probabilities for the sections regarded as the hazard zones of shield tunnels at Xiamen and Shanghai are displayed in Figure 3.26. According to these figures, a higher ratio of water to cement leads to a greater failure probability because of a faster deterioration process that is caused by worse anti-permeability in the segment. One hundred years after construction, the failure probability of the hazard section of the shield tunnels at Shanghai using the higher ratio of water to cement (i.e., W/C = 0.55) increases by two times, compared with the failure probability using the lower ratio of water to cement (i.e., W/C = 0.37). Also, the analyses for the shield tunnels located in Xiamen reveal similar results.

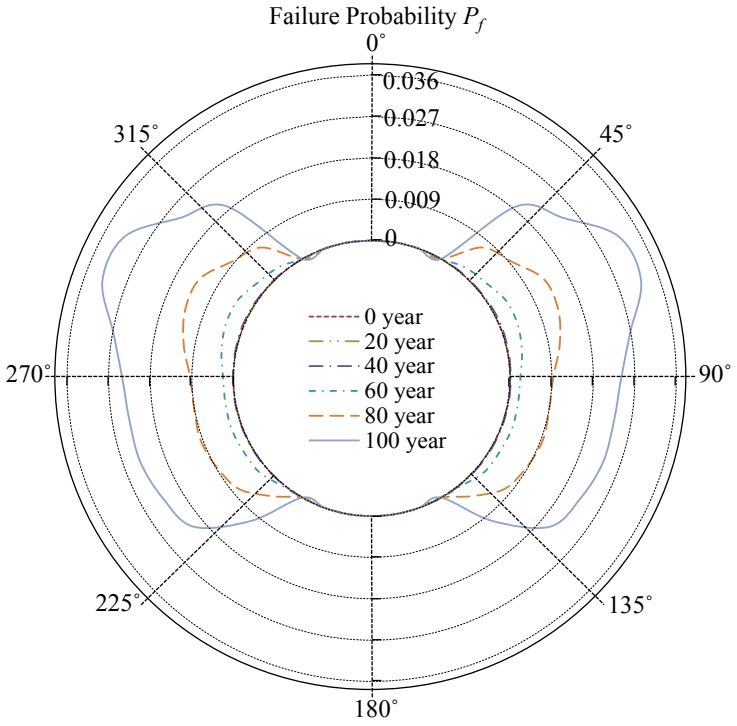

(a)

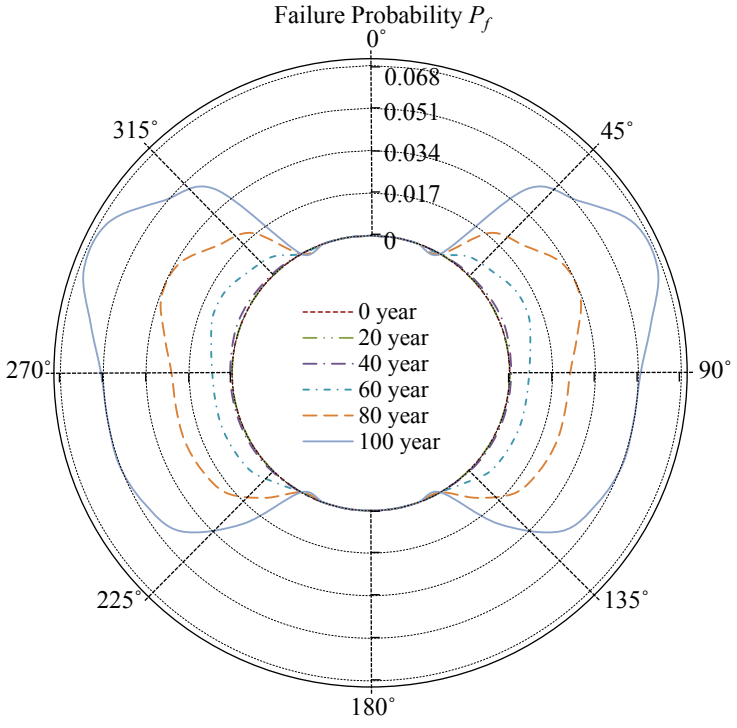

(b)

Figure 3.25 Failure probability of all sections of the shield tunnel in Shanghai (d_s = 0 km, P_w = 0 MPa) with ratios of water to cement that are equal to (a) 0.37 and (b) 0.55 at different years

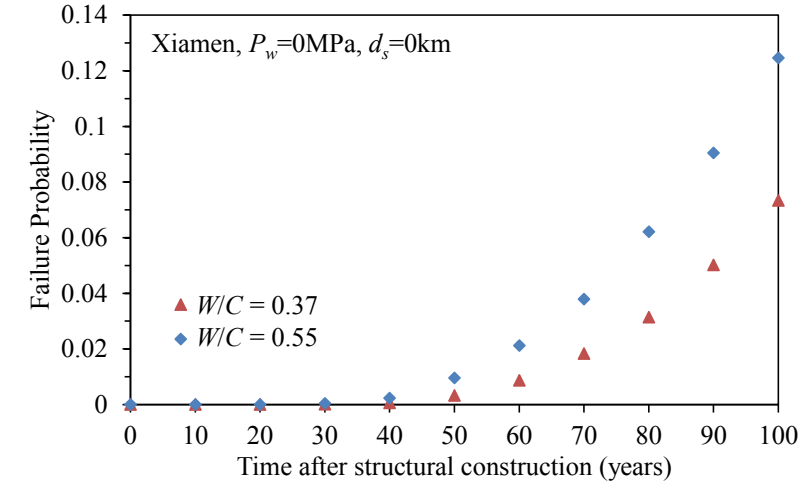

(a)

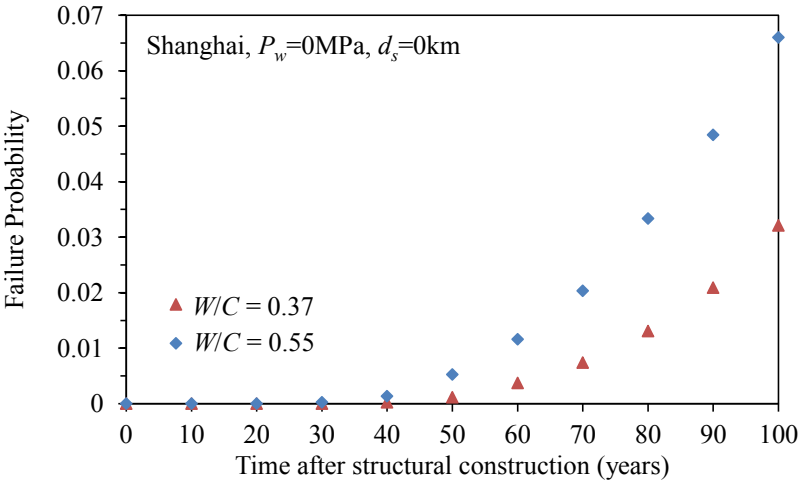

(b)

Figure 3.26 Max failure probability of the shield tunnels in (a) Xiamen and (b) Shanghai with different ratios of water to cement

Finally, the failure probabilities of a shield tunnel with a varying distance from the coastline are displayed in Figures 3.23 (a), 3.25(a), 3.27 and 3.28 assuming hydrostatic pressure equal to 0 MPa is illustrated here. As shown in Figure 3.28 (a), the failure probability of a shield tunnel in Xiamen increases with the structure's proximity to the marine environment because of a higher chloride hazard, similar to the results for a shield tunnel in Shanghai. Therefore, in term of the shield tunnels near to marine environment, it is necessary to conduct structural durability design, so that the target durability

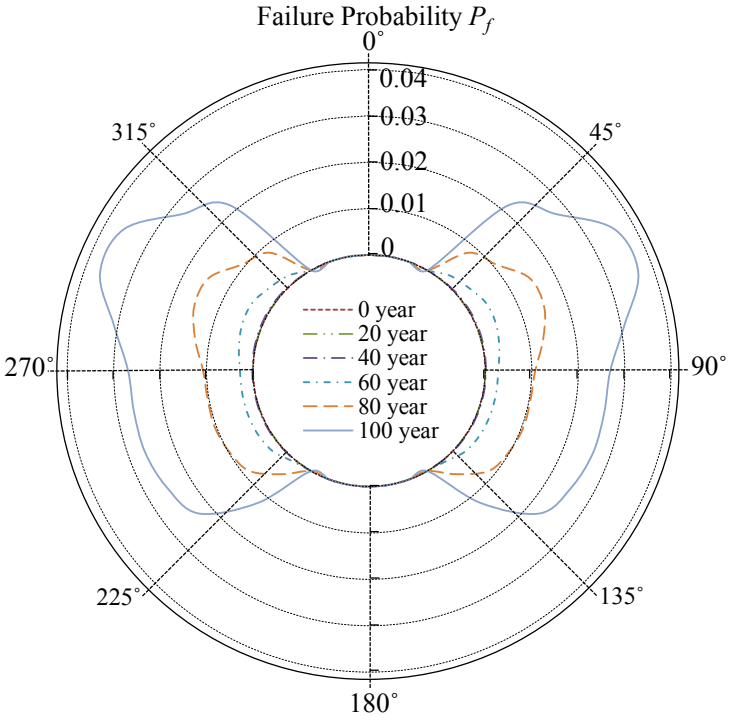

(a)

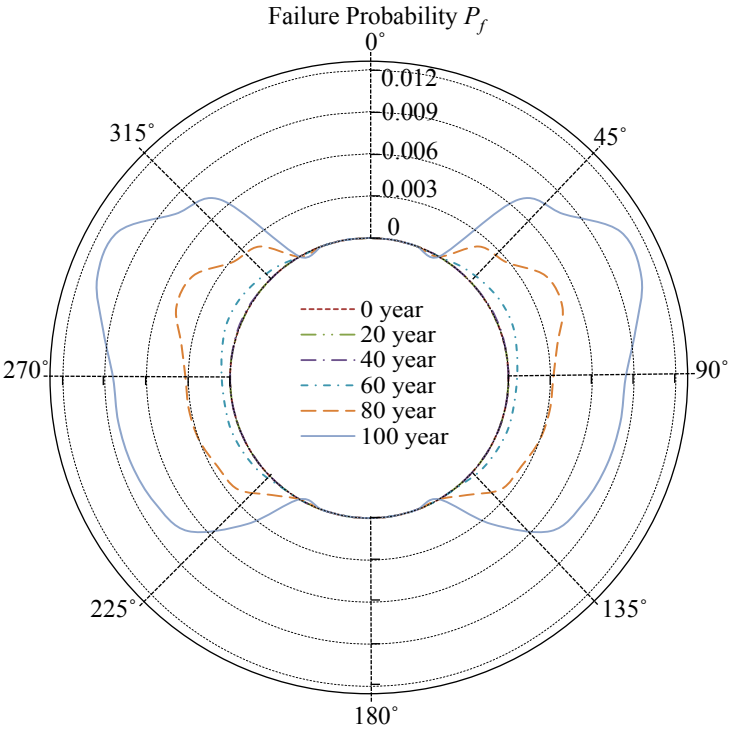

(b)

Figure 3.27 Failure probability of all sections of the shield tunnel in (a) Xiamen and (b) Shanghai (P_w = 0 MPa, W/C = 0.37) with a distance of 2 km from the coastline at different years

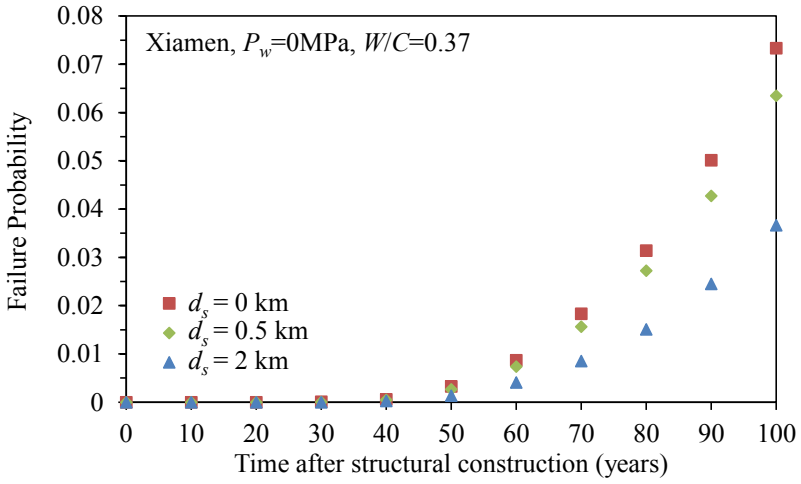

(a)

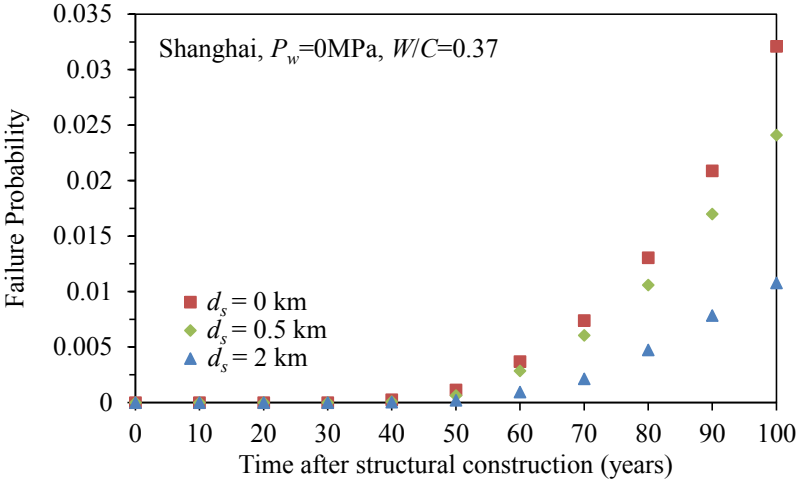

(b)

Figure 3.28 Max failure probability of the shield tunnels in (a) Xiamen and (b) Shanghai with different distances from the coastline

reliability level of shield tunnels during their lifetime will be satisfied.

3.6 Chapter Summary

(1) A novel time-variant framework for the structural performance assessment of shield tunnels in a marine environment was proposed. In this framework, the following five main components are considered: (a) chloride hazard assessment; (b) time-to-corrosion-initiation estimate with the impact of hydrostatic pressure; (c) deterioration process investigation based on corrosion-accelerated experimental tests; (d)

deteriorated structural performance evaluation; and (e) time-variant structural reliability analysis.

(2) A novel approach was proposed to establish the probabilistic hazard for chloride around a shield tunnel in a coastal region; this hazard can quantify the effect of the aggressive environment on the shield tunnel.

(3) The deterioration processes of segmental linings under the coupled effects were experimentally investigated using corrosion-accelerated specimens in a tunnel segment. Damage indices proposed include the initial and deteriorating damage as well as the steel corrosion of the segmental linings considering the loading effect.

(4) A probabilistic method to evaluate the chloride transport process in the segmental linings of shield tunnels with the impact of hydrostatic pressure was proposed. The time to corrosion initiation can be estimated by considering combined effects. Under high hydrostatic pressure, chloride ions can permeate the segmental linings more quickly due to coupling effect of diffusion and advection. This causes a higher failure probability of undersea shield tunnels.

(5) A computational procedure to integrate the chloride hazard around tunnel structures into the time-variant reliability of shield tunnels in coastal regions was proposed. This proposed method emphasized the structural performance degradation induced by steel corrosion, and the influence of hydrostatic pressure, structural location and material properties on the structural failure probability.

Chapter 4: Reliability-Based Durability Design of Shield Tunnels in Coastal Regions

4.1 Procedure for the reliability-based durability design of shield tunnels in a marine environment

Durability design, as an essential part of structural design, has widely been considered to ensure structures in an aggressive environment to provide acceptable service for extended periods of time. However, it should be recognized that the acquired knowledge on structural durability is far from complete, and not all durability requirements can be easily quantified (Li et al. 2015). Since the aggressive hazards might be underestimated or overestimated in design, poor quality concrete and/or inadequate concrete cover could lead to premature steel corrosion and severe concrete cracking for RC structures. As described in Chapter 3, owing to inadequate material parameters in design, these shield tunnels are at risk from deterioration process due to the coupling effects of high hydrostatic pressure and aggressive chemical attacks.

According to the description in Chapter 3, the degradation process of RC segmental linings is associated with several marine environmental factors, and the influence of these factors varies depending on time and space. Due to the uncertainties from environment and structure, the probabilistic concepts and methods should be taken into account for a reliable durability design of RC segmental linings in a marine environment. Meanwhile, in order to ensure the long-term structural performance of RC shield tunnels in an aggressive environment, controls of steel corrosion and concrete cracking should be considered in durability design as the basic requirements. Based on the new approach, the coupling effects of underground chloride hazards and high hydrostatic pressure are integrated in computing the probabilities of occurrence of steel corrosion and corrosion-

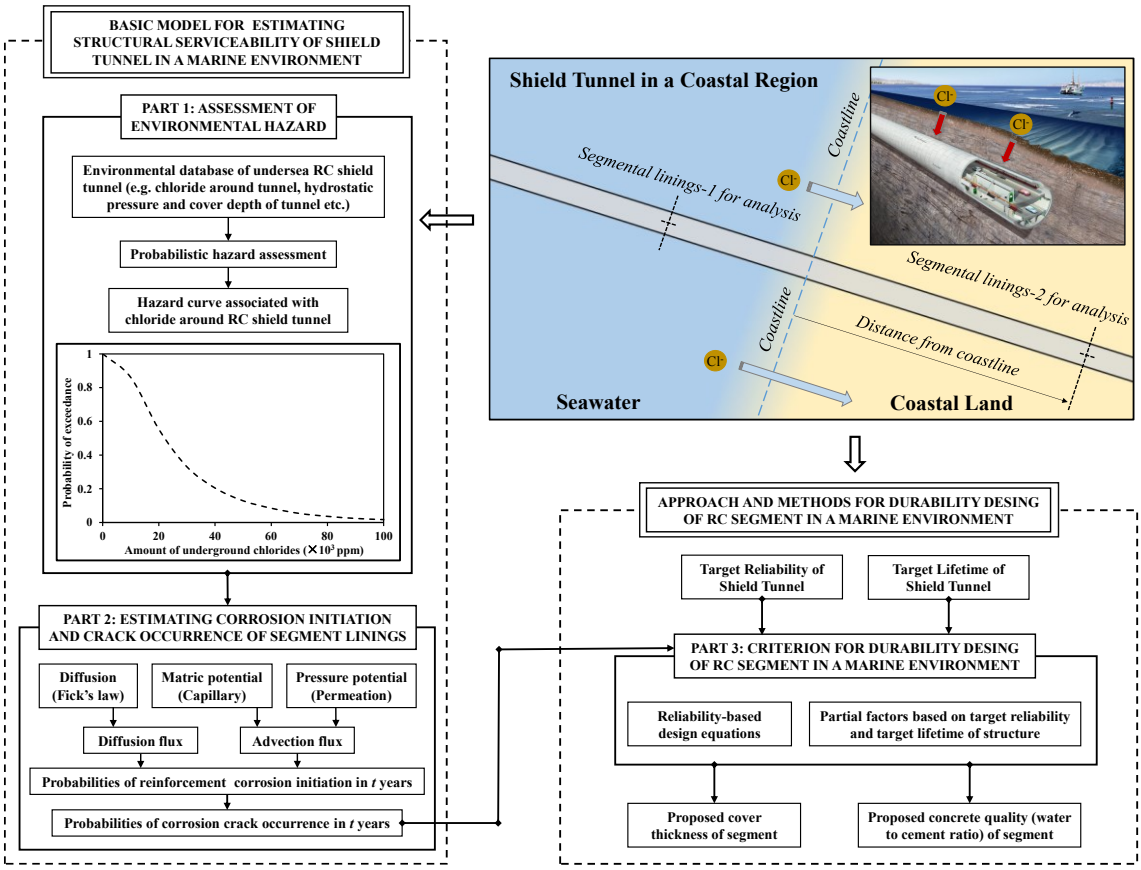

Figure 4.1 Flowchart for reliability-design approach of RC shield tunnels in a marine environment integrated with the coupling effects of underground chloride hazards and high hydrostatic pressure

induced cracking, and a flowchart for reliability-based design of segmental linings in a marine environment is illustrated in Figure 4.1.

According to the flowchart in Figure 4.1, two primary aspects are presented: (a) basic models for estimating structural serviceability of shield tunnels, and (b) an approach and method for durability design of RC segment in a marine environment. In terms of the aspect (a), it includes two steps: (1) defining the process of hazard assessment for underground chloride in a coastal regions (i.e. Part 1); (2) computing the time-dependent probability of steel corrosion and corrosion-induced cracking of the segmental linings with the impact of hydrostatic pressure (i.e. Part 2). Then, based on the basic models in aspect (a), a reliability-based durability design criterion of segmental linings was proposed in Part 3 included in aspect (b) to calculate the concrete cover and determine

the concrete quality (i.e. ratio of water to cement), so that the target durability reliability level of tunnel structures during their lifetime could be satisfied.

4.2 Basic models for estimating structural serviceability of shield tunnels due to corrosion

In Chapter 3, the probabilistic models associated with underground chloride hazard, steel corrosion and corrosion-induced cracking have been presented in detail. Herein, a brief summary of these models are described as follows.

4.2.1 Probabilistic model of hazard associated with underground chloride

Since the long-term performance of RC structures is strongly influenced by their environmental conditions, environmental hazards should be quantitatively assessed and considered in the durability design of RC shield tunnels in a marine environment. Considering the uncertainties involved in the prediction of underground chlorides around tunnels, parameters associated with model error should be included in the attenuation equations. Thus, the attenuation with model uncertainty is expressed as:

$$C_{Soil} = X_R \cdot \left[0.62 \cdot \left(X_S \cdot C_{Sea} \right) \cdot 0.63^d \right] \tag{3-7}$$

where X_R is a lognormal random variable related to estimation of chloride content in soil; and X_S is a normal random variable associated with the marine chloride content at different coastal regions.

The probability that C_{soil} at a specific site exceeds an assigned value c_{soil} is described as:

$$q(c_{Soil}) = P(C_{Soil} > c_{Soil}) = \int_0^\infty P(X_R > \frac{c_{Soil}}{0.62 \cdot X_S C_{Sea} \cdot 0.63^d}) \times f(X_S) dX_S \tag{3-8}$$

where $f(X_S)$ is the probability density function of X_S.

4.2.2 Performance function for steel corrosion

High hydrostatic pressure on tunnels lead structures to withstand a large water pressure gradient between the inside and outside walls, it could facilitate chloride ions transporting in concrete linings. As the total amount of chloride around rebar accumulates and reaches critical threshold of chloride content C_{cr} (kg/m^3), the corrosion of rebar begins. Considering the action of hydrostatic pressure and the water environment, the time t_1 to corrosion initiation can be obtained using the following event:

$$g_1 = X_2 C_{cr} - C(c,t) < 0 \tag{3-37}$$

where

$$C(c,t) = X_3 \frac{C_s}{2}\left[erf\left(\frac{c-ut}{\sqrt{4Dt}}\right) + e^{\frac{uc}{D}} erfc\left(\frac{c+ut}{\sqrt{4Dt}}\right)\right] \tag{3-38}$$

$$D = 10^{-6.77(W/C)^2+10.10(W/C)-1.14} \tag{3-39}$$

c is the concrete cover specified in design, mm; t is the time after construction, year; W/C is the ratio of water to cement; D is the chloride ion transportation coefficient in concrete, mm^2/year; u is the average velocity of chloride motion, mm/year; X_1 is a lognormal random variable representing model uncertainty; C_{cr} is assumed to be 2.8 kg/m^3, X_2 is a normal variable associated with the evaluation of C_{cr}; and X_3 is a lognormal variable representing the model uncertainty associated with estimation of $C(c, t)$.

4.2.3 Performance function for corrosion-induced cracking

As the passive film is broken by chloride ions, a large volume expansion of rust formation causes internal stress and induces cover concrete segment cracks when the total amount of steel corrosion product Q_b exceeds the critical threshold of corrosion associated with crack initiation Q_{cr}. And the probability of corrosion crack occurrence with time can be estimated by the following event:

$$g_2 = X_4 Q_{cr}(c) - Q_b(V_1, t_{co}, t) < 0 \tag{3-40}$$

where

$$Q_{cr}(c) = \eta(W_{c1} + W_{c2}) \tag{3-41}$$

$$Q_b(V_1, t_{co}, t) = X_5 \rho_s V_1 (t - t_{co}) \tag{3-44}$$

ρ_s is the steel density, 7.85 mg/mm^3; V_1 is the corrosion rate of the steel bar before the occurrence of a corrosion crack, mm/year, assumed as the corrosion rate is 7.7 μm/year; η is the correction factor; X_4 is a lognormal random variable representing the model uncertainty associated with the estimation of Q_{cr}; and X_5 is a lognormal random variable related to the corrosion rate.

4.2.4 Serviceability assessment of RC shield tunnels in a marine environment

To assess the serviceability of RC shield tunnels in a marine environment over their entire lifetime, Monte Carlo simulation (MCS) was also used herein. All parameters of the random variable X_i (i = S, R, 1, 2, 3, 4, and 5) involved in calculation are shown in Table 3.1. The probabilities associated with occurrence of two limit states (see Equation 3-37 and 3-40) at an assigned time, t, are defined as below, respectively.

$$P_f(t) = P(t_1 \le t) \tag{4-1}$$

$$P_f(t) = P(t_1 + t_2 \le t) \tag{4-2}$$

where t_1 is the time to corrosion initiation; t_2 is the time from corrosion initiation to occurrence of corrosion-induced cracking.

Equation 4-1 and 4-2 represent the time-dependent failure probability associated with corrosion initiation and occurrence of corrosion-induced cracking, respectively. And the probabilities can be transformed into a reliability index, β, as follows:

$$\beta(t) = -\Phi^{-1}(P_f(t)) \tag{4-3}$$

where Φ is the cumulative distribution function of the standard normal variable.

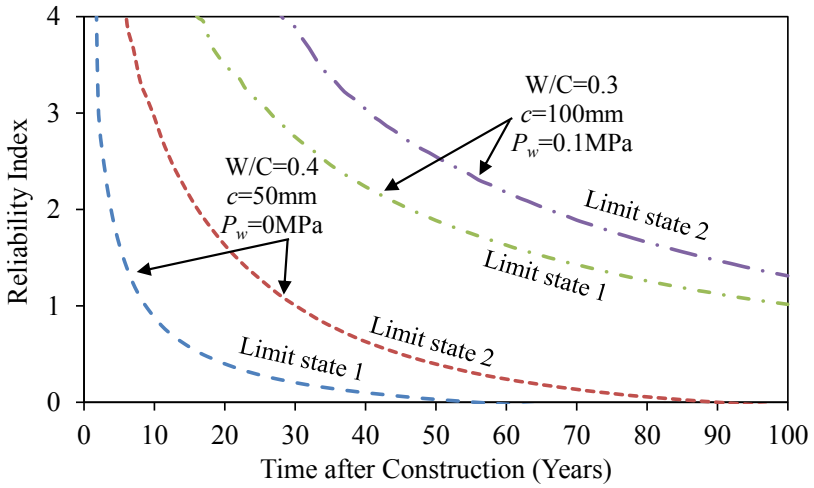

Figure 4.2 Reliability index for limit states depending on Equation 3-37 and 3-40

According to the hazard curves of underground chloride in Xiamen shown in Figure 3.3 (0.5 km from the coastline) and two limit states of structural serviceability (see Equation 3-37 and 3-40), the relationships between the reliability indices for structure with different designed parameters and time after structural construction are presented in Figure 4.2. As shown in Figure 4.2, the durability performance of RC segmental linings, under different marine environments (e.g. hydrostatic pressure and underground chloride contents), could be quantified based on this proposed approach.

4.3 Reliability-based design criterion

4.3.1 Proposed design criterion

In engineering, a target value, β_{target}, is given at structural design phase to ensure the serviceability of structures during their life-cycle. For the shield tunnels in coastal regions, because of the coupling effects of aggressive agents and high hydrostatic pressure, chloride transportation in concrete linings might not only include the diffusion process. Accordingly, a durability design method for shield tunnels in coastal regions is required based on the hazard assessment and effect of high hydrostatic pressure. Herein, the serviceability of structure is considered to be associated with the corrosion-induced cracks, and the limit state of structural serviceability is defined at the occurrence of first

corrosion-induced cracking. Next, a design criterion is proposed, so that the reliability index for the occurrence of corrosion cracking will be very close to the target value without complex reliability computations. After confirming that the time to occurrence, $T_{crack,d,}$ is larger than the lifetime of structure, T_d, the designers can determine the concrete cover and concrete quality. The design formulation proposed is:

$$T_d \le T_{crack,d} = \varphi\left(T_1 + T_2\right) \tag{4-3}$$

$$C_{S,d} = C_{Sea} \cdot 0.8^d \tag{4-4}$$

$$C_{\lim,d} = \frac{C_{S,d}}{2}\left[erfc\left(\frac{c_d - uT_1}{\sqrt{4DT_1}}\right) + e^{\frac{uc_d}{D}} erfc\left(\frac{c_d + uT_1}{\sqrt{4DT_1}}\right)\right] \tag{4-5}$$

$$T_2 = \frac{Q_{cr,d}}{V_d} \tag{4-6}$$

where φ is durability design factor taking into account the uncertainties in the computation of $T_{crack,d}$; T_1 and T_2 are the time of steel corrosion initiation and the time from steel corrosion initiation to occurrence of cracks, respectively; c_d is the design concrete cover; $C_{lim,d}$ is equal to C_t as the mean value; V_d is equal to V_1 as the media value; and $Q_{cr,d}$ is equal to Q_{cr} multiplied by X_4 as the median value.

To determine the durability design factor for tunnels in a marine environment, the procedure based on code calibration has the following steps:

(a) Set the target reliability index β_{target} and the life time of tunnel T_d.

(b) Set the calculation group under different marine environments (i.e. the design value of surface chloride content of tunnel using Equation 3-7 and design value of hydraulic pressure). In this study, 100 locations from 12 coastal cities of China are chosen to represent different marine environmental conditions.

(c) Assume the initial durability design factor φ.

(d) Determine the design concrete cover using Equation 4-5.

(e) Calculate β_i (i = 1, 2, …, 100) of tunnels under all cases that have the design concrete cover determined in step (d).

(f) Repeat steps (c) to (e) until

$$U = \sum_{i=1}^{100} (\beta_{\text{target}} - \beta_i(\varphi))^2 \tag{4-7}$$

is minimum, and the durability design factor is found.

4.3.2 Durability design factor

Specifications, like JSCE Standard Specifications (2002) and RILEM (1998), proposed the reliability indices ranging from 1.5 to 2.5 for serviceability limit state of RC structures. However, since the target lifetime of tunnels is generally almost 100 years or longer, it is very difficult to design using too high reliability indices. Thus, a target reliability index of Hong Kong-Zhuhai-Macau project for a working life of 120 years was suggested to be 1.3 (Li et al. 2015). Meanwhile, the Code for Durability Design of Concrete Structure of China (2008) suggests that failure probability of RC structures should range from 5% to 10% to ensure structural serviceability during its lifetime (i.e. β_{target} ranges from 1.282 to 1.645). In this study, β_{target} is set to be 1.1, 1.3 and 1.5, and the lifetime of tunnel is set to be 80 years, 100 years and 120 years. Minimum concrete cover is assumed 30 mm.

The calculated durability design factors for each target reliability index and lifetime are shown in Figure 4.3. This figure indicates that φ is more sensitive to β_{target} than to T_d. The reliability indices for structures under different requirements (i.e. prescribed lifetime, T_d, and target reliability value, β_{target}) and conditions (i.e. different cities, distance from coastline, d, hydrostatic pressure, P_w, and water to cement ratio, W/C) are listed in Table 4.1. As shown in Table 4.1, the reliability indices are very close to the target values. Therefore, based on the proposed design criterion and durability design factor, shield tunnels in a marine environment requiring target durability reliability indices for the prescribed lifetime can be designed.

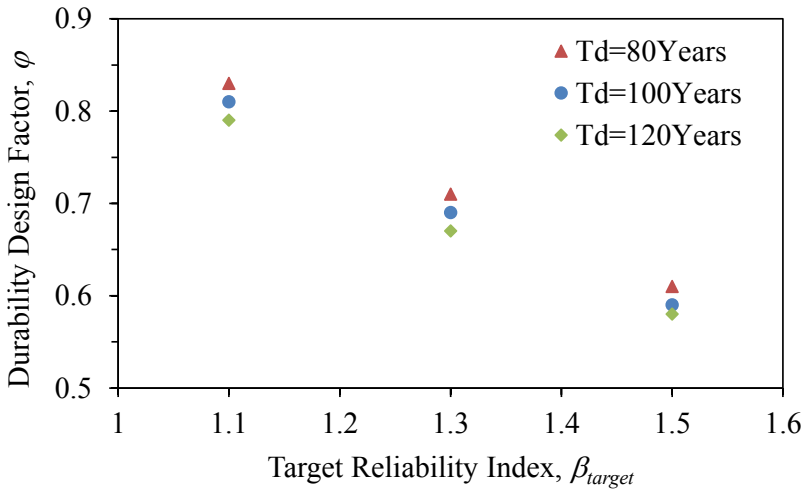

Figure 4.3 Relationship between lifetime of structures T_d, target reliability index β_{target} and durability design factor φ

Table 4.1 Reliability indices of RC tunnels using durability design factor

Coastal City in China	Case Considered								
	T_d=100Year β_{target}=1.3 P_w=0.2MPa d=0.3km			T_d=80Year β_{target}=1.5 P_w=0.08MPa d=0.5km			T_d=120Year β_{target}=1.3 P_w=0.6MPa d=0km		
	W/C = 0.3	W/C = 0.35	W/C = 0.4	W/C = 0.3	W/C = 0.35	W/C = 0.4	W/C = 0.3	W/C = 0.35	W/C = 0.4
Dandong	1.31	1.32	1.33	1.55	1.57	1.58	1.31	1.33	1.41
Tianjin	1.32	1.32	1.35	1.56	1.55	1.58	1.29	1.33	1.40
Yantai	1.30	1.31	1.34	1.53	1.55	1.58	1.29	1.34	1.40
Rizhao	1.21	1.23	1.24	1.44	1.44	1.44	1.21	1.25	1.33
Lianyungang	1.25	1.26	1.27	1.49	1.48	1.50	1.25	1.28	1.36
Ningbo	1.24	1.24	1.26	1.48	1.49	1.49	1.24	1.28	1.35
Zhoushan	1.19	1.20	1.22	1.43	1.41	1.44	1.20	1.24	1.31
Xiamen	1.27	1.28	1.31	1.51	1.52	1.55	1.29	1.31	1.38
Shantou	1.19	1.19	1.21	1.42	1.42	1.42	1.21	1.24	1.30
Shenzhen	1.26	1.28	1.30	1.49	1.51	1.51	1.27	1.29	1.37
Beihai	1.30	1.32	1.35	1.56	1.56	1.58	1.30	1.35	1.42
Zhanjiang	1.26	1.27	1.29	1.49	1.49	1.50	1.26	1.30	1.36
Mean	1.26	1.27	1.29	1.5	1.5	1.51	1.26	1.3	1.36
Standard Deviation	0.04	0.04	0.05	0.05	0.05	0.06	0.04	0.04	0.04
Coefficient of Variation	0.03	0.03	0.04	0.03	0.03	0.04	0.03	0.03	0.03

4.3.3 Maximum design ratio of water to cement associated with concrete cover and marine environments

As discussed in Chapter 3, in order to improve the long-term serviceability of shield tunnels in an aggressive environment, a lower ratio of water to cement and/or a thicker concrete cover of segment should be used. However, if the concrete cover of RC segment is too thick, higher tensile stress occurring in cover concrete would lead to more severe cracks, which is harmful to the structural durability. As a result, a limit value for maximum concrete cover of segments should be determined. According to a previous report (Song et al. 2009), which indicated an undersea tunnel in South Korea using designed concrete cover about 80 mm, a maximum design concrete cover of segment for shield tunnel in coastal regions is assumed to be 80 mm in this study.

For the segments with a concrete cover of 80 mm, the relationship between maximum ratio of water to cement and different marine environment (i.e. design water pressure and marine chloride concentration) are presented in Figure 4.4 to Figure 4.6 based on proposed design criterion. As shown in these figures, ratio of water to cement is suggested to be less than 0.35 for the RC shield tunnels in a marine environment, a similar suggestion has been proposed by Sun (2008). In addition, when the RC segmental linings are subjected to higher hydrostatic pressure, ratio of water to cement should be less than 0.3, so that these tunnels could satisfy the target reliability during its life-cycle.

For the undersea shield tunnels with target lifetime of 100 years under different target reliability (see Figure 4.4 (a), Figure 4.5(a) and Figure 4.6(a)), the functions of maximum ratio of water to cement depending on marine environments are proposed based on response surface method, as follows:

(a) Target lifetime of 100 years with target reliability of 1.1

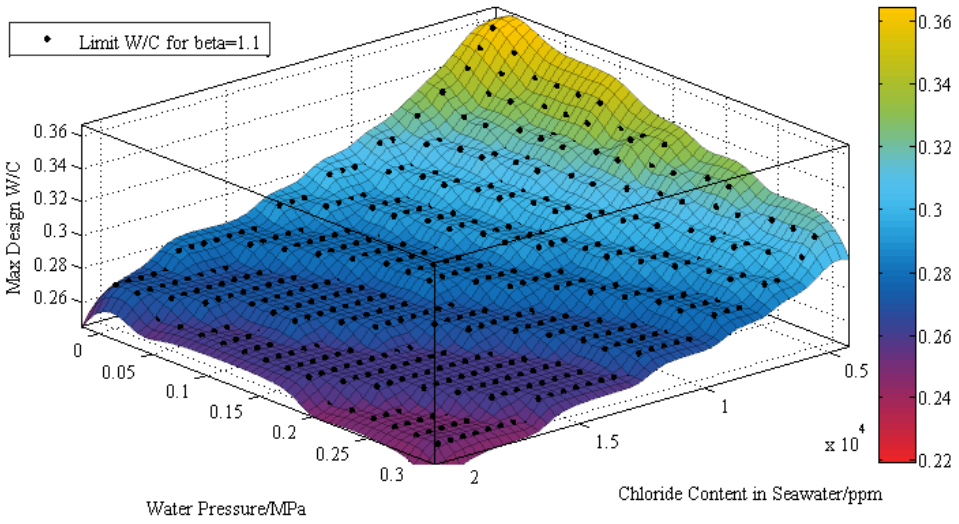

(a) Limit surface of water to cement ratio using MCS

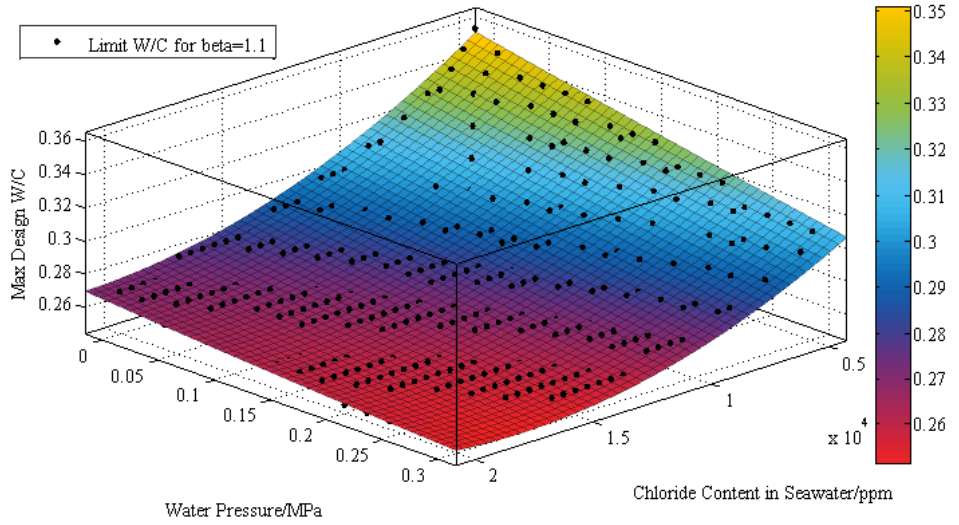

(b) Fitting surface of water to cement ratio using response surface method (RSM)

Figure 4.4 Maximum design ratio of water to cement for undersea shield tunnels with prescribed lifetime of 100 years and target reliability index of 1.1

$$[w/c]_{\max} = 0.3945 - 1.202\times10^{-5} C_{sea} - 0.1639 P_w + 2.884\times10^{-10} C_{sea}^{\ 2} + 5.062\times10^{-6} C_{sea} P_w + 0.02916 P_w^{\ 2} \quad (4\text{-}8)$$

(b) Target lifetime of 100 years with target reliability of 1.3

$$[w/c]_{\max} = 0.3612 - 9.739\times10^{-6} C_{sea} - 0.1192 P_w + 2.291\times10^{-10} C_{sea}^{\ 2} + 3.589\times10^{-6} C_{sea} P_w - 0.0094 P_w^{\ 2} \quad (4\text{-}9)$$

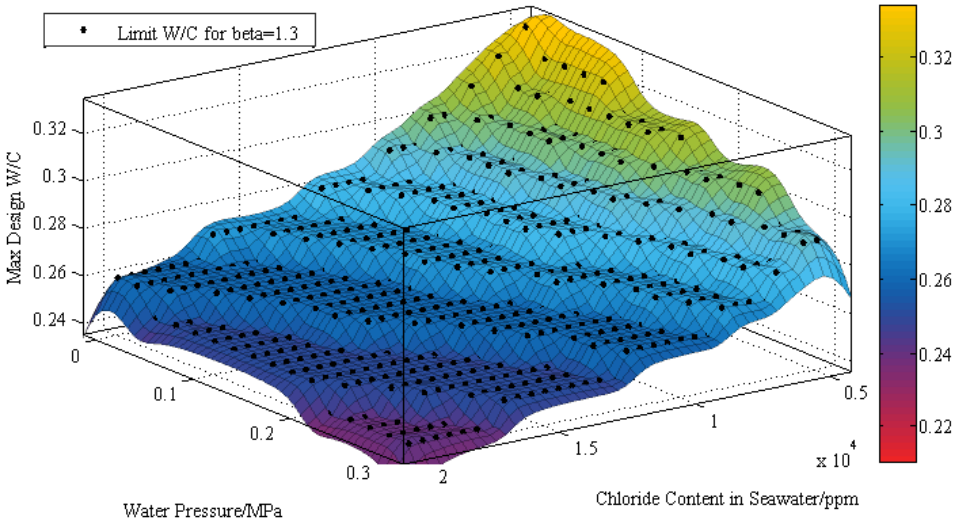

(a) Limit surface of water to cement ratio using MCS

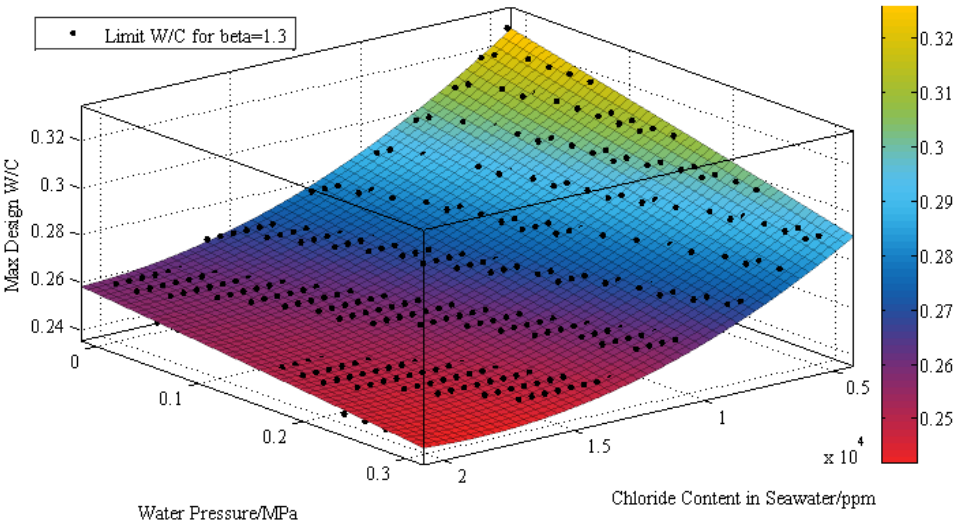

(b) Fitting surface of water to cement ratio using response surface method (RSM)

Figure 4.5 Maximum design ratio of water to cement for undersea shield tunnels with prescribed lifetime of 100 years and target reliability index of 1.3

(c) Target lifetime of 100 years with target reliability of 1.5

$$\begin{aligned}\left[w/c\right]_{\max} &= 0.3341 - 7.963\times10^{-6}C_{sea} - 0.09946P_w + 1.842\times10^{-10}C_{sea}^{\ 2} \\ &\quad + 2.721\times10^{-6}C_{sea}P_w + 0.0089P_w^{\ 2}\end{aligned} \tag{4-10}$$

The fitting surface for max design ratio of water to cement with different marine environments are presented in Figure 4.4(b), Figure 4.5(b) and Figure 4.6(b), based on Equations 4-8 to 4-10. These calculated surfaces can appropriately reflect the influence

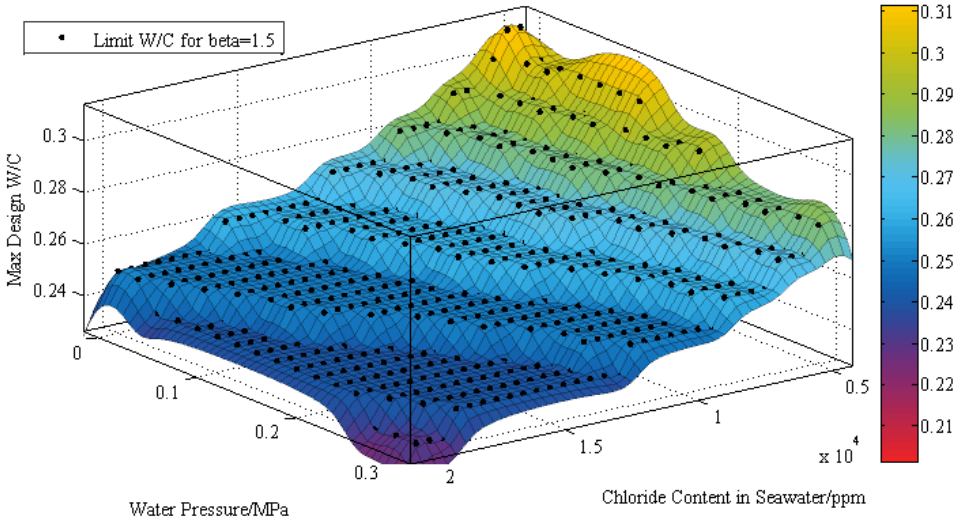

(a) Limit surface of water to cement ratio using MCS

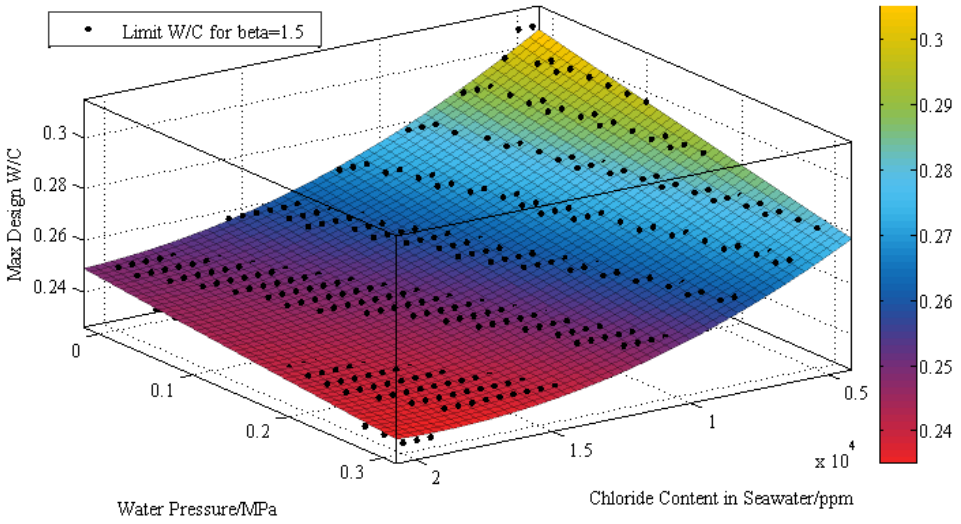

(b) Fitting surface of water to cement ratio using response surface method (RSM)

Figure 4.6 Maximum design ratio of water to cement for undersea shield tunnels with prescribed lifetime of 100 years and target reliability index of 1.5

of marine environments on the requirements of designing ratio of water to cement. However, if the RC segmental linings are under a severe marine environments, even though the ratio of water to cement is very low, the durability requirements of segmental linings cannot be satisfied as shown in Figures 4.4 to 4.6. Accordingly, other engineering measures to improve the durability of segmental linings should be taken into

consideration, such as protection coat on the surface of segment and reinforcement (Sun 2008).

4.4 Chapter Summary

(1) A computational procedure to integrate the chloride hazard around RC shield tunnel structures in a marine environment into reliability-based durability design using a partial factor was proposed. The effects of hydrostatic pressure and structural location on the durability reliability can be considered in the proposed method.

(2) A discussion about design criterion for RC segmental linings in a marine environment and durability design factors was presented to satisfy the target durability reliability level; Based on the proposed design criterion of RC segmental linings, the relationship between the marine environments and maximum design ratio of water to cement of RC segmental linings was revealed.

(3) According to this design method, proposed material parameters could generally ensure a higher long-term durability for structure during its life-cycle, compared to the design without considering environmental hazards. However, uncertainties of environmental hazards (e.g. underground chloride hazard), water pressure and prediction models, might be overestimated or underestimated at the design phase, thus maintenance activities are still needed after structural construction.

Chapter 5: Updating Structural Reliability of Existing Shield Tunnels

5.1 Procedure for the updated life-cycle reliability assessment of existing shield tunnels in a marine environment

Uncertainties including aleatory and epistemic cannot be neglected for the problems in the real world (Ang and Tang 2007; Frangopol 2011; Biondini et al. 2016). For a new RC shield tunnel in an aggressive environment, reliability-based durability design generally could ensure structure to provide an acceptable service during its life-cycle. However, in terms of the existing structures, those structures might be designed without durability measures, or using an overestimated /underestimated uncertainty at structural durability design phase. In order to accurately estimate structural performance of existing RC segmental linings during their remaining lifetime, inspection and monitoring activities has been widely adopted in engineering, so that the repair and maintenance action can be carried out in time to extend structural service life. For results of inspection and monitoring activities, they could not only provide an indicator reflecting structural deteriorating state, but also reduce the uncertainty related to structural performance assessment during structural life-cycle (Biondini et al. 2016).

Figure 5.1 depicts a flowchart for computing the life-cycle reliability of RC shield tunnels in a marine environment incorporating with the inspection information. As shown in Figure 5.1, new RC shield tunnels and existing RC shield tunnels are both considered in this framework. One of the main differences in the life-cycle reliability assessment process for new and existing RC shield tunnels is whether the observation information is available (i.e. part 5). In terms of the procedure from Part 1 to Part 4, it have been illustrated in Chapter 3 based on Figure 3.1. For the new structures and the existing

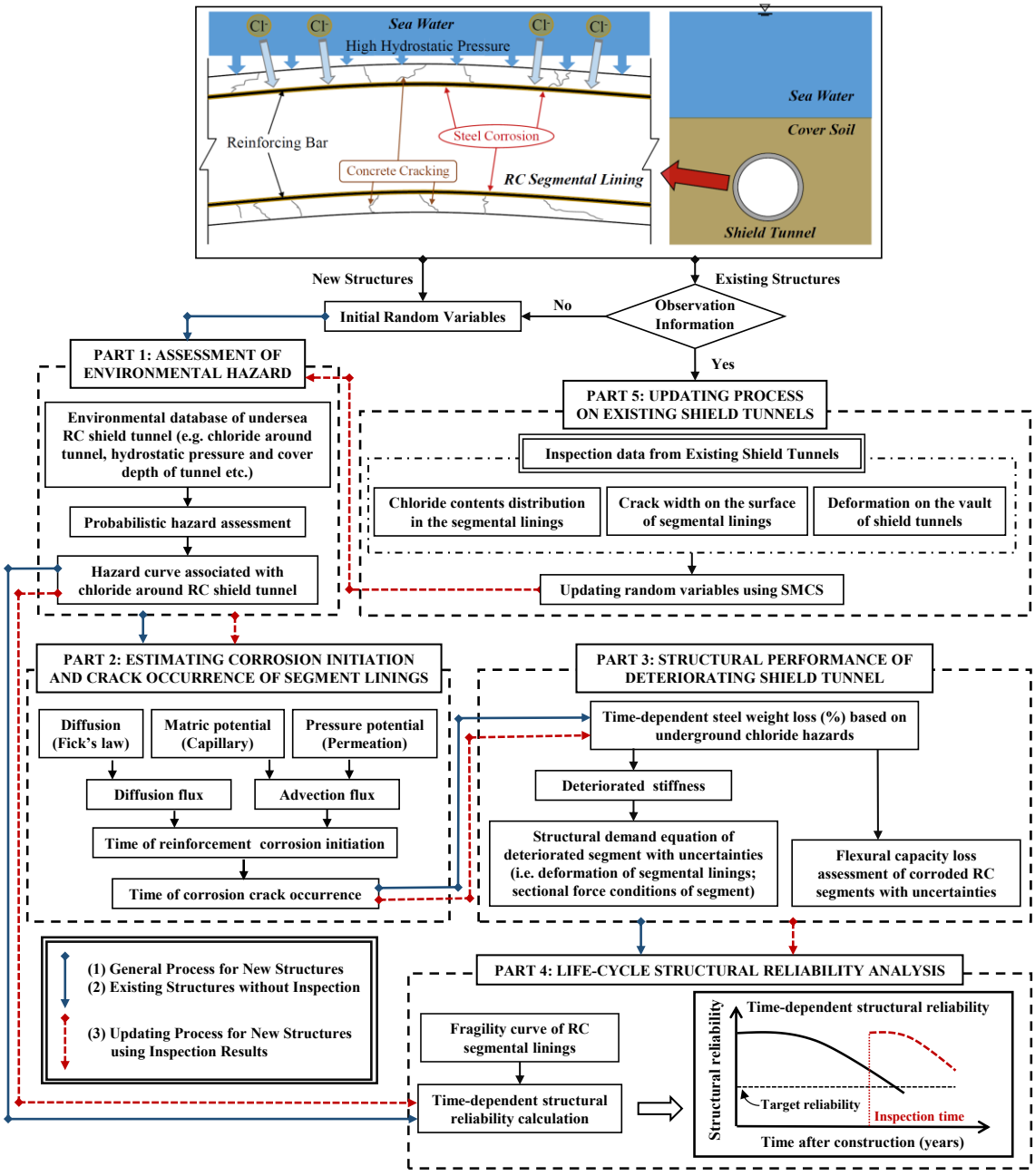

Figure 5.1 Flowchart to estimate the life-cycle reliability of RC shield tunnels in coastal regions using inspection information

structures without available observation information, the life-cycle reliability of RC shield tunnels can be calculated following this procedure using initial parameters of random variables. However, when the observation information is available for existing structures, the parameters of random variables can be updated via Sequential Monte Carlo Simulation (SMCS) as shown in Part 5. Finally, based on the procedure from Part 1 to

Part 4, the life-cycle reliability of existing RC shield tunnels can be updated by inspection information.

5.2 Algorithm of sequential Monte Carlo simulation

In general, to update reliability of existing structures based on the inspection data, the updating approach could be classified into two steps: (1) updating for the probability density functions (PDFs) of model parameters; (2) updating structural reliability using updated random variables. However, due to the complexity of observed data and random variables, it is not easy for the updated PDFs of model parameters to be expressed as a common distribution format, like normal distribution and lognormal distribution. Bayesian updating (Ang and Tang 2007) has been widely recognized to update structural reliability based on on-site information, but only when the prediction models are linear and/or random variables are normal distribution, a closed form solution of updated PDF could exist using this approach (Yoshida 2009), so that it is difficult to achieve the PDF updating according to a rigorous theoretical approach in engineering, because of less linear models or normal distribution for random variables in the real world (Yoshida 2009; Akiayam et al. 2010).

In order to solve this problem and implement the PDF updating with non-linear models and non-normal distribution of random variables, significant advances have been accomplished to get approximate solutions. Sequential Monte Carlo Simulation (SMCS) is one of those approaches with a convenient computation procedure, and it has been used to update structural reliability of existing RC structures (Yoshida 2009; Akiayam et al. 2010). In this study, SMCS was adopted in conjunction with the time-dependent reliability assessment of existing RC shield tunnels. With respect to the SMCS for existing structures, the updating procedure using SMCS includes time updating process and observation updating process, the detailed introduction could be found in Yoshida

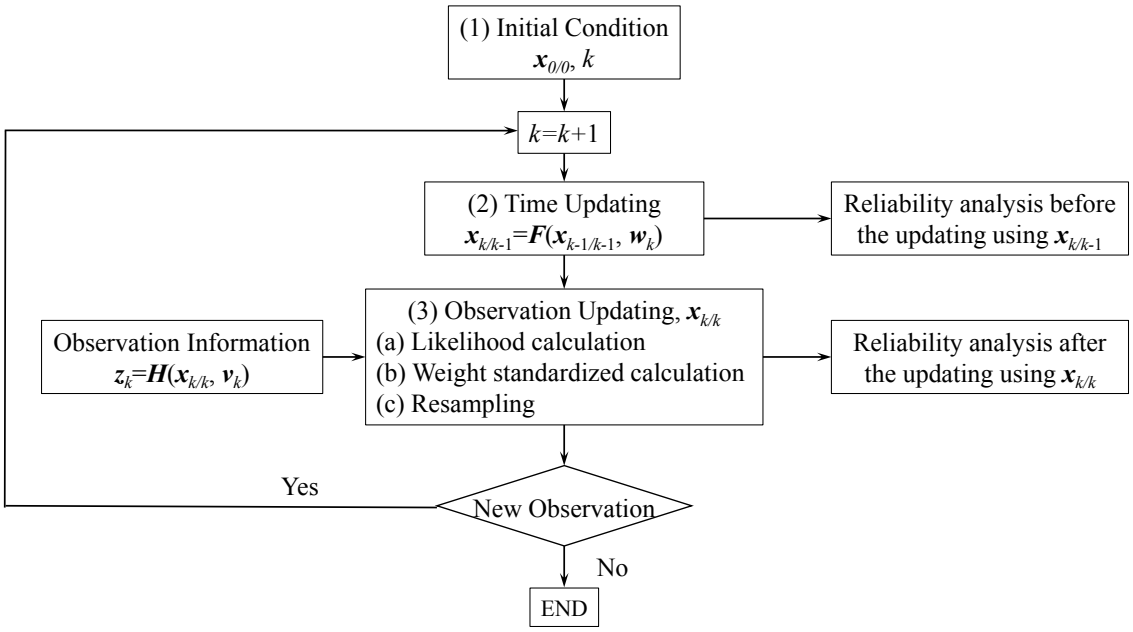

Figure 5. 2 Flowchart of updating reliability based on SMCS (Akiyama et al 2010)

(2009) and Akiyama et al. (2010). Herein, a brief summary of the SMCS approach for updating random variables is described based on Figure 5.2.

As shown in Figure 5.2, time updating process is the first step to predict the un-updated state vector at the k-th step (e.g. steel weight loss at 30th year before updating) using information at the (k-1)-th step (e.g. steel weight loss at 29th year), and the predicted state vector, $x_{k/k-1}$, can be expressed as a function as below:

$$x_{k/k-1} = F\left(x_{k-1/k-1}, w_k\right) \tag{5-1}$$

where w_k is the system noise associated with the uncertainty involved in the prediction process. For this equation, the cases associated with non-linear states and non-Gaussian random variables have been included.

In the observation updating process, updated state vector, $x_{k/k}$, could be gotten based on the predicted state vector, $x_{k/k-1}$, from Equation 5-1 and the observation information, z_k. For the observation information, z_k, it is assumed as a function of updated state vector $x_{k/k}$ and observation noise v_k, shown as follow.

$$z_k = H\left(x_{k/k}, v_k\right) \tag{5-2}$$

With respect to the PDFs of the noises, $p(w_k)$ and $p(v_k)$, in Equation 5-1 and 5-2, they are assumed known and independent in the updating process. Observation updating process using predicted state vector and observation information includes three sub-steps: (1) likelihood for each samples; (2) weight standardizing (likelihood ratio) and (3) resampling of random variables. Finally, updated reliability of structures could be gotten based on resampling results of random variables associated with the inspection information.

5.3 Modeling of observational data for deteriorating shield tunnels

For the existing RC shield tunnels in an aggressive environments, structural degradation level could be reflected using inspection information. According to different deterioration states of RC shield tunnels described in Chapter 3, three types of observed information are used here to update structural reliability, including the chloride contents in segmental linings, corrosion-induced cracks on the surface of segmental linings and the deteriorating deformation on the vault of shield tunnel.

(1) Modeling of observed chloride contents in segmental linings

With respect to the inspection data relating to chloride contents in segmental linings, it could provide more information to accurately evaluate the time of corrosion initiation of reinforcement in the segmental linings. This approach could decrease the uncertainty for estimating structural performance of deteriorating RC shield tunnels at initial stage. When chloride content distribution by on-site monitoring is given, the observed equation related to the inspection data of chloride contents is:

$$z_{cl} = 0.001 X_1 X_3 \frac{C_{soil}}{2}\left[erf\left(\frac{d'-ut}{\sqrt{4Dt}}\right) + e^{\frac{ud'}{D}} erfc\left(\frac{d'+ut}{\sqrt{4Dt}}\right)\right] + v_{cl} \tag{5-3}$$

where z_{cl} is the observed chloride contents at distance d' from the segment surface; v_{cl} is observation noise for chloride contents, assumed to be a standard normal distribution; D

is the chloride ion transportation coefficient in concrete, mm^2/year; u is the average velocity of chloride motion, mm/year; C_{soil} is the chloride content of the soil, ppm; X_1 is a lognormal random variable representing model uncertainty; and X_3 is a lognormal variable representing the model uncertainty associated with estimation of time-dependent chloride concentration.

(2) Modeling of observed corrosion-induced cracks on the surface of segmental linings

After the occurrence of corrosion initiation, expansion of rust formation results in cracking in the cover concrete of segmental linings. Generally, the corrosion-induced cracks is associated with the amount of steel weight loss. Since it is difficult to measure the steel weight loss in segmental linings directly and accurately, visual inspection for corrosion-induced crack width on the surface of segments, reflecting the amount of steel weight loss, was adopted as an observational information in SMCS.

Considering the relationship between amount of steel weight loss and corrosion-induced crack width generally is complex and uncertain, an observation model for visual inspection of corrosion crack width has been proposed by Akiyama (2010) via the survey of marine RC structures (Kodama et al. 2002). Four categories associated with corrosion-induced crack width, steel weight loss and deterioration state were classified. The probabilities for each categories of crack widths associated with different categories of steel weight loss are shown in Table 5.1. When the category of steel weight loss is given using estimating equations, the probability, used to calculate likelihood for each sample in observation updating process, could be determined based on the category of observational crack width shown in Table 5.1.

(3) Modeling of observed deformation on the vault of shield tunnel

With the decrease of structural stiffness due to steel weight loss and corrosion-induced cracking, structural deformation of segmental linings, reflecting the structural integrity

Table 5.1 Observation model of visual inspection of corrosion crack width (Akiyama et al. 2010)

Category based on steel weight loss	Category based on crack width			
	I (0-0.1mm)	II (0.1-0.2mm)	III (0.2-0.5mm)	IV (>0.5mm)
1 (SWL=0-2.3%)	0.811	0.159	0.031	0.000
2 (SWL=2.3%-5%)	0.268	0.410	0.313	0.009
3 (SWL=5%-20%)	0.019	0.120	0.600	0.261
4 (SWL>20%)	0.000	0.004	0.219	0.776

degradation, would increase significantly. As an important part of the on-site monitoring of a tunnel structure, the deterioration deformation of segmental linings could directly provide estimated results for structural serviceability at the inspection time. Meanwhile, according to the observed structural deformation, uncertainties associated with predicting the deformation of segmental linings could decrease in the remaining lifetime of shield tunnels. Thus, the observational equation based on the inspected structural deformation could be expressed as:

$$z_{disv} = Disv_{estimation} + v_{dis} \tag{5-4}$$

where z_{disv} is the observed deformation on the vault of shield tunnel; $Disv_{estimation}$ is the predicted deformation on the vault of shield tunnel at t-th year after structure construction according to the calculating procedure proposed in Chapter 3; and v_{dis} is the observation noise for deformation inspection with a standard normal distribution, depending on the magnitude of measuring error using measuring devices.

5.4 Time-dependent structural performance analysis based on inspection results

5.4.1 Structural reliability margin for existing shield tunnels

Structural serviceability is regarded as a significant part for structural durability, an appropriate serviceability limit based on structural degradation degree could guarantee structural safety to be satisfied during its lifetime. According to the durability demands

of RC shield tunnels reported by Sun (2008), serviceability limit state of segmental linings was proposed that the deformation of segmental linings should be less than 4% of the external diameter of shield tunnel. In this study, the time-dependent margin of structural serviceability, $Z(t)$, is described by the deformation on the vault of shield tunnel, $Disv(t)$, and the limit value for deformation of shield tunnel, $Disv_L$ (i.e. 4% of the external diameter of shield tunnel). Thus, the failure probability, $P_f(t)$, is expressed as:

$$P_f(t) = P\left[Z(t) = Disv(t) - Disv_L > 0\right] \tag{5-5}$$

The shield tunnel studied here is assumed to be located at Xiamen of China. The depth of the shield tunnel is assumed to be 12 m, structure is located in a layer of completely weathered granite, and the overlying stratum is sludge and residual sandy sticky clay with a depth of 5.4 m and 2.6 m. Meanwhile, the segmental linings are assumed to withstand water pressure of 0.1 MPa. The key parameters of the random variables to calculate structural reliability could be found in Table 3.4 and Table 3.5.

Considering the influence of observational information on decreasing uncertainty may be different, assumed observational data are listed in Table 5.2 and Table 5.3, including crack width, chloride contents distribution and structural deformation. Then, cumulative distribution function (CDF) of random variables before and after updating with different observation data are partial presented in Figure 5.3 and 5.4; Also, the distribution of predicted deformation on vault of segmental linings before and after updating and time-dependent reliability of existing segmental linings are shown from Figure 5.5 to 5.8.

5.4.2 Time-dependent reliability analysis of existing segmental linings

Figure 5.3 illustrated the CDFs for parameters of random variables before updating (Case 0) and after updating (Case 2, 5, 7 and 10) using different type of observed data. According to these figures, the influence of inspection information on the random

Table 5.2 List of assumed observation data

	Year of Inspection	Visual inspection (crack width)	Distribution of Chloride Contents	Vertical Deformation
0	-	-	-	-
1	70	I	-	-
2	70	II	-	-
3	70	III	-	-
4	70	-	A*	-
5	70	-	B*	-
6	70	-	C*	-
7	70	-	-	20 mm
8	70	-	-	30 mm
9	70	-	-	40 mm
10	70	II	B*	20 mm
11	50	-	-	20 mm

*Detail data shown in Table 5.4

Table 5.3 Assumed chloride contents distribution (kg/m^3) (Akiyama et al. 2010)

Distribution	Distance from concrete surface				
	10 mm	30 mm	50 mm	70 mm	90 mm
A	1.2	0.9	0.75	0.65	0.55
B	2.44	1.92	1.44	1.08	0.81
C	5.5	4	3	2	1.1

variables of X_R and X_4 is limited, and the COVs of these two random variables are almost same compared to the case without updating (case 0). Meanwhile, for the random variables associated with inspection information, the COVs of them are indicted to be decreased after updating using observed data (see Figure 5.3 (b), (c), (d), (e) and (g)). Similar results are also obtained for the other cases. In particular, for the random variable of X_2 shown in Figure 5.3(d), the difference is small before and after updating, but obvious decrease of COV could be seen in other cases as presented in Figure 5.4.

After updating the parameters of random variables, a new distribution for predicted deformation on the vault of shield tunnel can be calculated. As shown in Figure 5.5, the influence of each type of inspection information on the distribution of predicted

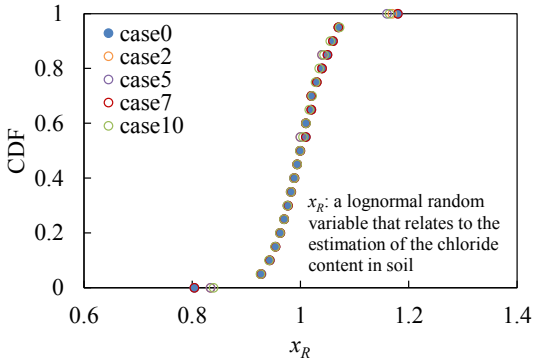

(a) X_R

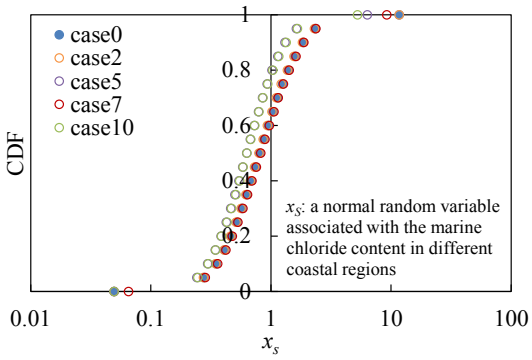

(b) X_s

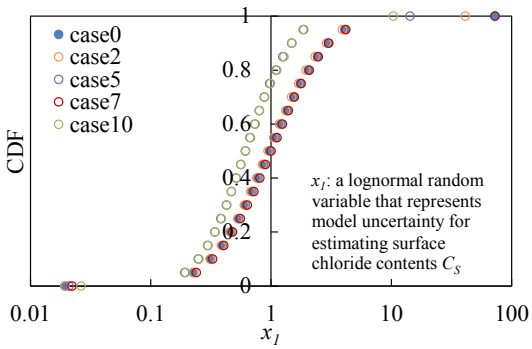

(c) X_1

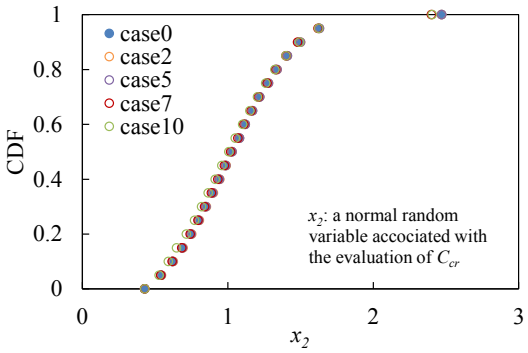

(d) X_2

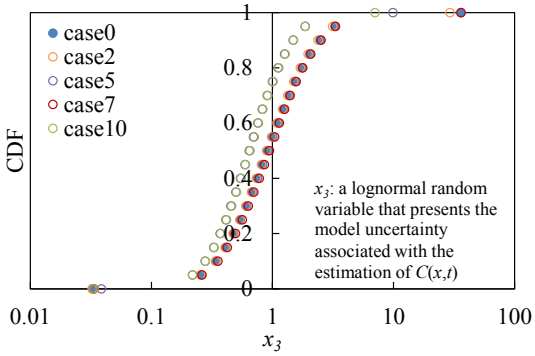

(e) X_3

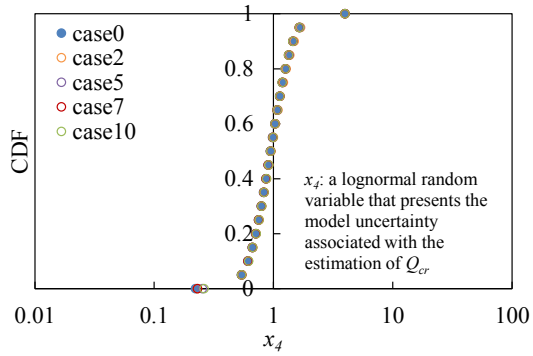

(f) X_4

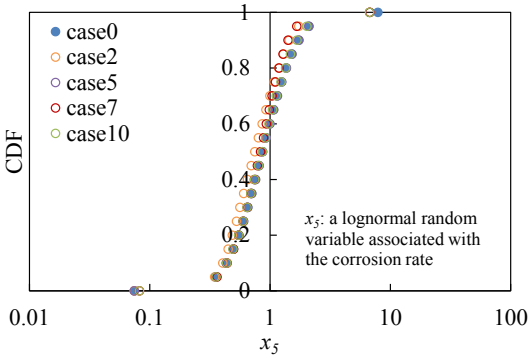

(g) X_5

Figure 5.3 CDF of random variables before and after updating (Case 0, 2, 5, 7, 10)

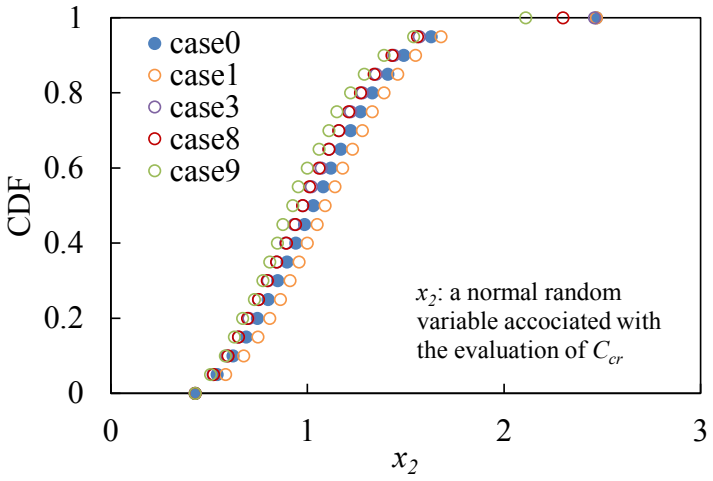

Figure 5.4 CDF of X_2 before and after updating (Case 0, 1, 3, 8, 9)

deformation on the vault are very different, the most sensitive observed results should be the measured deformation on the vault. Since the predicted deformation is updated by the measured deformation directly, COV of predicted deformation decreases most significantly. However, for the cases updated using the chloride contents in segmental linings, there is not so much different for the distribution of predicted deformation among each cases. Therefore, the measured structural deformation could provide the most accurate and helpful information for performing the structural performance assessment of existing shield tunnels.

According to the updated parameters of random variables presented in Figure 5.3, the time-dependent COVs of deformation on the vault of shield tunnels for these cases are depicted in Figure 5.6. As shown in this figure, the COVs of predicated deformation on the vault decrease after updating. Especially for the case 10 updated using the three types of observed data: crack width, chloride contents and measured displacement on the vault, the COV decreases most significantly, compared with the cases only using one type of inspection information. However, Figure 5.6 also reveals that the COVs of deformation would increase with time after updating, the reason for this phenomenon should be caused by the non-linear formulas for predicting the deformation. As a result, regular inspection,

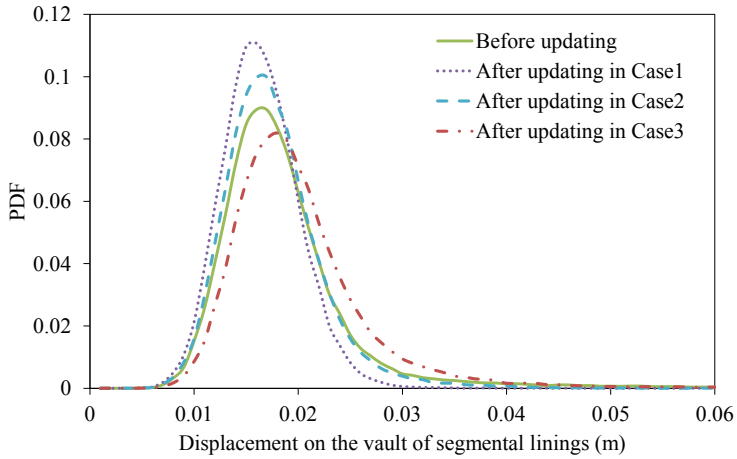

(a) Updating using crack width

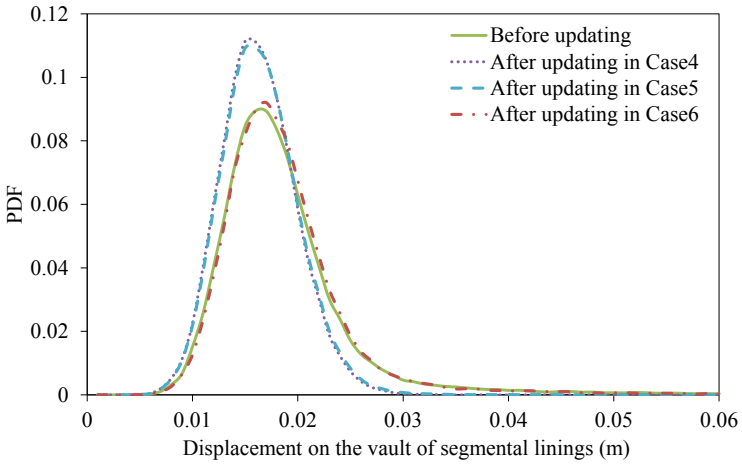

(b) Updating using chloride content distribution

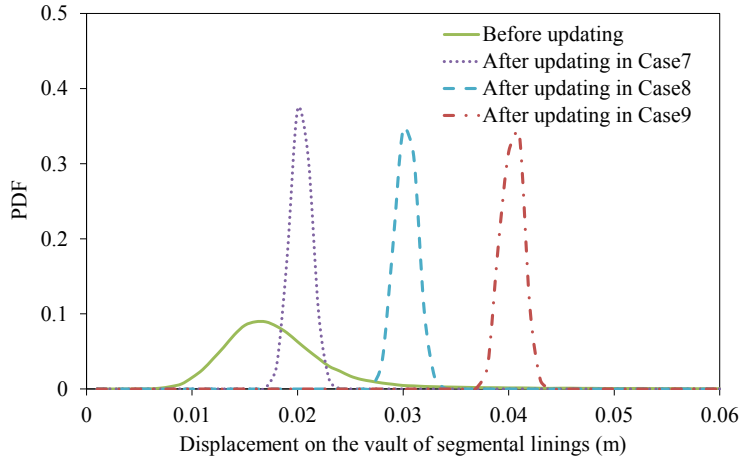

(c) Updating using measured displacement on vault

Figure 5.5 Distribution of predicted deformation on vault of shield tunnel before and after updating

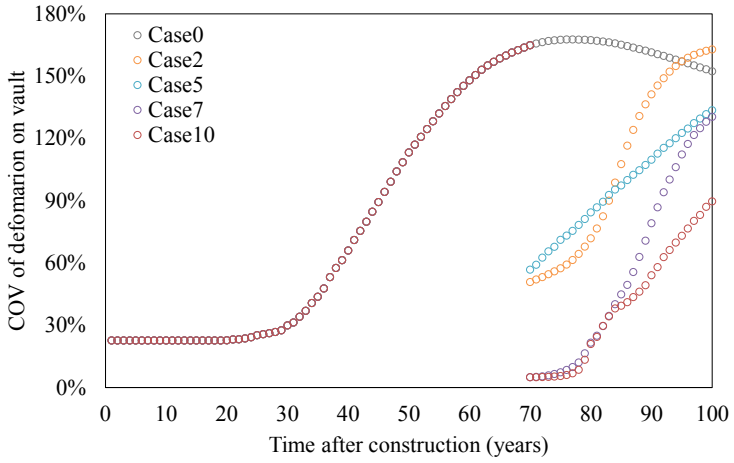

Figure 5.6 COV of deformation on the vault of shield tunnels (Case 0, 2, 5, 7, 10)

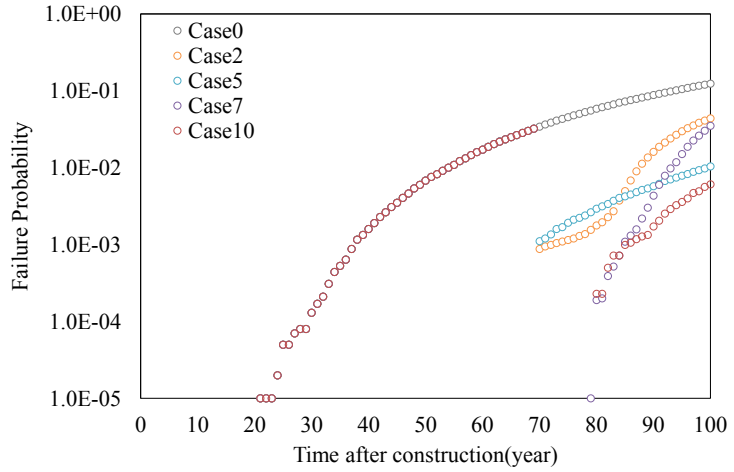

Figure 5.7 Time-dependent failure probability of shield tunnels (Case 0, 2, 5, 7, 10)

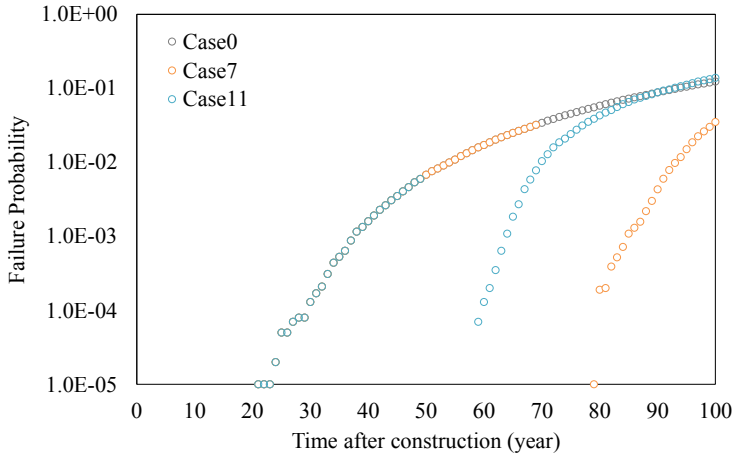

Figure 5.8 Time-dependent failure probability of shield tunnels (Case 0, 7, 11)

like time interval for inspection in 5 years or 10 years, is extremely advisable to predict structural performance of existing segmental linings more accurately, so that the maintenance actions could be carried out in time.

Furthermore, the time-dependent failure probability of segmental linings before updating and after updating are shown in Figure 5.7. Since the COV of predicated deformation on the vault of shield tunnels reduces, structural reliability should be more accurate than that without updating, and more inspection results could be beneficial for performing a more precise reliability assessment. Meanwhile, the failure probabilities for the shield tunnels updated at 50 years (case 11) and 70 years (case 7) by a same measured displacement of vault are presented in Figure 5.8. According to this figure, in order to ensure the structural serviceability and safety of RC shield tunnels over their entire life-cycle, a strict limit for the deformation of shield tunnel is required, especially for the structures with a longer remaining lifetime.

5.5 Chapter Summary

(1) A framework for estimating time-dependent structural performance of existing RC shield tunnels in a marine environments was proposed. In this framework, an updating process for structural reliability assessment using SMCS incorporating with inspection results, such as chloride contents distribution in segmental linings, corrosion-induced crack width and measured structural deformation, was illustrated.

(2) The effect of different type of inspection information on the updated estimates of RC segmental linings was discussed. With respect to the measured structural deformation, it could be regarded as the most helpful information for performing a more accurate structural reliability assessment of existing structures. This result should be taken into consideration for the decision-making process of establishing a reliability-based assessment criteria for existing RC shield tunnels using observed information.

(3) To decrease the uncertainty of structural reliability estimates, it is extremely advisable to increase the inspection frequency (i.e. a shorter time interval for inspection) during structural life-cycle and collect more inspection results. This procedure can improve the estimating precision and support the decision-making process for structural maintenance and repair during their remaining lifetime.

Chapter 6: Conclusions and Future Works

6.1 Conclusions

In this research, considering the corrosion-induced deterioration of segmental linings, life-cycle durability design and structural performance assessment of RC shield tunnels in coastal regions has been studied based on the probabilistic methodology. First of all, three original and novel flowcharts are proposed to consider the topics that (1) Time-variant structural performance analysis of shield tunnels in coastal regions; (2) Life-cycle reliability-based durability design of shield tunnels in coastal regions; (3) Updating time dependent structural reliability of existing shield tunnels. According to the flowcharts, six originally primary achievements in this study are summarized as below:

(1) A probabilistic model for estimating the hazard associated with the underground chloride in coastal regions was established. Based on this model, the effect of the aggressive environment on RC tunnel structures could be quantified.

(2) To study the corrosion-induced deterioration of concrete segments under the coupling effects of chloride attack and loading, the deterioration processes of segmental linings were experimentally illustrated using corrosion-accelerated specimens of a tunnel segment. Based on the experimental results, damage models associated with loading-induced and deteriorating damage in segmental linings was proposed. Meanwhile, steel corrosion in RC segments depending on loading effect was revealed.

(3) A novel probabilistic model for evaluating time-dependent distribution of chloride in segmental linings was established with the impact of hydrostatic pressure. And thus, the time to corrosion initiation can be estimated considering the combined effects of chloride contents and hydrostatic pressure. According to this probabilistic model, it reveals that, for undersea shield tunnels, the external reinforcement in segmental

linings generally undergoes high corrosion risks because of the high hydrostatic pressure and high concentration of aggressive agents.

(4) A computational procedure to integrate the underground chloride hazard around shield tunnel into time-variant reliability of shield tunnels in coastal regions was proposed. In this procedure, structural performance degradation induced by steel corrosion has been emphasized; meanwhile, the influences of hydrostatic pressure, structural location and material properties on structural failure were quantified.

(5) With respect to the new shield tunnel in coastal regions, a reliability-based durability design criterion for shield tunnel, considering the influence of chloride hazard and hydrostatic pressure, was proposed based on the partial factor method; According to this proposed design approach, a maximum design value of water to cement ratio for RC segment was suggested depending on different marine environments.

(6) In term of existing shield tunnel in coastal regions, a novel updating process for structural reliability using inspection results has been illustrated based on Sequential Monte Carlo Simulation. According to the updating results, measured structural deformation from on-site monitoring was indicated to have a significant influence on improving the estimating precision for structural performance of existing tunnels; meanwhile, a short inspection interval and more inspection results also strongly contribute to decrease the uncertainty of existing structures during their remaining lifetime.

6.2 Future works

This research presented a big framework to study life-cycle performance of RC shield tunnels in a marine environment, but it only emphasized on the deterioration of segmental linings due to external reinforcement corrosion. With respect to the durability of RC shield tunnels, structural performance during their life-cycle is influenced by multiply

factors, and structural degradation process is very complex. Therefore, further researches on life-cycle performance of RC shield tunnels should be carried out, and some suggestions for future works are proposed as follows.

(1) In engineering, segmental joints have high risks of seepage and leakage due to high water pressure and gap at the segment joint, it is easy to make the bolt corroded. To study the deterioration of joint, two primary contents should be considered. First, the transport process of seawater through the joint should be revealed, which could be used to estimate the time to corrosion initiation of bolts. Numerical simulation is suggested to study the transport process of seawater due to coupling effects of different material properties and complex component shape around joint. Second, the mechanical performance of deteriorated joint should be studied based on experimental testing, which could be used to improve the accuracy of structural performance assessment for deteriorated shield tunnels during structural lifetime.

(2) In terms of the internal reinforcement of segmental linings, they are subjected to attacks from air-born aggressive agents in the internal service environment of shield tunnels, such as carbonation-induced corrosion, chloride-induced corrosion for tunnels close to sea. Accordingly, the influence of air-bone aggressive agents in shield tunnels on deterioration of segmental linings should be considered. Next, the deterioration process of segmental linings due to corrosion of internal reinforcement and external reinforcement is recommended to be studied.

(3) In this study, structural integrity degradation of shield tunnels was considered. However, for the real structures, local deterioration of structures is more common than integrity deterioration. Accordingly, local deterioration mechanism for structural component should be revealed; next, an approach for estimating structural performance due to local deterioration are suggested to be established.

(4) With respect to the updating process for structural performance assessment of existing tunnels, it is complex for engineers to carry out this full-probabilistic approach based on inspection information. In engineering, semi-probabilistic approach using simple formula and probabilistic parameters is more easily accepted due to convenience. Therefore, it is suggested, based on the SMCS updating method, to establish a semi-probabilistic approach using inspection information to evaluate the structural performance of existing tunnels.

(5) Since China and Japan are located in Circum-Pacific Earthquake Zone, high seismic hazard generally causes RC shield tunnels in coastal regions of these two countries undergo a high risk of structural failure, especially for the deteriorated shield tunnels. Therefore, life-cycle reliability assessment of RC shield tunnels under multiple hazards, including underground chloride hazard and seismic hazard, should be carried out.

References

Akiyama, M., Frangopol, D.M. & Yoshida, I., 2010. Time-dependent reliability analysis of existing RC structures in a marine environment using hazard associated with airborne chlorides. *Engineering Structures*, 32, 3768-3779.

Akiyama, M., Frangopol, D.M., & Suzuki, M., 2012. Integration of the effects of airborne chlorides into reliability-based durability design of reinforced concrete structures in a marine environment. *Structure and Infrastructure Engineering*, 8(2), 125-134.

Ang, A.H.-S and Tang, W.H., 1984. *Probability concepts in engineering planning and design. Vol. II*. New York: John Wiley and Sons.

Ang, A.H.-S and Tang, W.H., 2007. *Probability concepts in engineering: Emphasis on applications to civil and environmental engineering*. 2nd edn. New York: Wiley.

Angst, U., Elsener, B., Larsen, C.K., & Vennesland, Ø., 2009. Critical chloride content in reinforced concrete-A review. *Cement and Concrete Research*, 39, 1122-1138.

Ann, K.Y., Ahn, J.H., & Ryou, J.S., 2009. The importance of chloride content at the concrete surface in assessing the time to corrosion of steel in concrete structures. *Construction and Building Materials*, 23, 239-245.

Bagnoli, P. et al., 2015. A method to estimate concrete hydraulic conductivity of underground tunnel to assess lining degradation. *Tunnelling and Underground Space Technology*, 50, 415-423.

Bertolini L., 2011. Steel corrosion and service life of reinforced concrete structures. *Structures and Infrastructures Engineering*, 26, 123-137.

Bhargava, K., Ghosh, A.K., Mori, Y., & Ramanujam, S., 2006. Analytical model for time to cover cracking in RC structure due to rebar corrosion. *Nuclear Engineering and Design*, 236, 1123-1139.

Bigaj, A., Kooiman, A., 2003. Monitoring durability aspects of the Green Heart Tunnel linings. *IABSE Symposium Report*, 87(2), 51-58.

Biondini, F., & Frangopol, D.M., 2016. Life-cycle performance of deteriorating structural systems under uncertainty: review. *Journal of Structure Engineering*, 142(9), 1-17.

Breitenbucher, R., Gehlen, C., & Schiessl, P., 1999. Service life design for the Western Scheldt Tunnel. *Durability of Building Materials and Components*, 8, 3-15.

Chen, D., & Mahadevan, S., 2008. Chloride-induced reinforcement corrosion and concrete cracking simulation. *Cement & Concrete Composites*, 30, 227-238.

Chen, H., Sun, F., & Wang, Y., 2008. Service life prediction of Xiamen Xiang'an subsea tunnel linings structure. *Proceedings of the International Conference on Durability of Concrete Structures*. November, 2008. Hangzhou, China, 992-997.

Costa, A., & Appleton, J., 2002. Case studied of concrete deterioration in a marine environment in Portugal. *Cement & Concrete Composites*, 24, 169-179.

Guo, Z., Huang, Y., Cai, M., & Liu, G., 2004. Nutrition Content and Indicator Value of Chlorion for Groundwater in Xiamen Island. *Site Investigation Science and Technology*, 3, 47-50. [In Chinese]

EI Maaddawy, T., Soudki, K., & Topper, T., 2005. Long-term performance of corrosion-damaged reinforced concrete beams. *ACI Structural Journal*, 102, 649-656.

Ellingwood, B.R., 2005. Risk-informed condition assessment of civil infrastructure: state of practice and research issues. *Structure and Infrastructure Engineering*, 1(1): 7-18.

Eurocodes, C.T.-S., 2002. EN 1990: 2002 Eurcode-Basis of structural design.

Estes, A.C., & Frangopol, D.M., 2005. Life-cycle evaluation and condition assessment of structures. Chapter 36, *Structural engineering handbook*, 2nd Ed., W.-F. Chen, and E.M. Liu, eds., CRC, Boca Raton, FL, 36-1-36-51.

Fagerlund, G., 1995. Penetration of chloride through a submerged concrete tunnel. *Report TVBM-7077*, 1-17.

Faroz, S.A., Pujari, N.N., & Ghosh, S., 2016. Reliability of a corroded RC beam based on Bayesian updating of the corrosion model. *Engineering Structures*, 126, 457-468.

fib, 2012. *Model Code 2010* — Vol. 1 & 2. Bulletins. Lausanne, International Federation for Structural Concrete (*fib*).

fib, 2018. *Safety and Performance Concepts — Reliability assessment of concrete structures*. Bulletin 86. Lausanne, International Federation for Structural Concrete (*fib*).

Francois, R. & Arliguie, G., 1999. Effect of micro-cracking and cracking on the development of corrosion in reinforced concrete members. *Magazine of Concrete Research*, 51(2), 143-150.

Frangopol, D.M., Lin, K.-Y., & Estes, C., 1997. Reliability of reinforced concrete girders under corrosion attack. *Journal of Structural Engineering*, 123(3), 286-297.

Frangopol, D.M., 2011. Life-cycle performance, management, and optimization of structural systems under uncertainty: accomplishments and challenges. *Structure and Infrastructure Engineering*, 7(6), 389-413.

Funahashi, M., 2013. Corrosion of underwater reinforced concrete tunnel structures. *Corrosion*, 1-15.

GB 50010-2002, 2002. *Code for design of concrete structures*. China Architecture & Building Press, Beijing, China.

GB/T 50476, 2008. *Code for durability design of concrete structures*. China Architecture & Building Press, Beijing, China.

Gong, C. et al., 2017. Long-term Field Corrosion Monitoring in Supporting Structures of China Xiamen Xiang'an Subsea Tunnel. *Acta Metallurgica Sinica*, 30 (4), 399-408.

Gonzalez, J. A., Andrade, C., Alonso, C., & Feliu, S., 1995. Comparison of Rates of General Corrosion and Maximum Pitting Penetration on Concrete Embedded Steel Reinforcement. *Cement and Concrete Research*, 25(2), 257-264.

Gouda, V.K., 1970. Corrosion and corrosion inhibition of reinforcing steel. I. Immersed in alkaline solutions, *British Corrosion Journal*, 5, 198–203.

Hausmann, D.A., 1967. Steel corrosion in concrete. How does it occur? *Materials Protection*, 6, 19–23.

He, C., Feng, K., Sun, Q., & Wang, S., 2017. Consideration on issues about structural durability of shield tunnels. *Tunnel Construction*, 37(11), 1351-1363.

Hoseini, M., Bindiganavile, V., & Banthia, N., 2009. The effect of mechanical stress on permeability of concrete: A review. *Cement & Concrete Composites*, 31, 231-220.

Japan Society of Civil Engineers (JSCE), 2002. *Standard specifications for concrete structures construction*. Tokyo, Japan: Maruzen.

Japan Society of Civil Engineers (JSCE), 2007. *Standard Specifications for Tunneling: Shield Tunnel* (2006th ed.). Tokyo: Japan Society of Civil Engineers. [In Japanese]

Japan Society of Civil Engineers (JSCE), 2010. *Tunnel library No.23-Segment design (Revision)*. Tokyo: Japan Society of Civil Engineers. [In Japanese]

Jin, W., & Zhao, Y., 2014. *Durability of Concrete Structures*. Beijing: Science Press. 129-132. [In Chinese]

Jin, Z., Zhao, T., Gao, S., & Hou, B., 2013. Chloride ion penetration into concrete under hydraulic pressure. *Journal of Central South University*, 20(12), 3723-3728.

John P. Broomfield., 2006. *Corrosion of steel in concrete: Understanding, Investigation and Repair*. CRC Press second edition.

Kimura, S., Kitani, T., & Koizumi, A., 2012. Development of performance-based tunnel evaluation methodology and performance evaluation of existing railway tunnels. *Journal of Transportation Technologies*, 2, 113-128.

Kudo, I., & Guo, S., 1994. Study on durability and anti-corrosion: Trans-Tokyo bay highway shield tunnel. *Collection of Translations on Tunnelling (Modern Tunnelling Technology)*, 10, 20-28.

Kodama, S., Tanabe, T., Yokota, H., et al. 2002. Development of maintenance management system for existing open-piled piers, Technical Note of the Port and Airport Research Institute, 1001. [In Japanese]

Lei, M., Peng, L., & Shi, C., 2015. Durability evaluation and life prediction of shield segment under coupling effect of chloride salt environment and load. *Journal of Central South University (Science and Technology)*, 46(8), 3092-3099.

Li, K., Li, Q., Zhou, X., & Fan, Z., 2015a. Durability Design of the Hong Kong-Zhuhai-Macau Sea-Link Project: Principle and Procedure. *Journal of Bridge Engineering*, 20(11), 1-11.

Li, Q., Li, K., Zhou, X., Zhang, Q., & Fan, Z., 2015b. Model-based durability design of concrete structures in Hong Kong-Zhuhai-Macau sea link project. *Structural Safety*, 53, 1-12.

Liu, S., He, C., Feng, K., An, Z., & He, Z., 2015. Research on the Influence of Segment Reinforcement Corrosion on the Mechanical Behaviors of Shield Tunnel Lining Structures. *Modern Tunneling Technology*, 52(4), 86-94. [In Chinese]

Liu, S., He, C., et al., 2017. Erosion degradation mechanism of shield tunnel lining structure in corrosive ion environment. *China Journal of Highway and Transportation*, 30(8), 125-133.

Liu, S., Sun, Q., Feng, K., & He, C., 2016. Research on chloride ion erosion and migration in segment joints of undersea shield tunnels. *Modern Tunneling Technology*, 53(6), 100-106. [In Chinese]

Liu, T., & Weyers, R.W., 1998a. Modeling the dynamic corrosion process in chloride contaminated concrete structures. *Cement and Concrete Research*, 28(3), 365-379.

Liu, X., 2011. *Continuum Damage Mechanics*. Beijing: National Defense Industry Press. [In Chinese]

Liu, Y., 1996. Modeling the time to corrosion cracking of the cover concrete in chloride contaminated reinforced concrete structures. Dissertation. Virginia Polytechnic Institute and State University, Blacksburg, Virginia.

Liu, Y., & Weyers, R.E., 1998b. Modeling the time-to-corrosion cracking in chloride contaminated reinforced concrete structures. *ACI Materials Journal*, 95(6), 675-681.

Maeda, S., Takewaka, K., & Yamaguchi, T., 2004. Quantification of chloride diffusion process into concrete under marine environment by analysis of salt damage data base. *Journal of Materials, Concrete Structures and Pavements*, JSCE, 63(760), 109-120.

Malumbela, G., Alexander, M., & Moyo, P., 2010. Variation of steel loss and its effect on the ultimate flexural capacity of RC beams corroded and repaired under load. *Construction and Building Materials*, 24, 1051-1059.

Mori, Y., & Ellingwood, B.R., 1993. Reliability-based service-life assessment of aging concrete structures. *Journal of Structural Engineering*, 119(5), 1600-1621.

Mori, Y., & Ellingwood, B.R., 1994. Maintaining reliability of concrete structures II: optimum inspection/repair. *Journal of Structure Engineering*, 120(3), 846-862.

Murata, J., Ogihara, Y., Koshikawa, S., & Itoh, Y., 2004. Study on watertightness of concrete. *ACI Materials Journal*, (101), 107-116.

Nakagawa, T., Seshimo, Y., Onitsuka, S., & Tsutsumi, T., 2004. Assessment of corrosion speed of RC structure under the chloride deterioration environment. *Proceedings of JCI symposium on the analysis model supporting the verification of long-term performance of concrete structure in design, JCI*. 325-330. [In Japanese]

Ogata, A., & Banks, R.B., 1961. A Solution of the differential equation of longitudinal dispersion in porous media. US Department of Interior, Washington, DC, USA.

Otieno, M., Beushausen, H., & Alexander, M., 2016. Chloride-induced corrosion of steel in cracked concrete — Part I: Experimental studies under accelerated and natural marine environments. *Cement and Concrete Research*, 79, 373-385.

Pan, H., Yang, L., & Tang, Y., 2005. Summary of actuality and development trend of the research on underground structure durability. *Chinese Journal of Underground Space and Engineering*, 1(5), 804-812.

Papakonstantinou, K.G., & Shinozuka, M., 2013. Probabilistic model for steel corrosion in reinforced concrete structures of large dimensions considering crack effects. *Engineering Structures*, 57, 306-326.

Post, M. L., Van de Linde, F. W. J., & Rademarker, E. J. C., 2004. The Westerchelde tunnel-using a sensor-based system for durability monitoring for the tunnel lining. *Tunnelling and Underground Space Technology*, 19(4-5), 325.

Qi, L., and Seki, H., 2001. Analytical study on crack generation situation and crack width due to reinforcing steel corrosion. *Journal of Materials, Concrete Structures and Pavements, JSCE*. 50, 161-171.

Rao, A.S., Lepech, M.D., Kiremidjian, A.S., & Sun, X.-Y., 2017. Simplified structural deterioration model for reinforced concrete bridge pipers under cycle loading. *Structure and Infrastructure Engineering*, 13(1), 55-66.

RILEM Technical Committee 130-CSL, 1998. *Durability design of concrete structures. RILEM*. Technical Research Center of Finland: E & FN SPON.

Skyora, M., Diamantidis, D., Holicky, M., & Jung, K., 2017. Target reliability for existing structures considering economic and societal aspects. *Structure and Infrastructure Engineering*, 13(1), 181-194.

Song, H., Pack, S., & Ann, K., 2009. Probabilistic assessment to predict the time to corrosion of steel in reinforced concrete tunnel box exposed to sea water. *Construction and Building Materials*, 23, 3270-3278.

Stewart, M.G., & Rosowsky, D.V., 1998. Time-dependent reliability of deteriorating reinforced concrete bridge decks. *Structural Safety*, 20, 91-109.

Sun, J., 2008. Durability design of segment lining structure in Chongming Yangtze river shield tunnel. *Journal of Architecture and Civil Engineering*, 25(1), 1-9.

Sun, J., 2011. Durability problems of lining structures for Xiamen Xiang'an subsea tunnel in China. *Journal of Rock Mechanics and Geotechnical Engineering*, 3(4), 289-301.

Tuutti, K., 1982. *Corrosion of steel in concrete*. Stockholm: Swedish Cement and Concrete Research Institute.

Val, D.V., & Stewart M.G., 2003. Life-cycle cost analysis of reinforced concrete structures in marine environments. *Structural Safety*, 25, 343-362.

Van der wegen, G., Bijen, J., & Van Selst, R., 1993. Behavior of concrete affected by sea-water under high pressure. *Materials and Structures*, 26, 549-556.

Venu, K., Balakrishnan, K., & Rajagopalan, K.S., 1965. A potentio kinetic polarization study of the behavior of steel in NaOH–NaCl system, *Corrosion Science*, 5, 59–69.

Walsh, M.T., & Sagues, A.A., 2016. Steel Corrosion in Submerged Concrete Structures — Part 1: Field Observations and Corrosion Distribution Modeling. *Corrosion Science Section*, 518-532.

Wang, J., Koizumi, A., & Tanaka, H., 2017. Framework for maintenance management of shield tunnel using structural performance and life cycle cost as indicators. *Structure and Infrastructures Engineering*, 13(1), 44-54.

Wang, M., Lu, F., Liu, D., & Yu, L., 2012. *Life-cycle safety monitoring measurement technology of subsea tunnel*. Beijing: China Communications Press. [In Chinese]

Xia, J., Jin, W-L., & Li., L-Y., 2016. Performance of corroded reinforced concrete columns under the action of eccentric loads. *Journal of Materials in Civil Engineering*, 28(1), 1-15.

Yoo, J.-H., Lee, H.-S., & Ismail, M. A., 2011. An analysis study on the water penetration and diffusion into concrete under water pressure. *Construction and Building Materials*, 25, 99-108.

Yoshida, I., 2009. Data assimilation and reliability estimation of existing RC structure. COMPDYN 2009. Rhodes, Greece.

Yu, L., Francois, R., Dang, V. H., L'Hostis, V., & Gagne, R., 2015. Structural performance of RC beams damaged by natural corrosion under sustained loading in a chloride environment. *Engineering Structures*, 96, 30-40.

Yuan, Y., Liu, T., & Liu, X., 2006. Investigation and evaluation of present state and serviceability of existing river-crossing tunnel. *Journal of southeast university (Natural Science Edition)*, 36, 83-89. [In Chinese]

Zhang, Y., Li X., Wei X. Yu G., Li W., & Huang Y., 2015. Water penetration in underwater concrete tunnel. *Journal of the Chinese Ceramic Society*, 43(4), 368-375.

Zhang, Y., Li, X., & Yu, G., 2016. Chloride Transport in Undersea Concrete Tunnel. *Advances in Materials Science and Engineering*, 1-10.

Zhao, J., 2004. Service life design of reinforced concrete structures exposed to chloride environment. *Concrete*, (1), 3-21.

Zhou, X., & Gao, B., 1999. Experimental study on metro stray current corrosion of rebars in reinforced concrete. *Journal of the China Railway Society*, 21(5), 99-105.

List of Published Papers

1. Academic Journals

(1) Zhengshu HE, Mitsuyoshi AKIYAMA, Chuan HE, Dan M. Frangopol, Sijin LIU. Life-cycle reliability analysis of shield tunnels in coastal regions: emphasis on flexural performance of deteriorating segmental linings. *Structure and Infrastructure Engineering*, 2019, 15 (7), 851-871.

(2) Zhengshu HE, Mitsuyoshi AKIYAMA. Time-dependent reliability assessment of shield tunnels under chloride and hydraulic pressure hazards. *Proceedings of Japan Concrete Institute*, 2018, 40 (2), 1387-1392.

(3) Zhengshu HE, Sijin LIU, Chuan HE, Mitsuyoshi AKIYAMA. Structural damage process of an underwater shield tunnel in an aggressive environment. *Proceedings of the Japan Concrete Institute*, 2017, 39 (2), 1333-1338.

(4) LIU Sijin, FENG Kun, HE Chuan, HE Zhengshu. Study on the bending mechanical model of segment joint in shield tunnel with large cross-section. *Engineering Mechanics*, 2015, 32 (12), 215-224.

(5) LIU Sijin, HE Chuan, FENG Kun, AN Zheli, HE Zhengshu. Research on the influence of segment reinforcement corrosion on the mechanical behaviors of shield tunnel lining structure. *Modern Tunneling Technology*, 2015, 52 (4), 86-94.

2. Conference Papers

(1) Zhengshu HE, Mitsuyoshi AKIYAMA, Dan M. Frangopol. Reliability-based durability design of shield tunnels in coastal regions. *Proceeding of 13th International Conference on Applications of Statistics and Probability in Civil Engineering* (ICASP13); May, 2019, Seoul, South Korea.

(2) Zhengshu HE, Mitsuyoshi AKIYAMA, Chuan HE, Dan M. Frangopol. Time-dependent structural reliability analysis of shield tunnels in coastal regions. *Proceeding of the 6th International Symposium on Life-Cycle Civil Engineering* (IALCCE2018); 1031-1037, Oct. 2018, Ghent, Belgium.

(3) Zhengshu HE, Sijin LIU, Chuan HE, Mitsuyoshi AKIYAMA. Performance Assessment of Shield Segments under Coupling Effects of Environmental Agent and Loading. *Proceeding of the 8th Asia and Pacific Young Researchers and Graduates Symposium* (YRGS2017); Sep. 2017, Tokyo, Japan.